Preparation of Atomically-Dispersed Gold on Lanthanum Oxide as Active and Stable Catalysts for the Low-Temperature Water-Gas Shift Reaction

A Thesis

Submitted by

Joseph D. Lessard

In partial fulfillment of the requirements

for the degree of

Master of Science

In

Chemical Engineering

TUFTS UNIVERSITY

May 2012

Advisor: Prof. Maria Flytzani-Stephanopoulos

to my parents
you taught me how to wonder

Acknowledgements

First and foremost I would like to thank my advisor, Professor Maria Flytzani-Stephanopoulos whose passion, drive, encouragement, and mentorship has brought me to this point. Professor Flytzani-Stephanopoulos has shown me what it means to be a chemical engineer and what it means to be a researcher through her questions, insight and attention to detail. She has also allowed me to grow this project from inception to the work presented here. I would also like to thank Professor Howard Saltsburg and Professor George Kyriakou who serve as members of my thesis committee and have provided valuable critique, honesty, and commentary along the way.

I would also like to thank my colleagues in the Nano Catalysis & Energy Lab at Tufts University. A special thanks is due to Dr. Yanping Zhai and Matt Boucher who served as my mentors when I was an undergraduate and first started in the lab. I gratefully acknowledge Ioannis Valsamakis with whom I have worked very closely on this project; his attention to detail and work ethic are remarkable. Additionally, I am very thankful to Branko Zugic for his analysis of my XPS, XAS and TEM data.

I also appreciatively acknowledge Dr. David Wilbur in the Chemistry Department at Tufts University for the use of the ICP instrument. Additionally, I would like to thank Professor Kurt Pennell in the Civil and Environmental Engineering Department at Tufts University and his student Anjuliee Mittelmann for the use of their group's ICP instrument. I also thank Dr. Elisabeth Shaw at the MIT Material Science and Engineering Center for her assistance with performing XPS measurements.

Finally, I would not be here without the loving support of my family and friends.

Abstract

Clean hydrogen has been touted as the fuel of the future because, when combusted, it only produces water, an environmentally innocuous by-product. The technology that would use this H_2 most efficiently is the fuel cell, which is capable of converting the chemical energy stored in H_2 into electrical energy that can be used to power daily life. Such a device, though, requires very pure H_2 as a fuel source without contaminating gases like CO that poison the platinum catalysts on the anode of low temperature fuel cells. The water-gas shift (WGS) reaction has been intensely studied as the most efficient way to remove CO from H_2 feeds to fuel cell systems. In such a design, a WGS reactor would operate upstream of the fuel cell, at low temperature, to remove most or all of the CO from the feed. Additional systems could also be implemented to further reduce the CO content and remove other impurities (e.g. H_2S).

The current catalysts used in industrial WGS reactors are $Cu/ZnO/Al_2O_3$. However, these catalysts are pyrophoric, require lengthy activation procedures and show little thermal stability. Noble metal (Au, Pt, Pd, etc.) catalysts have recently received significant attention as potential alternatives to the industrial catalysts because they are non-pyrophoric and can be made more stable. In this thesis, Au highly dispersed on La_2O_3 was investigated as a novel catalyst for the WGS reaction. In particular, an anion adsorption technique was developed to deposit Au onto the La_2O_3 surface in a manner that would favor a strong interaction between the Au and the support.

In this work, catalysts were prepared with four different techniques: colloidal deposition, co-precipitation, deposition-precipitation, and anion adsorption. These materials were characterized with electron microscopy (TEM), X-ray absorption spectroscopy (XAS), BET surface area measurements, X-ray photoelectron spectroscopy (XPS), and temperature

programmed reduction (CO-TPR) studies. Additionally, Au/La_2O_3 was studied under WGS reaction conditions in both product-free and full reformate gas environments.

Anion adsorption was found to produce the most active WGS catalyst compared to other gold preparation techniques on lanthana. Additionally, it was observed that high temperature treatments of 1% Au/La_2O_3 further activated these materials for the WGS reaction. In an effort to improve our understanding of the importance of reducible versus irreducible metal oxide supports in the WGS reaction, the surface oxygen of the active gold catalysts was examined and quantified. It was discovered that normalization of the reaction rates over Au/La_2O_3 by the amounts of active surface oxygen were comparable to the similarly normalized rates of Au supported on reducible metal oxides like CeO_2 and FeOx.

Table of Contents

List of Figures and Tables

Chapter 1. Introduction

1.1 Background

The growing industries of today's global economy consume energy at an unprecedented rate, leading to increased pollution, conflict over energy sources, and an unequal distribution of resources. In 2009, over 80% of the world's energy supply was derived from fossil fuels, principally oil[1]. The conversion of fossil fuels to usable energy – i.e. electricity – is an inherently inefficient process that produces significant amounts of by-products that contribute to global warming and climate change. To offset these socio-political and environmental pressures, technologists and politicians are searching for alternative energy solutions that are safer, cleaner, more sustainable and more efficient. One of the most attractive technologies that addresses many of these criteria is the fuel cell.

1.2 Fuel Cells

A fuel cell is an electrochemical device that converts the energy stored in chemical bonds into electrical energy, which can be used to power daily life. This energy conversion is accomplished by harnessing the electrons transferred in a redox reaction by forcing them through a load-bearing external circuit. A fuel cell consists of an anode and a cathode to which an reductant and oxidant are supplied, respectively. The porous electrodes, usually comprised of carbon with dispersed platinum particles, are separated by an ion-conducting electrolyte. Fuel cells are differentiated based on the nature of the ion-conducting electrolyte; of the several variations, polymer electrolyte membrane fuel cells (PEMFCs) are the most

interesting because they show the most promise for residential heaters, portable devices and transportation applications. PEMFCs offer many advantages over other types of fuel cells because they have low operation temperatures, sustained operation at high current densities, small size and weight, potentially low production costs, and durability during start-up and shut-down cycles[2].

In the PEMFCs of interest to this work, H_2 is the reductant (Equation 1) and O_2 is the oxidant (Equation 2). The H^+ produced at the anode travels through the polymer electrolyte membrane (usually a fluorinated polysulfonate) where it combines with the oxygen ions and forms water at the cathode.

$$2H_2 \rightarrow 4H^+ + 4e^- \qquad \textbf{(Eq. 1)}$$

$$4H^+ + 4e^- + O_2 \rightarrow 2H_2O \qquad \textbf{(Eq. 2)}$$

The overall reaction has an electrical potential of 1.3 V, which allows for PEMFC stacks in transportation applications with power outputs on the order of 5 – 50 kW[3].

A major concern to be addressed before PEMFCs can be fully commercialized in the transportation sector involves the means by which H_2 will be supplied to the vehicle. An obvious choice would be to develop systems for H_2 distribution, supply, and refueling like those already in place for gasoline and diesel fuels. Fueling a vehicle with compressed H_2 and onboard storage as either compressed H_2, cryogenic H_2 or metal hydrides are the currently considered approaches[4]. An alternative solution, which was abandoned in the earls 2000s due to complexity and cost, would be the onboard production of H_2 from more

easily stored fuels – e.g. alcohols or hydrocarbons. This may be the way we will power the fuel cell cars in the future.

The onboard reforming of an alcohol or hydrocarbon into H_2 is appealing as it eliminates much of the complexity associated with H_2 storage. However, the poisoning of the Pt anode by the CO also produced in this process is a significant challenge that must be overcome. Due to its favorable adsorption onto the Pt surface, CO can out-compete H_2 for active sites at the anode. For this reason, CO concentrations must be below a few ppm in the fuel feed[5]. This CO concentration reduction can be accomplished, in most part via the water-gas shift (WGS) reaction over active catalysts upstream of the PEMFC.

1.3 Water-Gas Shift Reaction

The water-gas shift (WGS) reaction (Equation 3) has been known to scientists since 1888, but it did not gain a foothold in industry until 1914 when Bosch and Wild began using Fe/Cr catalysts to produce H_2 via the WGS reaction for the synthesis of ammonia[6].

$$CO_{(g)} + H_2O_{(g)} \leftrightarrow CO_{2(g)} + H_{2(g)} \qquad \textbf{(Eq. 3)}$$

$$\Delta H = -41.3 \text{ kJ mol}^{-1}$$

$$\Delta G = -28.5 \text{ kJ mol}^{-1}$$

Because the reaction is exothermic, equilibrium is more favored to the products at lower temperatures; a catalyst must then be used to achieve appreciable reaction rates. There are three major classes of catalysts in use in industry today, with the differentiation between them based primarily on their operating conditions. Promoted Fe (and Fe-Cr) catalysts operate in the high temperature regime (350 –

450 °C) and are dubbed high-temperature shift (HTS) catalysts. In the low temperature – low-temperature shift (LTS) – regime (190 – 250 °C), Cu-ZnO catalysts are used. Finally, when the feed contains appreciable amounts of sulfur, which can poison catalytic surfaces, Co-MoS catalysts are used, and are called sour gas shift catalysts[7]. In a typical WGS reactor scheme, a series of adiabatic reactors are used with HTS reactors preceding LTS ones so that the final stages can achieve favorable equilibrium conversions to H_2. This industrial set up is able to reduce CO concentrations from 10-50% in the feed to 0.3 wt% in the reactor effluent.

While the Fe-Cr and Cu-ZnO have become industry standards for large scale H_2 production, they do not hold much promise for crossover into the consumer market for application in onboard PEMFC H_2 production. In such applications, the catalyst bed must be small and compact. Additionally, the catalyst must be able to tolerate rapid start-up and shut-down cycles without a requisite elaborate pre-reduction procedure. Finally, for safety reasons, the catalyst should be non-pyrophoric and oxidation-tolerant. In recent years, the development of catalysts with supported noble metals (Pt and Au) has begun to address these issues.

1.3.1 Gold-Based WGS Catalysis

Gold was long considered a completely inert metal, hence its classification as a noble metal, with little or no potential in catalysis. However, with the pioneering work of Haruta in the late 1980s and early 1990s, it was demonstrated that if brought to the nanoscale, Au was an excellent catalyst in a host of

reactions[8]. Having worked first with CO oxidation, Haruta extended his Au-based catalysts into the realm of the WGS reaction when he studied the preferential oxidation of CO in H_2-rich streams (PROX)[9]. In this work, it was shown that small Au particles (<1-5 nm) were present in the most active materials. Andreeva et al. further showed that high conversions of CO were possible below 200 °C on a Au/α-Fe_2O_3 catalyst with high Au dispersion[10]. This high activity over reducible metal oxide supports was further extended to Au/CeO_2 wherein it was shown that ionic gold was present in the most active materials[11]. The Au/CeO_2 materials were treated with a solution of NaCN that was capable of removing all weakly bound and metallic Au species, leaving only strongly bound ionic species. Both the catalytic performances and the apparent activation energies were the same for the parent and leached materials. In these materials it was also demonstrated that the addition of Au to the support significantly altered the local electronic structure of the CeO_2. Bare CeO_2 has two reduction peaks, one at 440 °C assigned to surface oxygen and one at 800 °C assigned to bulk oxygen. However, the addition of Au drastically lowers the reduction temperature of the surface oxygen to below 100 °C[12].

A precise understanding of how Au factors in the WGS catalysis is still sought. At the core of this investigation is the interaction between Au and CO. In another test reaction, CO oxidation, the influence of the Au oxidation state on the adsorption of CO has been heavily studied[13]. In their review, Flytzani-Stephanopoulos and Gates highlight the most recent findings that suggest cationic Au species are responsible for the adsorption of CO.

Gold-based catalysts face significant challenges in overcoming the deactivation usually observed with time on stream in WGS conditions. This deactivation is usually attributed to the sintering of the Au particles and concomitant loss of low coordinated Au sites. To address this issue, researchers have investigated the performance of bimetallic Au-based catalysts via the introduction of other metals – e.g. Pt, Pd – with results indicating improved performance[14]. Additionally, other groups have doped the support with metal cations – e.g. Fe, and rare earth group metals – to improve the Au stability, and improve the support's reducibility and oxygen mobility[15].

1.3.2 Lanthanum in WGS Catalysts

In Au/CeO_2 catalysts, La ion doping has been used to stabilize the CeO_2 support to prevent crystallite growth and maintain high surface area[16]. Similar effects have been demonstrated when La (or La_2O_3) is doped in Fe_2O_3 and CeO_2 for CO oxidation and the PROX reaction[17]. A sulfated form of lanthana, $La_2O_2SO_4$, was recently shown to be active for the HT-WGS reaction, in the absence of any metals[18]. Lanthanum oxide alone is not an active oxide for the WGS reaction since, unlike CeO_2 or Fe_2O_3, it is not reducible. In her thesis work, Yanping Zhai prepared gold on lanthana by deposition-precipitation of gold, but the resulting materials were of relatively low activity below 250 °C[19]. Even less active (<5% CO conversion at 310 °C) materials were similarly prepared by Wang et al.[15a].

Gold supported on La_2O_3 has been shown to be active for the dry CO oxidation reaction. This system was first investigated in 2005 by Fierro-Gonzalez,

et al. when they demonstrated that addition of Au to La_2O_3 via an organometallic precursor produced mononuclear Au(III) species that were highly active for CO oxidation[20]. Further investigation of the Au/La_2O_3 system showed that Au can be deposited onto La_2O_3 in a variety of ways to produce highly stable, ionic Au species that are highly active for CO oxidation and show interesting redox behavior with CO_2[21]. A similar material prepared by deposition-precipitation has also been shown to be active and selective for the oxidative dehydrogenation of butane[22]. In this work it was shown that when the gold was loaded in very small amounts (<0.2 at%), it was highly dispersed and remained cationic even at temperatures of 550 °C.

1.4 Thesis Motivation and Objectives

The Au/La_2O_3 catalysts that have previously been investigated in the literature have been successful at achieving highly dispersed Au species that appear to be stable under certain reaction conditions. Because La_2O_3 seems capable of supporting highly oxidized Au – and has already been shown to be active in reactions for which oxidized gold is desirable – it seems that it could potentially be an active WGS catalyst. However, work at producing highly dispersed ionic Au species has been limited to materials with very low Au contents (<0.2 at%).

The aim of this thesis was to investigate the use of La_2O_3-based Au catalysts for the LT-WGS reaction. In particular, an anion adsorption technique was developed to prepare Au/La_2O_3 materials, which were then investigated for their structural properties and WGS activity. This thesis is comprised of five

chapters. An introduction and background information is provided in Chapter 1. Chapter 2 outlines the experimental principles and methods used for the characterization of the materials. The results of WGS reaction studies for materials prepared by colloidal deposition, co-precipitation, and deposition-precipitation are presented in Chapter 3. The preparation details, and catalytic activity of materials prepared by anion adsorption are discussed in Chapter 4. Chapter 5 includes a summary of the work completed, conclusions drawn from the results, and recommendations for future work.

1.5 References

[1] International Energy Agency, Paris, **2011**, pp. 1-10.

[2] J.-H. Wee, *Renewable and Sustainable Energy Reviews* **2007**, *11*, 1720-1738.

[3] a. J. J. Hwang, D. Y. Wang, N. C. Shih, *Journal of Power Sources* **2005**, *141*, 108-115; b. A. Folkesson, C. Andersson, P. Alvfors, M. Alaküla, L. Overgaard, *Journal of Power Sources* **2003**, *118*, 349-357.

[4] X. Li, *Principles of Fuel Cells*, 1 ed., Taylor & Francis, New York, **2005**.

[5] C. Song, *Catalysis Today* **2002**, *77*, 17-49.

[6] a. L. Mond, C. Langer, Britain, **1888**; b. C. Bosch, W. Wild, Canada, **1914**.

[7] C. Ratnasamy, J. P. Wagner, *Catalysis Reviews* **2009**, *51*, 325-440.

[8] a. M. Haruta, N. Yamada, T. Kobayashi, S. Iijima, *Journal of Catalysis* **1989**, *115*, 301-309; b. M. Haruta, T. Kobayashi, H. Sano, N. Yamada, *Chemistry Letters* **1987**, *16*, 405-408.

[9] M. Haruta, S. Tsubora, T. Kobayashi, H. Kageyama, M. J. Genet, B. Delmon, *Journal of Catalysis* **1993**, *144*, 175-192.

[10] a. D. Andreeva, V. Idakiev, T. Tabakova, A. Andreeva, R. Giovanoli, *Applied Catalysis A: General* **1996**, *134*, 275-283; b. D. Andreeva, V. Idakiev, T. Tabakova, A. Andreeva, *Journal of Catalysis* **1996**, *158*, 354-355.

[11] Q. Fu, H. Saltsburg, M. Flytzani-Stephanopoulos, *Science* **2003**, *301*, 935-938.

[12] Q. Fu, W. Deng, H. Saltsburg, M. Flytzani-Stephanopoulos, *Applied Catalysis B: Environmental* **2005**, *56*, 57-68.

[13] M. Flytzani-Stephanopoulos, B. C. Gates, *Annual Review of Chemical and Biomolecular Engineering* **2012**, *3*, 545-574.

[14] M.-A. Hurtado-Juan, C. M. Y. Yeung, S. C. Tsang, *Catalysis Communications* **2008**, *9*, 1551-1557.

[15] a. Y. Wang, S. Liang, A. Cao, R. L. Thompson, G. Veser, *Applied Catalysis B: Environmental* **2010**, *99*, 89-95; b. W. Deng, C. Carpenter, N.

Yi, M. Flytzani-Stephanopoulos, *Topics in Catalysis* **2007**, *44*, 199-208; c. F. Moreau, G. C. Bond, *Catalysis Today* **2006**, *114*, 362-368.

[16] Q. Fu, A. Weber, M. Flytzani-Stephanopoulos, *Catalysis Letters* **2001**, *77*, 87-95.

[17] a. R. Liu, C. Zhang, J. Ma, *Journal of Rare Earths* **2010**, *28*, 376-382; b. G. Avgouropoulos, M. Manzoli, F. Boccuzzi, T. Tabakova, J. Papavasiliou, T. Ioannides, V. Idakiev, *Journal of Catalysis* **2008**, *256*, 237-247.

[18] I. Valsamakis, M. Flytzani-stephanopoulos, *Applied Catalysis B: Environmental* **2011**, *106*, 255-263.

[19] Y. Zhai, Ph.D. Dissertation, Dept. of Chemical & Biological Engineering, Tufts University, **2011**.

[20] J. C. Fierro-Gonzalez, V. A. Bhirud, B. C. Gates, *Chemical Communications* **2005**, 5275-5277.

[21] a. M. Mihaylov, E. Ivanova, Y. Hao, K. Hadjiivanov, H. Knözinger, B. C. Gates, *Journal of Physical Chemistry C* **2008**, *112*, 18973-18983; b. M. Mihaylov, E. Ivanova, Y. Hao, K. Hadjiivanov, B. C. Gates, H. Knözinger, *Chemical Communications* **2008**, *2*, 175-177; c. A. Goguet, M. Ace, Y. Saih, J. Sa, J. Kavanagh, C. Hardacre, *Chemical Communications* **2009**, 4889-4891; dT. Takei, I. Okuda, K. K. Bando, T. Akita, M. Haruta, *Chemical Physics Letters* **2010**, *493*, 207-211.

[22] J. Sá, M. Ace, J. J. Delgado, A. Goguet, C. Hardacre, K. Morgan, *ChemCatChem* **2011**, *3*, 394-398.

Chapter 2. Materials & Methods

2.1 Catalyst Preparation

This section describes in detail the methods used to prepare the lanthanum-based Au catalysts used in this work. The analysis and activity tests of these materials are presented in subsequent chapters. First, the hydrolysis method used to prepare the lanthanum oxide (La_2O_3) is described, followed by the methods used to deposit Au onto the support surface. These methods are colloidal deposition, deposition-precipitation and anion adsorption. Finally, a co-precipitation technique was investigated to produce Au/$La(OH)_3$. All Au deposition procedures were performed in the dark to minimize light-induced reduction of the Au precursor.

2.1.1 Precursors

The chemicals and reagents used in this work are listed in Table 2.1. All materials were used as provided by suppliers without further purification.

2.1.2 Hydrolysis Support Preparation

The hydrolysis technique used in this work was adapted from a preparation described by Wang et al[1]. In the literature, a urea gelation coprecipitation (UGC) technique is often used to prepare rare earth oxides[2]. However, the hydrolysis technique is used here because it yields a $LaO(OH)_x$ (specifically called a La2O3 by Wang et al.[1]) material with higher surface area without the inclusion of bulk carbonate, which is introduced in UGC as the urea

decomposes. Sodium (from the NaOH used to precipitate the $La(OH)_3$) was not found in the final $LaO(OH)_x$ product when tested by ICP. The procedure to prepare approximately 10 g of $LaO(OH)_x$ is as follows:

i. Dissolve 27.9 g of the lanthanum nitrate salt in 100 mL of deionized H_2O with continuous stirring.
ii. In a separate beaker, heat 250 mL of deionized H_2O to 80 °C and then dissolve 35.4 g of NaOH with continuous stirring.
iii. Add the lanthanum precursor solution to the hot solution of NaOH. The highly insoluble $La(OH)_3$ precipitates out of solution as a white solid.
iv. Keep the suspension stirring overnight at 80 °C.
v. Filter the lanthanum solids and wash with approximately 300 mL aliquots of deionized water to remove excess NaOH until the pH of the filtrate is 7 (usually 3 – 4 washes).
vi. Dry the lanthanum-based cake overnight in a room temperature vacuum chamber.
vii. Crush the dried material and sieve to 270 mesh to yield a fine, white powder of $La(OH)_3$.
viii. Calcine the material in static air at 650 °C for 4 h with a temperature ramping rate of 2 °C min^{-1} to produce $LaO(OH)_x$.

The material obtained after the calcination is a highly amorphous form of lanthana most accurately described as $LaO(OH)_x$ because it includes OH and crystalline H_2O in its lattice. However, for simplicity, this material will be denoted as La_2O_3

throughout the remainder of the text because this is how this material is often reported in the catalysis literature.

2.1.3 Colloidal Deposition

This technique was used to prepare Au/La_2O_3 catalysts with relatively large metallic Au particles. This method has been used elsewhere to prepare metallic Au particles of varying particle size distributions as both catalytically active materials and as control materials for comparison[3]. Colloidal (>3-5 nm) Au particles are first prepared by reducing a Au salt in the presence of the capping agent polyvinylpirrolidone (PVP) with sodium borohydride ($NaBH_4$); these particles are then deposited onto the La_2O_3 in a step analogous to excess solution impregnation. By varying the Au:PVP ratio it is possible to achieve Au particles of different sizes[3a]. To prepare approximately 1.7 g of 0.5% Au/La_2O_3 (C) (where 0.5% refers to the atomic ratio Au/(Au + La) and (C) refers to the colloidal preparation) with a design particle size distribution of 3-5 nm, the following procedure is performed:

i. Suspend 1.7 g of La_2O_3 in 100 mL of deionized H_2O with stirring and sonication.
ii. In a separate beaker, dissolve 0.06 g of the PVP in 50 mL of deionized H_2O with stirring and sonication.
iii. Dissolve 0.02 g of the Au precursor in 50 mL of deionized H_2O and add dropwise to the PVP mixture. This step allows the gold complex to interact with the PVP with the goal of dispersing Au along the PVP polymer chains.

iv. Dissolve 0.004 g of $NaBH_4$ in 30 mL of deionized H_2O and add dropwise to the Au/PVP mixture. The solution turns from a pale yellow to a deep purple as the Au is reduced to Au(0) colloidal particles. Continue stirring the mixture at room temperature for approximately 1 h.

v. Add the Au/PVP mixture to the La_2O_3 suspension dropwise with vigorous stirring at 70 °C. Continue stirring the mixture at temperature for 6-8 h.

vi. Filter the material and wash three times with 300 mL aliquots of deionized water at room temperature. The first filtrate should be clear, indicating that all of the Au has been deposited onto the La_2O_3 surface.

vii. Dry the material overnight in vacuum.

viii. Calcine the material in static air at 280 °C for 4 h with a temperature ramping rate of 2 °C min^{-1} to burn off the PVP. The catalyst is purple indicating the presence of >2 nm metallic Au nanoparticles.

2.1.4 Deposition-Precipitation

Deposition-precipitation (DP) has been used extensively with supported Au catalysts to prepare Au nanoparticles on a variety of supports. Our group at Tufts has used DP to successfully prepare Au/CeO_2 materials with particles <5 nm in diameter, and about 10% of the gold in an atomically dispersed state, the latter being the active sites for the WGS reaction[4]. In this technique, Au is precipitated from an aqueous solution and deposited onto a support surface. The precipitation is driven by the pH of the solution, which is maintained around 8. A major concern with this method is that any residual chlorides left on the catalyst

can compromise the stability of Au[5]. The following procedure is used to prepare 1.0 g of 1% Au/La_2O_3 (DP):

i. Suspend 1.0 g of La_2O_3 in 100 mL of room temperature deionized H_2O with stirring. The pH of this mixture should be 9-10.

ii. In a separatory funnel dissolve 0.02 g of the Au precursor in 50 mL of deionized H_2O.

iii. Add the Au precursor solution to the La_2O_3 suspension dropwise while maintaining the pH of the mixture around 8.5-8.6 with 1 M $(NH_4)_2CO_3$. This pH is chosen to precipitate the Au precursor as a hydroxide onto the La_2O_3 surface.

iv. Age the mixture at room temperature with stirring for 1 h. The pH may rise during this time to approximately 9.

v. Filter and wash the material 2 – 3 times with 300 mL aliquots of warm (70 °C) deionized H_2O.

vi. Dry the material overnight in vacuum at room temperature and calcine in flowing O_2 (30 mL min^{-1}, 20% O_2 – He) at 250 °C for 2 h with a temperature ramping rate of 2 °C min^{-1}. At this point the material should be light gray in color.

vii. In select experiments, this material was further heated to 400 °C for 1 h with a temperature ramping rate of 10 °C min^{-1} after the initial calcination at 250 °C in either flowing He (30 mL min^{-1}), O_2 (30 mL min^{-1}, 20% O_2 – He), H_2 (30 mL min^{-1}, 20% H_2 – He), or CO_2 (30 mL min^{-1}, 10% CO_2 –

He) to investigate the effect of pretreatment conditions on the catalytic activity.

2.1.5 Anion Adsorption

Anion Adsorption (AA) seeks to mitigate some of the inherent difficulties presented by DP. In DP, reagents are used to maintain the pH at a desired set point. In this study, $(NH_4)_2CO_3$ was used and could therefore introduce carbonates to the system. In other DP preparations, alkali-containing reagents are used, which can further complicate the system due to the alkali effect. Additionally, residual chlorides often remain on the support surface during DP preparation and hot H_2O or hot NH_3 is required to remove them.

In AA, originally developed by Ivanova, et al., the Au precursor is speciated to the hydroxylated form by adjusting the preparation temperature and concentrations – i.e. without any additional chemicals[6]. The preparation conditions are also chosen to establish an electrostatic attraction between the negatively charged Au precursor complex and the positively charged support surface. In order to choose the preparation conditions properly, the point of zero charge (PZC) of La_2O_3 and the speciation behavior of the Au precursor must be known, these are described in Chapter 4. To prepare 2.0 g of 1% Au/La_2O_3 (AA) the following procedure is used:

i. Suspend 2.0 g of La_2O_3 in 200 mL of warm (70 °C) deionized H_2O. The pH of this mixture is generally between 9 and 10.
ii. Dissolve 0.05 g of the Au precursor in 100 mL of deionized H_2O and add dropwise to the La_2O_3 suspension (at a rate of approximately 1 mL min^{-1}).

The pH will initially drop to approximately 7.0-7.5 and will rise to approximately 7.5 – 8 once all of the Au solution has been added.

iii. Age the mixture for 1 h at 70 °C with continuous stirring. At the end of the aging the pH will have dropped to 8.

iv. Filter the material and wash twice with 300 mL aliquots of room temperature deionized water.

v. Dry the catalyst overnight in vacuum at room temperature and calcine in flowing O_2 (30 mL min^{-1}, 20% O_2 – He) at 250 °C for 2 h with a temperature ramping rate of 2 °C min^{-1}. At this point the material should be light gray in color.

vi. In select experiments, this material was further treated at 400 °C for 1 h with a temperature ramping rate of 10 °C min^{-1} after the initial calcination in either flowing He (30 mL min^{-1}), O_2 (30 mL min^{-1}, 20% O_2 – He), H_2 (30 mL min^{-1}, 20% H_2 – He), or CO_2 (30 mL min^{-1}, 10% CO_2 – He) to investigate the effect of pretreatment conditions on the catalytic activity.

2.1.6 Co-Precipitation

Co-precipitation (CP) is a technique wherein salts of the support and salts of the supported noble metal are dissolved together and then precipitated simultaneously to produce a mixed salt. In such a procedure the noble metal is often included in the lattice of the support; in some cases treatments with H_2 can be used to bring the noble metal to the surface. As it changes with the gas composition and temperature/time treatment, it is often tedious to quantify the amount of noble metal on the surface and in the bulk with CP. However, this

method allows for more extensive interaction of metal and oxide, and often produces very active catalysts, e.g. the Au/CeO_2 catalysts prepared by CP in Qi Fu's thesis work[4].

Takei, et al. used CP to make a $Au/La(OH)_3$ catalyst that was highly active for the low temperature CO oxidation reaction[7]. Oxidized Au, surrounded with hydroxyl (OH) groups, was present. However, the temperature at which this material could be tested was limited by the relatively low thermal stability of $La(OH)_3$. This technique was investigated here to see if the material could be used as a LT-WGS catalyst. To prepare 1.0 g of 5% Au/La_2O_3 (CP), the following procedure was used:

i. Dissolve 2.3 g of the La precursor and 0.1 g of the Au precursor in 56 mL of room temperature deionized H_2O.
ii. Add the precursor solution to warm (70 °C) solution of 0.763 g of NaOH in 191 mL of deionized H_2O. $La(OH)_3$ is seen to precipitate immediately upon addition of the La-precursor solution to the NaOH solution.
iii. Age the mixture at 70 °C for 1 h with continuous stirring.
iv. Filter the materials and wash with 300 mL aliquots of room temperature deionized H_2O until the pH of the filtrate is <8 (usually 2 – 3 washes).
v. Dry the catalyst overnight in vacuum at room temperature and calcine in flowing O_2 (30 mL min^{-1}, 20% O_2 – He) at 150 °C for 4 h at a heating rate of 2 °C min^{-1}.

2.2 Catalyst Notation

Catalysts are denoted *n*% Au/*support* (*x,y,z*) where *n* represents the atomic metal percent loading, Au / (Au + La) x 100%; *x* represents the preparation technique used – C: colloidal deposition, DP: deposition-precipitation, AA: anion adsorption, and CP: co-precipitation; *y* represents the differentiation between parent (P) or leached (L) materials (if no *y* is listed then the material is assumed to be the parent; *z* represents the pretreatment (see the individual sections on catalyst preparation for precise pretreatment conditions) – He: He pretreatment, O_2: O_2 pretreatment, CO_2: CO_2 pretreatment, if no *z* is listed then the material can be assumed to have been used fresh (i.e. calcined at 250 °C with no further high temperature treatment). Finally, the lanthanum support prepared by the hydrolysis technique is represented as La_2O_3, although it might be more accurately described as $LaO(OH)_x$.

2.3 Catalyst Characterization Methods

2.3.1 Bulk Compositional Analysis

For bulk compositional analysis the catalyst powders were dissolved in HCl (36.5-38%, Alrdich) that contained a small amount of H_2O_2 (29-32%, Aldrich) and diluted with deionized H_2O. The resulting solutions were analyzed by Inductively Coupled Plasma Atomic Emission Spectroscopy (ICP-AES, Leeman Labs, Inc.). Standard ICP solutions of Au and La were purchased from Alfa Aesar and diluted to produce calibration curves.

2.3.2 Electron Microscopy

Electron microscopy is used to resolve nanometer, and in some cases sub-nanometer-sized features by using high-energy electrons. Transmission electron microscopy (TEM) was used to estimate the particle size distribution in this work. The sample was sonicated in ethanol and deposited on a lacey carbon, 200 mesh copper grid. Samples were analyzed at the MIT Center for Materials Science and Engineering on a JEOL 2100 instrument, operating at 200 kV with a lanthanum hexaboride cathode.

2.3.3 X-Ray Diffraction (XRD) Analysis

X-ray diffraction (XRD) is a bulk technique used to determine the crystalline phases present in a sample; it can also be used to measure the size of supported nanoparticles if the particles are large enough (>2 nm). Measurements were taken on a Rigaku RU300 with a rotating anode generator and a monochromatic detector. Cu $K\alpha_1$ radiation was used with a power setting of 50 kV and 300 mA.

2.3.4 BET Surface Area Measurements

BET surface area measurements were performed using single-point N_2 adsorption-desorption cycles with a Micromeritics model AutoChem II 2920 apparatus. In a typical experiment 0.2 g of the sample was loaded between beds of quartz wool and pretreated in He to 150 °C for 30 minutes to remove any adsorbed H_2O. The analysis gas used was 30% N_2 – He. Each measurement was repeated three times; the reported surface areas are the averages of the three repeats.

2.3.5 CO Temperature Programmed Reduction (CO-TPR)

Temperature Programmed Reduction (TPR) is a technique in which the surface reduction of an oxide is monitored while the temperature of the sample is ramped in a programmed fashion with time. This analysis can yield insight into the type of oxygen groups present on a support surface. In CO-TPR, the surface is reduced under a flow of CO and the process is monitored by an online quadrupole mass spectrometer (SRS residual gas analyzer). Analysis was performed on a Micromeritics model AutoChem II 2920 apparatus.

In a CO-TPR experiment the sample was tested untreated either after a reaction or immediately after *in situ* pretreatment. The sample was first purged at room temperature in a flow of He for 15 – 30 minutes. The flow was then switched to 10% CO – He (30 mL min^{-1}) and the temperature was ramped to 400 °C at 10 °C min^{-1}; in general the temperature was held at 400 °C for 1 h. In cyclic experiments, a room temperature rehydration between cycles was performed wherein the sample was treated with a flow of 3% H_2O – He (10 mL min^{-1}) for 30 minutes followed by a 5 minute purge in He (30 mL min^{-1}). The amount of surface hydroxyls was calculated by integrating the peak areas of the CO_2 and H_2 produced. The integrated area, whose units are [% gas • s], is then converted to moles of activated oxygen using a calibration curve created by performing a series of similar CO-TPRs over Ag_2O in which the amount of CO_2 is stoichiometrically equivalent to the total oxygen in the sample.

2.3.6 UV-Visible (UV-Vis) Spectroscopy

UV-visible (UV-Vis) spectroscopy is a technique that can be used to examine the electronic transition states of metals based on the absorption intensity of varying wavelengths of light in the range of 200 – 800 nm. In particular with Au catalysts, the oxidation state and the coordination environment can be qualitatively measured based on the shape and position of different absorption bands. In this work, UV-Vis spectra were taken on a Thermo Scientific Evolution 300 instrument with *in situ* heating capabilities. Samples were suspended in spectroscopic grade ethanol (Sigma) or deionized H_2O and placed in a quartz cuvette with a path length of 1 cm. Materials were analyzed for absorption in the range of 220 – 800 nm.

2.3.7 X-Ray Photoelectron Spectroscopy (XPS)

X-ray photoelectron spectroscopy is a surface analysis technique that is used to characterize the composition, chemical shift and oxidation states of a material. In XPS, an X-ray beam irradiates the sample causing the release of core-level electrons. These electrons are collected and analyzed for their number and kinetic energy, which is correlated to their binding energy. Since each element's electrons have a distinct binding energy, the resulting spectrum of intensity plotted against binding energy can be used to determine the relative composition of a sample, along with the oxidation state of its components due to the chemical shift of any peaks. Additionally, since the photoelectrons released in this experiment have an escape depth of only several nanometers, this is an excellent

technique to determine the "surface" concentration and oxidation state of supported metal catalysts.

XPS measurements were performed at the MIT Center for Materials Science and Engineering on a Kratos AXIS Ultra. Materials were pressed into a self-supporting wafer on conductive carbon double-sided tape that was pressed onto copper foil. These materials were examined using a pass energy of 20 eV; the spectra were aligned during analysis to the C 1s peak at 284.5 eV. Spectra were analyzed using CasaXPS software.

2.3.8 X-Ray Absorption Near Edge Structure (XANES) Spectroscopy

X-ray absorption near edge structure (XANES) spectroscopy is used to examine the oxidation state of metals. In a XANES experiment, the sample is irradiated with X-rays of increasing energy; below a characteristic energy (known as the absorption edge), the X-rays are not absorbed. However, at the absorption edge, the X-rays have sufficient energy to excite core-level electrons into vacant higher energy orbitals; sometimes a sharp peak known as the white line is present at the top of this absorption edge. The intensity of the white line can give insight into the degree of oxidation of the metal being examined.

In this work, XANES was used to monitor *in situ* the oxidation state of the Au during reaction or treatments. XANES spectra were collected at the National Synchnotron Light Source (NSLS) at Brookhaven National Lab (BNL) on the X18B beamline. Samples were loaded into a Kapton tube and packed with quartz wool and then fitted into a reactor assembly that allowed for gas flow through the sample and heating of the sample. The spectra were taken in the fluorescence

mode with a Ge 13-element detector placed at an angle of 90° to the incident X-ray beam; the sample was placed at an angle of 45° to both the X-ray beam and the detector (Figure 2.1). Spectra were then taken at room temperature in product-free gas (20 mL min^{-1}, 5% CO – 3% H_2O – He) and during a temperature ramp (5 °C min^{-1}) to 300 °C and isothermal hold at 300 °C for 1 h.

2.3.9 Temperature Programmed Surface Reaction (TPSR)

The reactivity of the catalysts was tested dynamically using temperature programmed surface reaction (TPSR). The onset temperature of catalytic activity and achievement of 100% conversion of the feed was followed by tracking the CO (m/z = 28), CO_2 (m/z = 44), and H_2 (m/z = 2) signals. These experiments were performed in a Micromeritics model AutoChem II 2920 apparatus with an online quadrupole mass spectrometer (SRS residual gas analyzer). After any necessary pretreatments, samples were exposed to 10% CO – 3% H_2O – He (30 mL min^{-1}). The water content was achieved by passing the 10% CO – He feed through H_2O in a vapor generator that was kept at room temperature. The temperature of the reactor was then ramped linearly to 400 °C (10 °C min^{-1}). In some tests, an isothermal hold was performed after the linear ramp.

2.3.10 Steady-State Kinetics Tests

While TPSR can be used to give the dynamic, unsteady-state performance of a catalyst, light-off and kinetic tests can be used to evaluate the steady-state performance of a material. In these experiments, 0.1 – 0.3 g of the sample was loaded between two beds of quartz wool into a quartz tube reactor. The feed gases, all certified mixtures of He (Airgas), were controlled by mass flow controllers and

mixed prior to entering the reactor. Water was injected by a calibrated syringe pump and vaporized prior to entering the reactor through a heated line. Water was condensed at the reactor exit with an ice water bath. The inlet and outlet gases were analyzed by a SRI 310C gas chromatograph (GC) using a thermal conductivity detector (TCD). In the full reformate gas feed used for kinetic and stability tests, a feed composition of 11% CO – 26% H_2O – 26% H_2 – 7% CO_2 – He (207 mL min^{-1}) was used. During the kinetics experiments, the reactor was operated in differential mode with the total CO conversion kept below 15%.

The rate of CO_2 production was used to calculate the reaction rate:

$$Rate = \frac{N_t^{out} \times CO_2^{out} - N_t^{in} \times CO_2^{in}}{W_{cat}} \; [mol\, g^{-1}\, sec^{-1}]$$

where N_t is the total molar flow rate (mol sec^{-1}) and W_{cat} is the weight of the catalyst used. Since N_t^{out} cannot be monitored continuously, it is calculated from the carbon mass balance:

$$N_t^{out} = N_t^{in} \times \frac{CO_2^{in} + CO^{in}}{CO_2^{out} + CO^{out}}$$

where the N_t^{in} is measured before the reaction and is constant, and the CO and CO_2 concentrations are measured by GC. This rate expression is based on the rate of CO consumption being equal to the rate of CO_2 production. There was no methane production observed during these experiments.

2.4 References

[1] X. Wang, X. Sun, D. Yu, B. Zou, Y. Li, *Advanced Materials* **2003**, 15-18.

[2] L. Kundakovic, M. Flytzani-Stephanopoulos, *Applied Catalysis A: General* **1998**, *171*, 13-29.

[3] a. F. Porta, L. Prati, M. Rossi, S. Coluccia, G. Martra, *Catalysis Today* **2000**, *61*, 165-172; b. S. K. Beaumont, G. Kyriakou, R. M. Lambert, *Journal of the American Chemical Society* **2010**, *132*, 12246-12248.

[4] Q. Fu, Ph.D. Dissertation, Dept. of Chemical & Biological Engineering, Tufts Univerisity, **2004**.

[5] H.-S. Oh, J. H. Yang, C. K. Costello, Y. M. Wang, S. R. Bare, H. H. Kung, M. C. Kung, *Journal of Catalysis* **2002**, *210*, 375-386.

[6] S. Ivanova, C. Petit, V. Pitchon, *Applied Catalysis A: General* **2004**, *267*, 191-201.

[7] T. Takei, I. Okuda, K. K. Bando, T. Akita, M. Haruta, *Chemical Physics Letters* **2010**, *493*, 207-211.

Table 2.1 Precursors and Reagents

Element or Compound	Precursor	Source
La	Lanthanum nitrate hydrate, 99.9%	Sigma
Au	Hydrogen tetrachloroaurate (III) hydrate, 99.99%	Alfa Aesar
NaOH	Sodium hydroxide, 98%	Alfa Aesar
PVP	Polyvinylpirrolidone, MW 8000	Alfa Aesar
$NaBH_4$	Sodium borohydride, 99%	Sigma
$AgNO_3$	Silver nitrate, 99%	Sigma
$(NH_4)_2CO_3$	Ammonium carbonate	Alfa Aesar
CH_3CH_2OH	Ethanol	Sigma

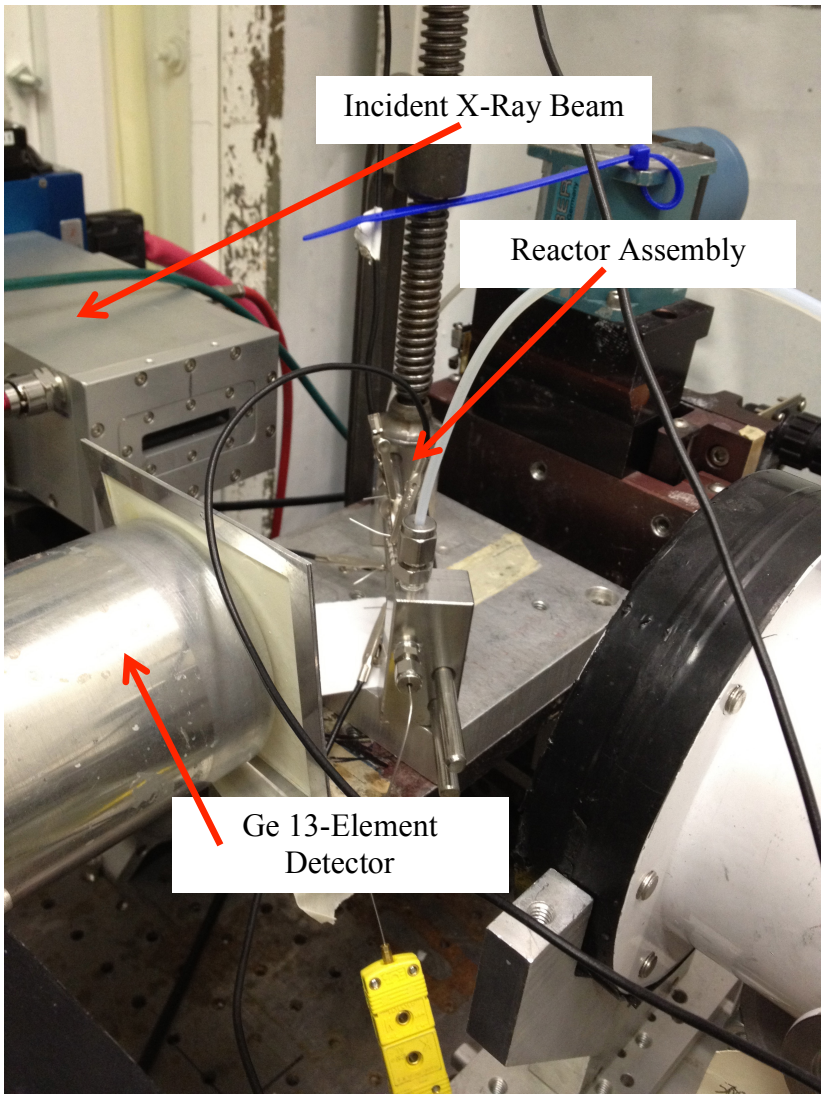

Figure 2.1 XANES Reactor Assembly

Chapter 3. Preparation Effects on Water-Gas Shift Reactivity

3.1 Comparison of Preparation Techniques

The four preparation techniques investigated in this work – colloidal deposition, deposition-precipitation, co-precipitation and anion adsorption – differ by the means in which Au is added to the La_2O_3 support and the type of Au species so deposited. These differences have marked effects on the water-gas shift (WGS) activity of the catalysts, as well as their stability. To first understand the effect of the different preparation techniques, a brief discussion of the La_2O_3 support used is warranted.

3.1.1 La_2O_3 Support Preparation and Properties

3.1.1.1 Calcination Temperature and Specific Surface Area

Lanthanum oxide was prepared by the hydrolysis method because the alternative method (UGC) results in a bulk material that contains carbonates (XRD analysis shows an hexagonal $La_2O_2CO_3$ species) with a low surface area (5 $m^2\ g^{-1}$)[1]. Because reactions take place at the surface of the catalyst, materials with the highest possible specific surface area are desired. In the hydrolysis preparation, the final product is a $La(OH)_3$. These materials calcined at 400 °C show the highest surface area (75 $m^2\ g^{-1}$) (Table 3.1). When Au/La_2O_3 catalysts prepared using this La_2O_3 are tested up to 400 °C, H_2 is evolved that cannot be linked to WGS conversion. This H_2 is, in fact, due to further crystallization of the

bulk La_2O_3 as hydroxyls in the bulk are reduced. Upon calcination at temperatures >400 °C the $La(OH)_3$ is converted to La_2O_3, which is largely amorphous when analyzed by XRD. However, with increasing calcination temperature, a loss in surface area is observed and the structure crystalizes to cubic La_2O_3 (Table 3.1). It should be noted that La_2O_3 calcined at 400 °C has been used as a support previously in our group, but was only tested in WGS conditions up to 350 °C[2].

In order to eliminate any changes in the bulk support during high-temperature isothermal tests, a La_2O_3 that had been calcined at 650 °C in static air was used during this work. Dr. Rui Si from our lab had previously shown[3] that this material was largely amorphous according to XRD analysis. This material has a surface area of ~55 m^2 g^{-1} (Table 3.1).

3.1.1.2 Point of Zero Charge (PZC)

The point of zero charge (PZC) of a metal oxide is the pH of an aqueous suspension of the material at which it carries no net charge (Figure 3.1). A net surface charge can be developed on the surface as exposed hydroxyl groups are protonated at pHs below the PZC (forming $–OH_2^+$) and deprotonated at pHs above the PZC (forming $–O^-$). Because this charge can affect electrostatic interactions in the metal oxide suspension, the PZC is a very important parameter in deposition of charged metal precursors onto metal oxide support surfaces.

The PZC of La_2O_3 was determined in this work to (1) better understand the solution dynamics during Au deposition and (2) determine the most desirable preparation pH during anion adsorption. PZC was measured using a mass titration technique previously reported by Noh, et al.[4] and Park, et al.[5]. In this method a

spear-tip probe is used to measure the pH of an aqueous slurry of La_2O_3. The pH is monitored as La_2O_3 is slowly added to the slurry; as the slurry approaches the "infinite mass/volume ratio," the pH plateaus at the PZC. The La_2O_3 prepared in this work (hydrolysis La_2O_3 then calcined at 650 °C) had an PZC of 10, which is in good agreement with results reported elsewhere.

3.1.2 Differences in Au Deposition Techniques

3.1.2.1 Colloidal Deposition

The preparation of colloidal Au particles has been known since Faraday's time. Michael Faraday first synthesized Au colloids to investigate their optical properties[6]. Since then, they have been studied extensively for applications both in catalysis and other fields, *e.g.* sensing, immunology, etc. Turkevich performed much of the early work in colloidal Au chemistry, particularly in investigating the role different capping and reducing agents play in determining the size of the particles obtained[7]. During the formation of the Au colloids it is necessary to include a protective "capping agent" that prevents particles from agglomerating to a significant extent. The preparation used here has been adapted from the work of Porta, et al. wherein polyvinylpirrolidone (PVP) is used as a capping agent and sodium borohydride ($NaBH_4$) is used to reduce the Au(III) salt to Au(0)[8]. PVP contains a polar amide group in its monomer unit that interacts favorably with the Au(III) salt and is able to stabilize Au particle seeds against agglomeration during reduction and colloid formation (Figure 3.2)[9]. By varying the PVP:Au weight ratio it is possible to produce Au particles of selected average particle sizes. The

ratio chosen here (6:1) was chosen to produce particles of approximately 3 – 5 nm in diameter (Figure 3.3).

A significant excess of $NaBH_4$ is added to the preparation mixture to ensure that all of the Au(III) salt is reduced. For this reason, it is expected that only Au(0) should be present in the catalyst. XPS analysis of this material confirms that only Au(0) is present without any Au(I) or Au(III) visible (Figure 3.4). Operating under the hypothesis that ionic Au is the active species in WGS catalysis[10], Au/La_2O_3 (C) serves as a control material for WGS activity.

The 1% Au/La_2O_3 (C) was first calcined in static air at 280 °C for 4 hours with a heating rate of 2 °C min^{-1}. The material was then tested in WGS-TPSR mode (0.2 g s mL^{-1}, 10% CO – 3% H_2O – He) up to 400 °C at a heating rate of 10 °C min^{-1}. During the first cycle of TPSR a significant amount of CO_2 and H_2 were evolved without the consumption of CO, indicating the decomposition of PVP still on the surface after the calcination procedure. This material was held isothermally at 400 °C for 4 h and the conversion stabilized at 15% CO conversion (Figure 3.5a). During a second cycle of WGS-TPSR, the light-off temperature of the material was established to be 250 °C with a CO conversion of approximately 20% at 400 °C (Figure 3.5b). At the contact time used here, the addition of Au to La_2O_3 showed little catalytic improvement when compared to bare La_2O_3 indicating that no additional active sites – sites active for low-temperature WGS, in particular – had been introduced when metallic Au particles were added.

3.1.2.2 Co-Precipitation

Co-precipitation (CP) was investigated in this work in the hopes of applying a highly active CO oxidation catalyst developed by Takei, et al. to the low-temperature WGS reaction[11]. In their work, Takei, et al. prepared $Au/La(OH)_3$ in various ratios to determine the most active formulation for CO oxidation. While CO oxidation and the WGS reaction likely operate through different mechanisms, the $Au/La(OH)_3$ materials had characteristics one normally looks for in a WGS catalyst. Most notably, the authors claimed that upon calcination at 150 °C, they were able to bring Au atoms to the surface, which form small Au clusters "decorated" with –OH groups. Additionally, these Au clusters, or at least the Au at their periphery, are cationic in nature, with the charge balance likely obtained by nearby oxygen groups. However, upon exposure to CO at temperatures as low as 100 °C, the surface Au is reduced.

Recent computational studies by Jiang, et al. have suggested that Au clusters (specifically on the order of 10 atoms) interact quite favorably with hydroxide-rich surfaces[12]. DFT calculations show that Au clusters covalently bond with surface –OH forming a stable Au-OH bond with the surface. Interestingly, while the Au atoms directly bonded to the surface display slightly positive ionic character, if the cluster is small enough (~10 atoms), it will carry a net negative charge on the whole.

Between a hydroxyl-rich surface and ionic Au, this $Au/La(OH)_3$ would seem a valid candidate for screening the WGS reaction[2, 13]. However, it is apparent that great care must be taken in order to preserve the desired surface

species, lest they be reduced at high temperatures. The Au/$La(OH)_3$ (CP) with a design loading of 5 at% Au, was tested for WGS activity in TPSR mode (Figure 3.6). It is apparent through the first and second cycles of TPSR that there is significant reduction of the $La(OH)_3$ support during the temperature ramp at temperatures >150 °C. The CO_2 and H_2 do not coincide, especially at low temperatures. According to the work of Takei, et al., the ionic Au species decorated with hydroxyls are only stable to ~100 °C. Given that this Au/$La(OH)_3$ does not seem to light off until 175 – 200 °C, it is unclear which species are present/active during the WGS reaction. At these elevated temperatures the underlying $La(OH)_3$ support also is reduced to La_2O_3 or $LaO(OH)_x$.

3.1.2.3 Deposition-Precipitation

Deposition-precipitation (DP) is a technique that was first applied to Au catalysts by Haruta et al.[14], and is used quite frequently to prepare Au catalysts for the WGS reaction[15]. In our group, DP has been used to successfully prepare Au/CeO_2 catalysts for the WGS reaction with Au particles with diameters <5 nm[10, 13a, 13b]. During DP, the $[AuCl_4]^-$ complex is precipitated onto the support as a $[Au(OH)_xCl_{4-x}]^-$ species. This speciation is driven by the pH of the solution, which is controlled by the addition of a weak base, $(NH_4)_2CO_3$ in this work (for details on Au complex speciation see Chapter 4). Ammonium carbonate is used here because (1) it does not introduce alkali metals that can further complicate the Au catalysis and (2) it drastically reduces the amount of Au remaining in solution (compared to Na_2CO_3, for example)[13c, 13d]. Subsequent filtration and washes with hot deionized H_2O are used to remove residual chloride ions still present. While

washes with hot aqueous NH_3 can be used to remove chloride more aggressively, this has been avoided because Au can form explosive compounds (fulminating gold) when it interacts with concentrated NH_3[15]. However, fulminating Au is formed, most likely, only when Au is present in solution[16]. With this safety caution in mind, Au/La_2O_3 that had been calcined – and was thus unlikely to lose Au to solution – was washed with concentrated NH_3 in a separate study to investigate whether any residual Cl^- were still present. After neutralizing the NH_3 wash solution, it was tested with $AgNO_3$; the lack of white precipitate indicated that Cl^- were absent. This visual inspection is accurate to at least 600 ppm because this is the concentration of Cl^- in the preparation after addition of the Au precursor when addition of $AgNO_3$ addition clearly shows the presence of a white precipitate, which indicates that at least some Cl^- has not been adsorbed onto the sample. After the hot H_2O washes calcination in O_2 is performed to decompose the Au-OH species into oxidic and metallic Au.

DP has previously been used to prepare highly ionic Au/La_2O_3 materials[17]. In these works, the atomically dispersed Au was prepared by keeping the total Au loading extremely low (<0.2 at%). There is no mention of using these material as catalysts for the WGS reaction, but the presence of highly ionic, thermally stable Au shows promise.

During this preparation, it is routinely observed that Au is left in the solution after the first filtration. The presence of Au is confirmed by the color change from transparent to deep purple with the addition of $NaBH_4$ to the supernatant of the sample after it had aged 1 h during the preparation.

Additionally, ICP tests performed on the preparation wash solutions indicate that Au is in the wash even after the second hot H_2O wash. The pH of the preparation is maintained at 8.5, which is below the PZC of La_2O_3 suggesting that the surface should carry a net positive charge and therefore a favorable electrostatic interaction between the Au complex and the La_2O_3 should exist. However, as noted by several groups, there often exists a maximum achievable Au loading as a function of pH during DP preparations[15, 18]. Additionally, the presence of the weak base seems to negatively affect the Au species, as it leads to the formation of particles (1-2 nm) on the La_2O_3 support.

In addition to the ineffectual Au loading, leaching of these Au/La_2O_3 (DP) materials with NaCN removes nearly 70% of the Au, suggesting that the Au does not interact strongly with the support surface (Table 3.2). The leaching procedure has been adapted from the industrial process used to extract Au from mineral ores[19]; Fu et al., first showed its efficacy in isolating Au cations in cyanide-leached Au/CeO_2[10]. During this procedure, the catalyst was treated with an excess of 2 wt% NaCN in an aqueous NaOH solution (pH > 12). Great care must be taken when working with NaCN because if the pH of the solution drops below 8-9, poisonous HCN gas may be formed. This procedure operates under the principle that strongly bound, ionic Au species are unable to be leached from the surface, while weakly bound, metallic Au species, and oxidized clusters, are easily solvated to cyanide complexes of Au. The reactions for this cyanide solvation are:

$$4Au + 8CN^- + 2H_2O + O_2 \leftrightarrow 4[Au(CN)_2]^- + 4OH^-$$

$$Au^{+} + 2CN^{-} \leftrightarrow [Au(CN)_2]^{-}$$

$$Au^{3+} + 3CN^{-} + 2OH^{-} \leftrightarrow [Au(CN)_2]^{-} + H_2O + CNO^{-}$$

The equilibrium constant for the formation of the $[Au(CN)_2]^{-}$ is 2 x 10^{38}[20]. Gold bound to the surface as $Au(OH)_x$ species are non-leachable because the Au-OH bond is much stronger than the Au-CN bond:

$$Au + 3OH^{-} \leftrightarrow Au(OH)_3$$

The equilibrium constant for the formation of $Au(OH)_3$ is 1.8 x 10^{45}[20], which is significantly higher than that of the $[Au(CN)_2]^{-}$. Upon leaching of the Au/La_2O_3 (DP) materials, a significant fraction of the Au is removed from the support (Table 3.2), indicating that a majority of the Au does not interact strongly with the support. Lanthanum was not found in the leachate.

With this in mind, Au/La_2O_3 (DP) was screened for WGS activity by WGS TPSR. Both the parent 0.9% Au/La_2O_3 (DP,P) and the leached material 0.3% Au/La_2O_3 (DP,L) were tested in cyclic and isothermal holds (Figures 3.7, 3.8). The parent and leached materials did not exhibit the same activity in WGS TPSR mode; the parent material reached approximately 85% conversion of the H_2O (the limiting reactant) at 400 °C with a light off temperature of 175 °C. Additionally, the parent material deactivates from the first cycle to the second cycle and then shows stable performance from the second and third cycles (Figure 3.7). This deactivation might be due to the loss of active sites through sintering – further evidence that the Au deposited during DP is not strongly bound to the surface. The leached material, on the other hand, reaches only 30% H_2O

conversion at 400 °C and shows rapid deactivation during an isothermal hold at 400 °C (Figure 3.8).

An interesting phenomenon was observed in working with the Au/La_2O_3. While the fresh material (simply calcined in static air at 250 °C for 2 h) exhibited moderate activity, a subsequent He treatment at 400 °C for 1 h followed by WGS-TPSR produced a catalyst that reached 100% H_2O conversion at 350 °C (Figure 3.9) However, a similar treatment with O_2 at 400 °C for 1 h significantly deactivated the material with only 65% H_2O conversion at 400 °C achieved (Figure 3.9). The mass spectra signals for both pretreatments are presented in Figure 3.10 and seem to indicate the decomposition of hydroxyl groups during the He pretreatment and loss of H_2O from the underlying support in the O_2 pretreatment. These results suggest a more complex picture of the surface, particularly how Au, La and O are interacting at various temperatures. This phenomenon, and a similar one with the anion adsorption Au/La_2O_3, will be further discussed in Chapter 4.

In her thesis work, Yanping Zhai demonstrated that Au/La_2O_3 prepared by a DP method is a moderately active WGS catalyst[2]. She speculated that this activity was due to the presence of Au-O-OH-La species on the surface, making note that the La_2O_3 support is in fact more accurately described as $LaO(OH)_x$. Her 5% Au/La_2O_3 showed comparable activity to the Au/La_2O_3 (DP) presented here when the latter is scaled to account for the differences in Au loading, and surface areas. The most important feature to take from the DP work presented here and the work performed by Zhai[2] is that addition of Au to La_2O_3 dramatically

improved the reducibility of its –OH groups, a phenomenon previously observed in the most active Au/CeO_2 and Au/FeOx catalysts[13a, 13b]. Zhai concluded that a preparation method in which Au can be better dispersed and stabilized on La_2O_3 might yield a more active material; for this reason anion adsorption was investigated in this thesis work (Chapter 4).

3.2 Summary

Lanthanum oxide prepared via a hydrolysis technique and calcined at 650 °C was chosen as the support for this work because it struck a favorable balance between surface area and thermal stability. Subsequently, three different schemes to prepare Au/La_2O_3 materials have been presented with a particular focus paid to how the preparation chemistry affects the final product. Materials prepared by colloidal deposition demonstrate that large metallic Au particles show almost no activity for the WGS reaction, with the negligible activity attributable to the very small fraction of Au sites at the periphery of large Au particles that interact with the underlying support. On the other hand, co-precipitation provides a very interesting route to prepare a Au catalysts in an hydroxide-rich environment. However, this material sits on a highly unstable $La(OH)_3$ support and shows very little WGS activity in the low temperature range in which $La(OH)_3$ is thermally stable. The third approach, deposition-precipitation, is a tried-and-true method used to prepare supported Au catalysts. Here it is shown that Au/La_2O_3 (DP) is a material with promising application. However, a means by which the Au dispersion (and Au-OH interaction) can be improved is sought. This is addressed in the next chapter of this thesis.

3.3 References

[1] L. Kundakovic, M. Flytzani-Stephanopoulos, *Applied Catalysis A: General* **1998**, *171*, 13-29.

[2] Y. Zhai, Ph.D. Dissertation, Dept. of Chemical & Biological Engineering, Tufts University, **2011**.

[3] R. Si, Dept. of Chemical & Biological Engineering, Tufts University, **2007**, unpublished work.

[4] J. Noh, J. Schwarz, *Journal of Colloid and Interface Science* **1989**, *130*, 157-164.

[5] J. Park, J. R. Regalbuto, *Journal of Colloid and Interface Science* **1995**, *175*, 239-252.

[6] M. Faraday, *Philosophical Transactions of the Royal Society* **1857**, *147*, 145.

[7] a. J. Turkevich, G. Garton, P. C. Stevenson, *Journal of Colloid Science* **1954**, *9*, S26-S35; b. J. Turkevich, C. Stevenson, J. Hillier, *Journal of Physical Chemistry* **1953**, *57*, 670-673; c. J. Turkevich, P. C. Stevenson, J. Hillier, *Discussions of the Faraday Society* **1951**, *11*, 55.

[8] F. Porta, L. Prati, M. Rossi, S. Coluccia, G. Martra, *Catalysis Today* **2000**, *61*, 165-172.

[9] B. Santiago González, M. J. Rodríguez, C. Blanco, J. Rivas, M. A. López-Quintela, J. M. G. Martinho, *Nano letters* **2010**, *10*, 4217-4221.

[10] Q. Fu, H. Saltsburg, M. Flytzani-Stephanopoulos, *Science* **2003**, *301*, 935-938.

[11] T. Takei, I. Okuda, K. K. Bando, T. Akita, M. Haruta, *Chemical Physics Letters* **2010**, *493*, 207-211.

[12] D.-E. Jiang, S. H. Overbury, S. Dai, *The Journal of Physical Chemistry Letters* **2011**, *2*, 1211-1215.

[13] a. Q. Fu, Ph.D. Dissertation, Dept. of Chemical & Biological Engineering, Tufts Univerisity, **2004**; b. W. Deng, Ph.D. Disseration, Dept. of Chemical & Biological Engineering, Tufts University, **2008**; c. A. Weber, M.S. Thesis, Dept. of Chemical & Biological Engineering, Tufts University,

1999; d. Q. Fu, A. Weber, M. Flytzani-Stephanopoulos, *Catalysis Letters* **2001**, *77*, 87-95.

[14] S. Tsubota, M. Haruta, T. Kobayashi, A. Ueda, Y. Nakahara, *Preparation of Highly Dispersed Gold on Titania and Magnesium Oxide*, Elsevier, Louvain-la-Neuve, **1991**.

[15] *Catalysis by Gold, Vol. 6*, Imperial College Press, London, **2006**.

[16] S. Ivanova, V. Pitchon, Y. Zimmermann, C. Petit, *Applied Catalysis A: General* **2006**, *298*, 57-64.

[17] a. A. Goguet, M. Ace, Y. Saih, J. Sa, J. Kavanagh, C. Hardacre, *Chemical Communications* **2009**, 4889-4891; b. J. Sá, M. Ace, J. J. Delgado, A. Goguet, C. Hardacre, K. Morgan, *ChemCatChem* **2011**, *3*, 394-398.

[18] *Catalyst Preparation*, CRC Press, Boca Raton, FL, **2007**.

[19] N. Hedley, H. Tabachnik, (Ed.: A. C. Company), Wayne, **1968**.

[20] J. A. Dean, *Lange's Handbook of Chemistry*, 15 ed., McGraw-Hill, Columbus, **1998**.

Table 3.1 Calcination Temperature and Surface Area

Preparation	Calcination Temperature [°C] (in static air)	S_{BET} [m^2 g^{-1}]
La_2O_3 (UGC)	650	5
La_2O_3 / $LaO(OH)_x$ (hydrolysis)	400	75
	650	55
	800	25

Table 3.2 Au Content in Au/La_2O_3 (DP) Before (P) and After (L) Leaching with 2 wt% NaCN in aqueous NaOH (pH > 12)

Sample	Design Loading (at. %)	Actual Loading (at. %)
Au/La_2O_3 (DP,P)	1.0	0.9
Au/La_2O_3 (DP,L)		0.3

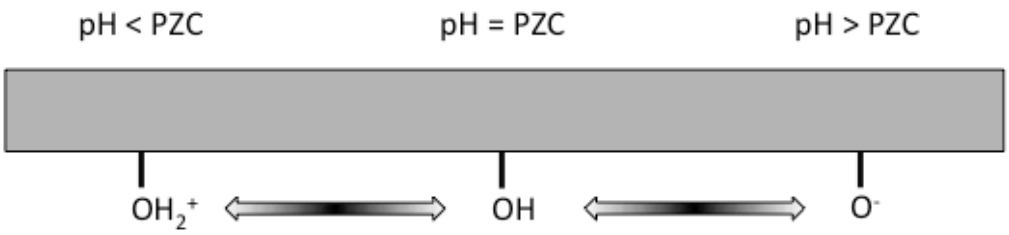

Figure 3.1 Surface Protonation-Deprotonation as a Function of pH

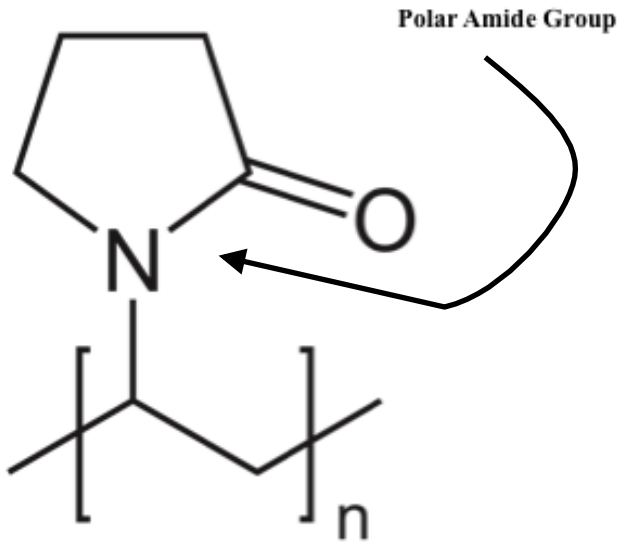

Figure 3.2 Polyvinylpirrolidone (PVP) Monomer

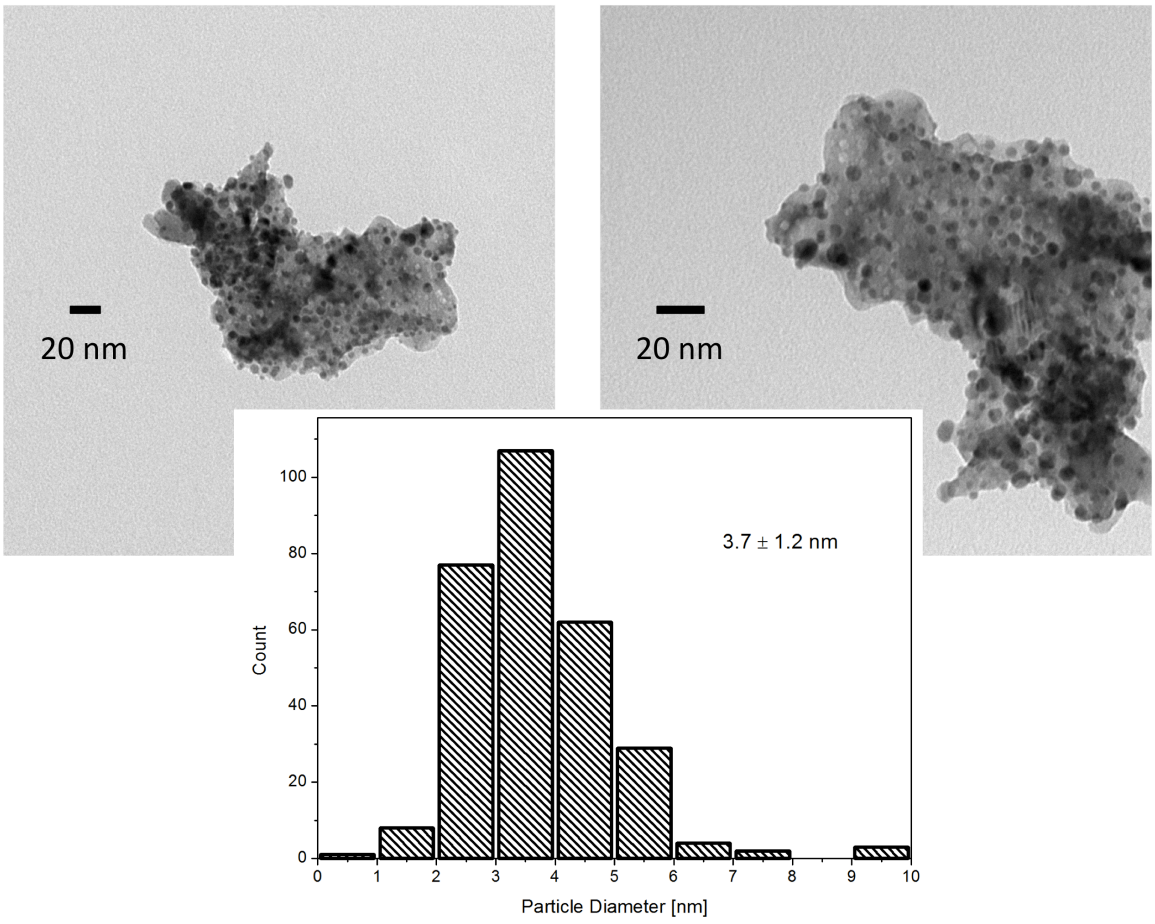

Figure 3.3 Transmission Electron Micrograph (TEM) Image of 1% Au/La_2O_3 (C)

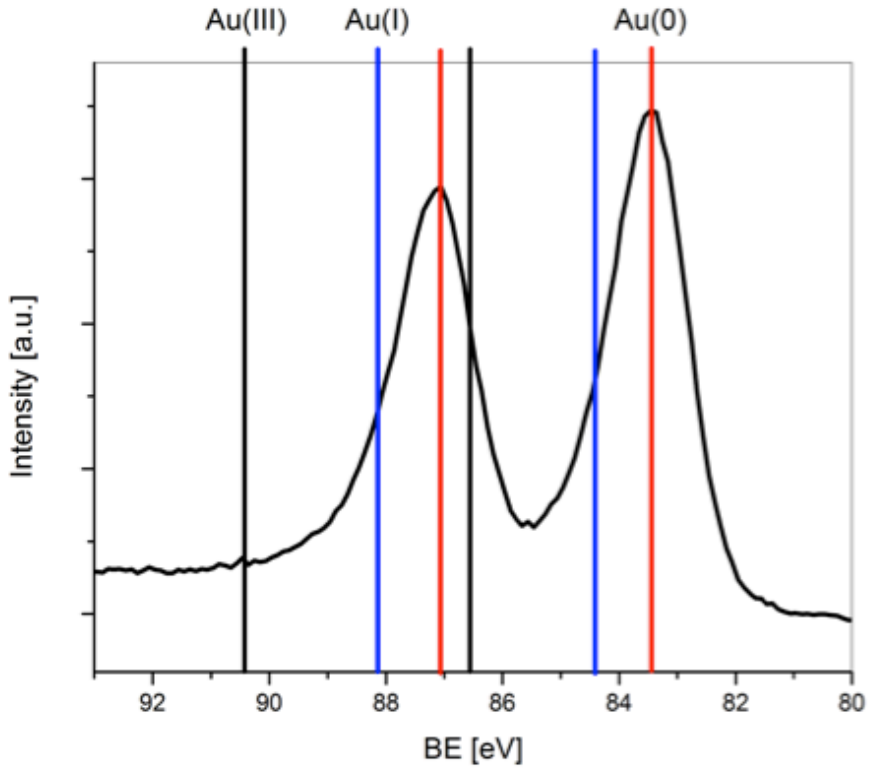

Figure 3.4 X-Ray Photoelectron Spectrum (XPS) of Au/La_2O_3 (C)

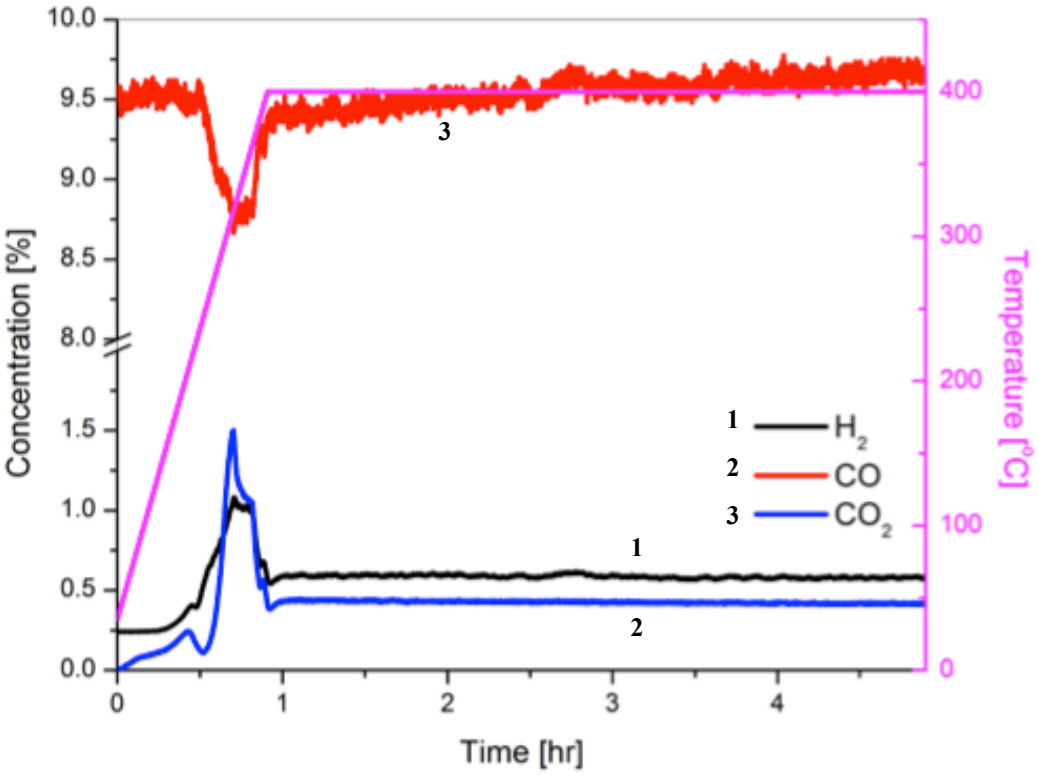

Figure 3.5a WGS TPSR and Isothermal Hold Performance of 1% Au/La_2O_3 (C)

10% CO – 3% H_2O – He, contact time 0.2 g s mL^{-1}

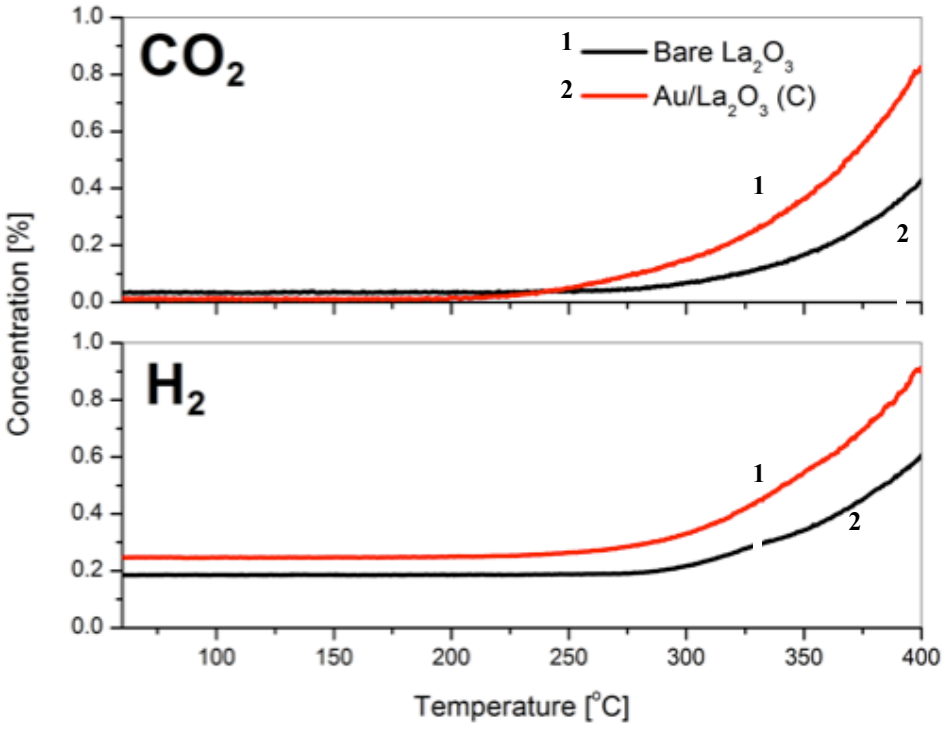

Figure 3.5b WGS TPSR Second Cycle Performance of 1% Au/La_2O_3 (C)

10% CO – 3% H_2O – He, contact time 0.2 g s mL^{-1}

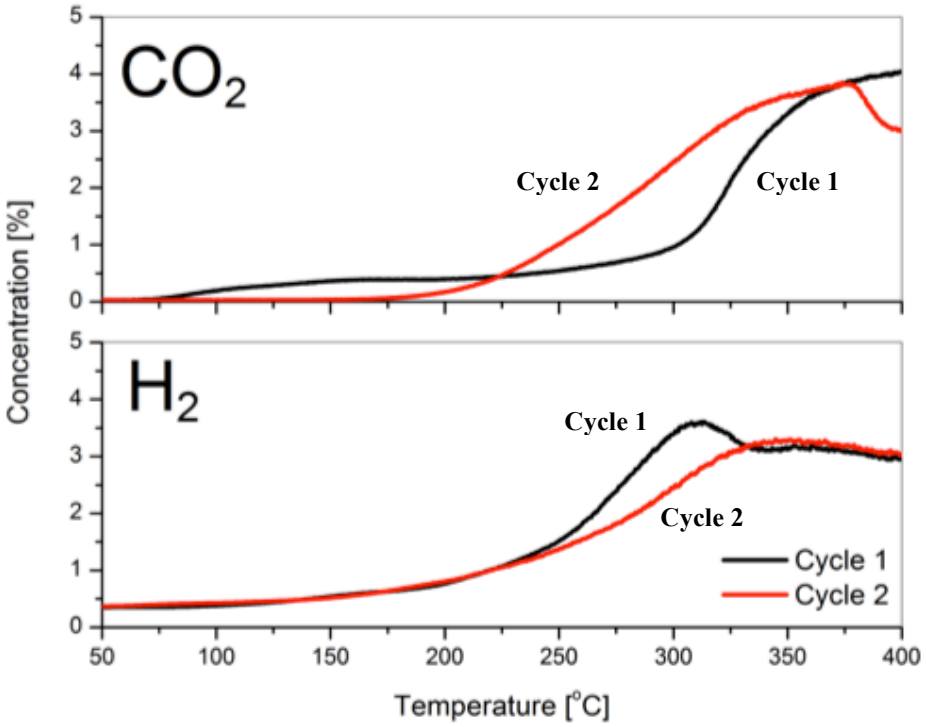

Figure 3.6 Cyclic WGS TPSR Performance of 5% $Au/La(OH)_3$ (CP)

10% CO – 3% H_2O – He, contact time 0.2 g s mL^{-1}

Sample cooled to room temperature in He between cycles

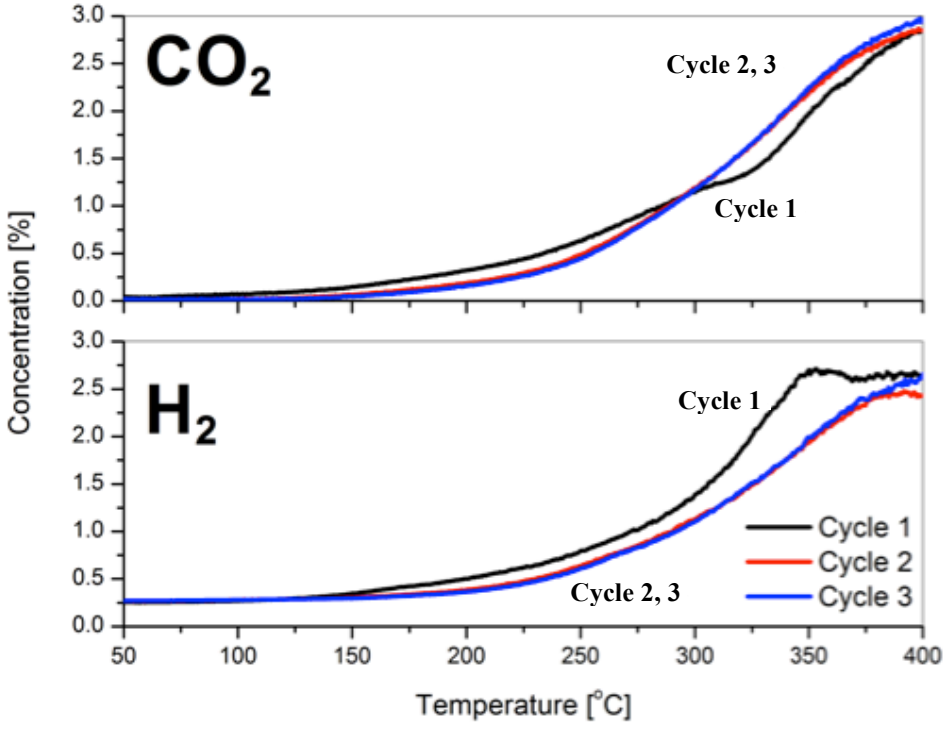

Figure 3.7 Cyclic WGS TPSR Performance of 0.9% Au/La_2O_3 (DP,P)

10% CO – 3% H_2O – He, contact time 0.2 g s mL^{-1}

Sample cooled to room temperature in He between cycles

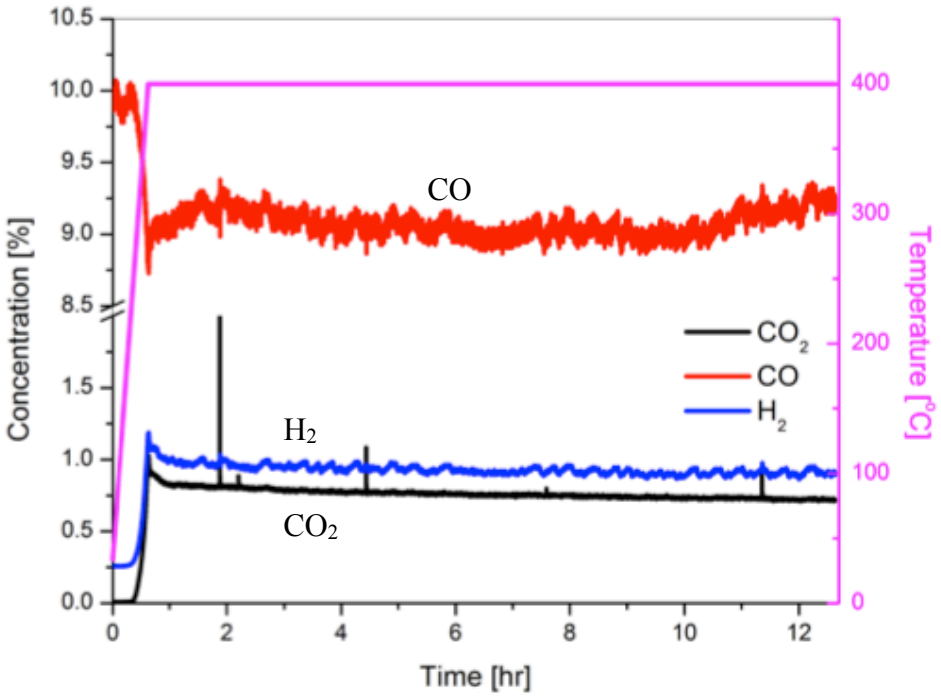

Figure 3.8 WGS TPSR and Isothermal Hold

Performance of 0.3% Au/La_2O_3 (DP,L)

10% CO – 3% H_2O – He, contact time 0.2 g s mL^{-1}

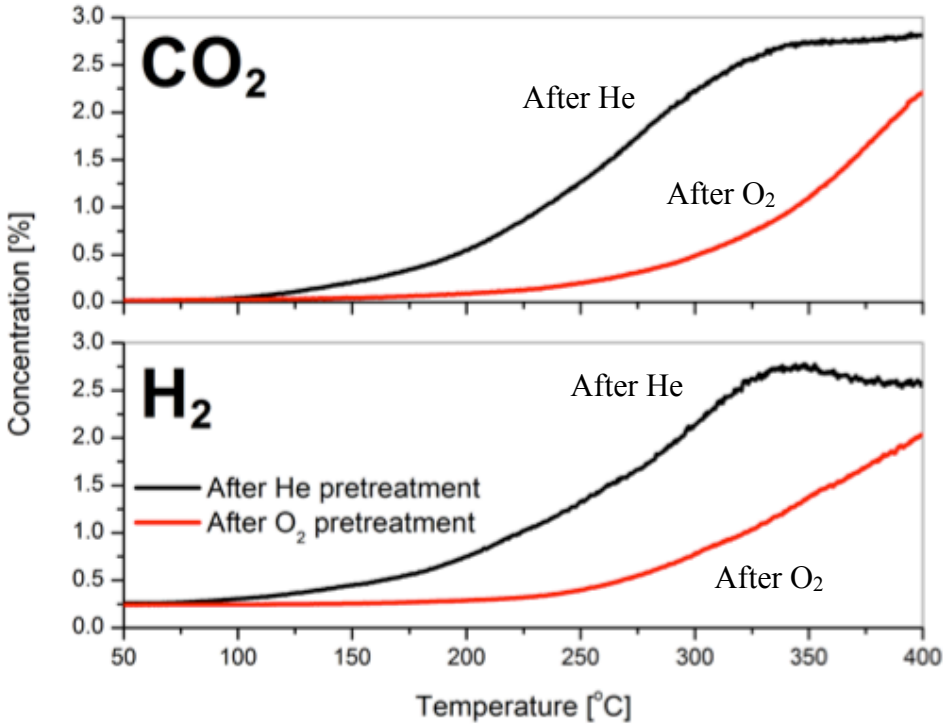

Figure 3.9 He and O_2 Pretreatment Effects on WGS TPSR Activity of 0.9% Au/La_2O_3 (DP,P)

Pretreatments: 30 mL min^{-1} (He or 20% O_2 – He), room temperature to 400 °C for 1 h with a heating rate of 10 °C min^{-1}

WGS TPSR: 10% CO – 3% H_2O – He, contact time 0.2 g s mL^{-1}

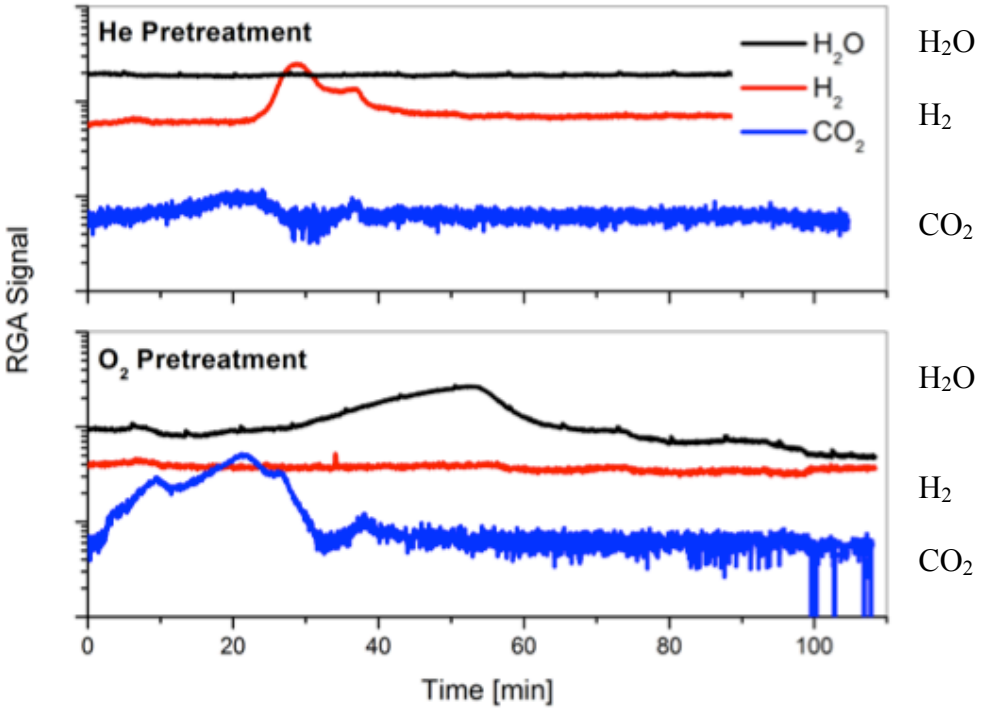

Figure 3.10 Mass Spectra of He and O_2 Pretreatments of

0.9% Au/La_2O_3 (DP,P)

30 mL min^{-1} (He or 20% O_2 – He), room temperature to 400 °C for 1 h with a

heating rate of 10 °C min^{-1}

Chapter 4. Anion Adsorption

4.1 Au Precursor Speciation and Adsorption onto La_2O_3

The speciation of the $[AuCl_4]^-$ precursor to the $[Au(OH)_4]^-$ complex is of key importance in anion adsorption (AA). It is well established that residual Cl^-, even in ppm levels, can lead to significant deactivation of Au catalysts[1]. This deactivation is due to sintering of the supported Au particles via Au-Cl "bridges" that promote particle agglomeration. It is advantageous, therefore, to use preparation techniques that eliminate Cl from the final catalyst. As mentioned in Chapter 3, different post-preparation washes can be used to remove residual Cl. Several parametric studies have investigated the use of hot H_2O and various basic (NaOH, NH_3, etc.) wash solutions[1b, 2]. Alternatively, Cl-free Au precursors can be used. Gates, et al., have used an organic Au precursor $Au(CH_3)_2(acac)$ adsorbed onto La_2O_3 from a n-pentane solution to investigate atomically dispersed Au/La_2O_3 for CO oxidation[3]. However, this Au precursor is an order of magnitude more expensive than conventional $HAuCl_4$ precursors and requires handling in anoxic environments. Anion adsorption has been used in other Au/metal oxide systems in the past decade as a means to prepare Cl-free catalysts for both the CO oxidation and the WGS reactions[2b, 2d, 4].

During AA, the speciation to the fully hydroxylated complex is driven by the prevailing solution conditions during the preparation. It is well understood that pH, temperature and salt concentration greatly affect the equilibrium established between the different $[Au(OH)_xCl_{4-x}]^-$ species in solution[1b]. The $[AuCl_4]^-$ is

converted to $[Au(OH)_4]^-$ by the stepwise hydrolysis of the four Au-Cl bonds with H_2O, which quickly dissociates to form a hydroxylated complex[4a, 5]. Low concentrations of the $[AuCl_4]^-$ favor speciation to the hydroxylated species. Additionally, higher pHs are required to speciate to the fully hydroxylated complex. Increasing temperature will also favor speciation. There is some disagreement in the literature about which $[Au(OH)_xCl_{4-x}]^-$ species are obtained at a given pH and concentration, but it is generally accepted that when the $[AuCl_4]^-$ is on the order of 1 x 10^{-3} M, the fully hydroxylated $[Au(OH)_4]^-$ is present at pHs above 7[1b] (Table 4.1).

Peck, et al., have shown that this speciation can be measured by UV-Vis spectroscopy[5]. Bonds between Au and Cl absorb light in the UV range (approximately 250 – 350 nm) due to the ligand-to-metal charge transfer (LMCT). This phenomenon is the absorption of energy as electrons are transferred from the π orbitals of Cl to the strongly antibonding σ^* orbitals of Au. However, when Cl^- ligands are replaced with OH^- groups, this LMCT is no longer possible and a decrease in absorption, along with a blue shift, is observed. Eventually, as the complex is fully speciated to $[Au(OH)_4]^-$, an absorption peak is no longer visible. It should also be noted that absorption peaks in the visible range (approximately 500 – 600 nm) are assigned to Au(0) in solution[6].

The concentration of the Au precursor used in this work (Chapter 2) is approximately 4 x 10^{-4} M. A solution of this concentration was prepared to investigate the speciation process by UV-Vis spectroscopy. The fresh Au solution (pH = 3.4) was first tested. The initial spectrum shows a clear absorption peak at

295 nm with a blue shift and decrease in the absorption intensity as the solution was heated to 70 °C; no peak in the 500 – 600 nm range was seen (Figure 4.1). This result indicates that at this low pH, an equilibrium between different $[Au(OH)_xCl_{4-x}]^-$ species is established. In order to investigate the equilibrium established at higher pHs (pHs closer to the pH of the preparation solution), a separate solution of equal concentration was prepared and then neutralized to pH = 7 with NaOH. Analysis of this solution by UV-Vis showed that even at room temperature the Au complex had completely speciated to the $[Au(OH)_4]^-$; additionally, raising the temperature to 70 °C did not change the distribution of species present (Figure 4.2).

With an understanding of how the Au precursor speciates under preparation conditions, the overall AA preparation can be put into perspective. When the La_2O_3 is first placed in deionized H_2O the pH of the slurry as measured by a pH probe is 9.5 (at this point the surface is approximately 75% $-OH_2^+$ and 25% -OH). As the Au precursor solution is added dropwise (approximately 1 mL min^{-1}), the pH of the mixture drops to 7 – 7.5 within the first minute (at this point the surface is >99% $-OH_2^+$). As the mixture is aged for 1 h the pH is seen to rise to 7.5 – 8 and then remain stable (Figure 4.3). The pH plateau can be used as an indicator that an equilibrium has been reached between the species adsorbed on the surface and the species remaining in solution. As shown in Figures 4.1 and 4.2, the conditions of the Au addition favor the complete speciation of the Au precursor to the fully hydroxylated species. This is the species believed to be on

the surface at the end of the aging process. Further evidence of this hypothesis will be presented shortly.

After the aging, the material is vacuum filtered. The filtrate was collected and tested separately with $NaBH_4$ and $AgNO_3$. The $NaBH_4$ test showed that no Au was present in solution, as was further confirmed by ICP. Complete adsorption of Au on the surface is routinely observed and the design loading is consistently the loading achieved when using AA (Table 4.2). Additionally, the $AgNO_3$ test showed the presence of Cl^- in the filtrate. Washes with room temperature H_2O were then performed and when tested with $NaBH_4$ and $AgNO_3$ the wash filtrates were negative for both Au and Cl^-. To further investigate whether residual Cl^- might have remained on the surface the samples were washed with hot H_2O and hot NH_3 in isolated tests. When these wash solutions were tested with $AgNO_3$ Cl^- ions were not detected. This indicates that the level of Cl^- is at least below the level of visual detection (~600 ppm). As a further control test, bare La_2O_3 was slurried with NaCl at a concentration equivalent to that during preparation conditions (1.8 mM). When this material was washed in a similar manner as above, Cl^- was only detected after the first room temperature wash, again indicating that Cl^- had not adsorbed to the surface. Additionally, a chloride ion selective electrode (Cole-Parmer) was used to measure the Cl^- concentration in the filtrate solution; the amount detected was consistent with the conclusion that no Cl^- was adsorbed onto the La_2O_3 surface (*i.e.* the Cl^- ion balance was closed). The absorption of Cl on La_2O_3 has only been observed at high temperatures (260 – 950 °C) from the gas phase when La_2O_3 acts as a sorbent[7].

When 1% Au/La_2O_3 (AA,P) was leached with NaCN (see Chapter 3), the resulting material was found to contain 0.7 at% Au. This result suggests two features of this material in its fresh state (i.e. after calcination in flowing 20% O_2 – He at 250 °C for 2 h, 2 °C min^{-1}). Firstly, the Au is possibly atomically dispersed and therefore interacting strongly with the La_2O_3. As discussed by Qi Fu in her thesis work, strongly bound Au species cannot be leached with NaCN[8]. Secondly, the Au still bound to hydroxyl groups, $Au(OH)_3$, cannot be leached with NaCN[9].

Gold particles are not visible in the 1% Au/La_2O_3 (AA,P) when imaged by TEM suggesting that the Au species are highly dispersed (Figure 4.4). Pulsed CO chemisorption was tried as a means to estimate the Au dispersion[10] but results were inconsistent and therefore unreliable. XPS results indicate that the Au is oxidized in the fresh state comprising a mixture of Au(III) (20%) and Au(I) (80%) (Figure 4.5).

4.2 Performance of 1% Au/La_2O_3 (AA,P) and CO_2 Adsorption and Activation

Different Au loadings (1%, 3%, 5%) of Au/La_2O_3 (AA,P) were initially investigated in this work. As was expected, with higher Au loadings the performance of the Au/La_2O_3 was improved in WGS-TPSR mode (Table 4.2). The higher Au loading provided a higher initial content of ionic Au that was able to participate in the WGS reaction. However, upon leaching these materials, only 1% Au remained on the surface. Additionally, in cyclic experiments, the materials with a Au loading >1% showed a marked deactivation. The 1% Au/La_2O_3 (AA,P)

on the other hand, as will be shown below, retained its Au loading after NaCN leaching and was stable in cyclic experiments. For this reason, the 1% Au loading was used.

WGS-TPSR studies were used to investigate the catalytic performance of the fresh 1% Au/La_2O_3 (AA,P). Cyclic tests showed that during the first cycle the H_2 evolves stoichiometrically, *i.e.* for complete conversion of CO by WGS, as CO is consumed; however, no CO_2 is evolved (Figure 4.6). During the second cycle both the CO_2 and H_2 are evolved in a stoichiometric manner with CO consumption. Hence, it appears that the CO_2 was completely adsorbed on the surface during the first cycle.

In order to confirm that the CO_2 was adsorbed onto the surface, a temperature-programmed desorption (TPD) was performed on the 1% Au/La_2O_3 (AA,P) after reaction (Figure 4.7). The TPD was performed by ramping the temperature of the sample from room temperature to 400 °C at 10 °C min^{-1} while flowing He over it at 30 mL min^{-1}; the temperature was held constant at 400 °C to allow the desporption peak to resolve fully. By comparing the amount of CO_2 adsorbed during the first cycle to the amount desorbed during TPD, it is found that approximately 30% of the CO_2 desorbed during TPD, with the remaining CO_2 likely bound very strongly up to 400 °C.

It is well known that La_2O_3 adsorbs CO_2 quite readily, even at room temperature, to form surface hydroxycarbonate species ($La_2(OH)_4CO_3$) when exposed to air, which can then be decomposed to form surface $La_2O_2CO_3$ at 500 °C[11]. The carbonate species then can be decomposed to La_2O_3 when heated

in excess of 600 °C. The bulk carbonate is formed very rapidly in a CO_2 atmosphere at a ~800 °C[12]. Therefore, under the conditions used here, it would be expected that the CO_2 produced during WGS-TPSR would adsorb onto the underlying La_2O_3 support and form the hydroxycarbonate.

To investigate the extent of this carbonation, a CO_2 saturation procedure was run wherein the bare La_2O_3 support was exposed to a flow of 10% CO_2 – He (30 mL min^{-1}) while the temperature was ramped at 10 °C min^{-1} to 400 °C and held constant for 1 hour, followed by a TPD in He (Figure 4.8). During the saturation (Figure 4.8a), the CO_2 adsorption began at ~250 °C with a total adsorption of 830 μmol CO_2 g^{-1}. During the TPD, the CO_2 eluted at ~250 °C with a total amount of 270 μmol CO_2 g^{-1} (Figure 4.8b). The amount of CO_2 adsorbed onto and desorbed from the 1% Au/La_2O_3 (AA,P) was 760 μmol CO_2 g^{-1} and 210 μmol CO_2 g^{-1}, respectively. As a very rough approximation of the surface coverage, it can be assumed that 5% of the mass of the support oxide is on the surface when the surface area is 55 m^2 g^{-1} (Table 3.1) and the particles are approximately 20 nm in diameter. As such, further assuming a rough 1:2 La to O ratio, it can be calculated that, with a 1:1 or 1:2 CO_2 to La binding stoichiometry, that the monolayer coverage would be approximately between 300 to 600 μmol CO_2 g^{-1}. A more accurate estimation requires detailed crystallographic data. In summary, though, it would appear that the CO_2 adsorbed is of order of a monolayer.

From these values it seems that the carbonation involves only the surface layer of the material. In general a small fraction of the CO_2 originally adsorbed is

able to desorb between ~250 and 400 °C, suggesting this species is a weakly bound carbonate. During the WGS-TPSR, there is little difference between the amount of CO_2 adsorbed over the samples whether or not Au is present. However, as will be shown below, during a presaturation with CO_2 it is apparent that the presence of Au greatly increases the ability of the material to adsorb CO_2.

Having established that CO_2 adsorption saturates the 1% Au/La_2O_3 (AA,P) surface during the first cycle of WGS-TPSR, and that complete conversion and stable catalytic performance is possible in subsequent cycles, the material was pretreated with a 10% CO_2 – He (30 mL min^{-1}) gas mixture and heated at 10 °C min^{-1} to 400 °C where it was held for 1 hour. This material is designated 1% Au/La_2O_3 (AA,P,CO_2). However, instead of seeing the material perform as it did in the second cycle of Figure 4.6, it was markedly more active with a lower light-off temperature and ~100% H_2O conversion at ~325 °C (Figure 4.9). The difference between the CO_2 and H_2 signals in Figure 4.9 is due to CO_2 that desorbs from the surface at the elevated temperatures and therefore leads to a higher reported CO_2 concentration. As seen in isothermal tests, the CO_2 eventually returns to the same level as the H_2 signal once the decomposition of the surface is complete.

In a more systematic examination of the effect of the CO_2 pretreatment, the material was pretreated with CO_2 (Figure 4.10) and then a TPD was performed (Figure 4.11). Similarly to what was previously observed, only approximately 50% of the CO_2 that was adsorbed during the saturation step was desorbed during the TPD. The total amount of CO_2 irreversibly adsorbed, though, was

approximately 50% more than the amount irreversibly adsorbed by the bare support. This may be because some CO_2 was used to oxidize the Au (see below) and was therefore unavailable to desorb. It may also indicate that the addition of Au to the support improves the stability of carbonates and/or the hydroxycarbonate species by providing more –OH species with which adsorbed CO_2 can form stable hydroxycarbonates. A WGS-TPSR and a 12 hour isothermal test at 400 °C (Figure 4.12) of this 1% Au/La_2O_3 (AA,P,CO_2) again demonstrated that this material is significantly more active than the fresh material and is stable at high temperatures. After these tests, a TPD test was performed (Figure 4.13); the amount of CO_2 desorbed was very low and seemed to have no effect on a subsequent TPSR (Figure 4.14). This CO_2 may be attributed to residual CO_2 that was adsorbed reversibly onto the material during the previous cycles of WGS reaction and was in fact equal to the amount desorbed during the first TPD (Figure 4.11). In both the CO_2 pretreatments and CO_2 adsorption over fresh 1% Au/La_2O_3 (AA,P), the carbon balance is closed when the TPD is run to higher temperatures (~650 °C) and the remaining CO_2 that did not desorb at 400 °C is seen to desorb. This material was not tested for WGS activity after this high-temperature test.

These cyclic saturation-TPD-TPSR studies seem to indicate that the CO_2 is in some way activating the surface of the 1% Au/La_2O_3 (AA,P,CO_2). Gates and co-workers have investigated Au/La_2O_3 for CO oxidation; in that work the researchers found that CO_2 has a very interesting effect on highly dispersed Au

atoms and clusters[3b, 3c]. It was determined that CO_2 was capable of oxidizing Au(0) through a dissociation mechanism:

$$2Au^0 + CO_2 \rightarrow Au^+\text{-}O^{2-}\text{-}Au^+ + CO$$

This hypothesis was made based on IR measurements wherein after introduction of CO_2 the only observed product was surface adsorbed CO. In the data collected in this study, CO_2 was seen to adsorb onto the surface, but no appreciable amount of CO was seen to desorb. The CO produced as a result of this dissociation has been shown by Gates et al.[3c] and by the Bernal group[11a] to be bound to the support; Gates et al. were unable to conclude whether the CO was also adsorbed on the Au. While the fresh 1% Au/La_2O_3 (AA,P) was shown to be highly oxidized (Figure 4.5), *in situ* XANES data collected for the 1% Au/La_2O_3 (AA,P) during WGS TPSR showed that the white line intensity decreased significantly as temperature was increased (Figure 4.15), suggesting that the Au was at least partially reduced. It may also be possible that CO was adsorbed on the Au, making it appear partially reduced.

Under this "reoxidation" hypothesis, it can be suggested that CO_2 treatment of a fresh Au/La_2O_3 (AA) material after it had undergone two cycles of WGS TPSR should further activate this material. A summary of this test is presented in Figure 4.16. It should be noted that this test was performed with the leached 0.7% Au/La_2O_3 (AA,L) material, not the parent material. As previously discussed, there is a slight deactivation from the first to the second cycle of the TPSR with the fresh material. However, upon treatment with CO_2 the activity of the 0.7% Au/La_2O_3 (AA,L) is improved to a level commensurate with that of a

separate 0.7% Au/La_2O_3 (AA,L,CO_2) previously performed (also shown in Figure 4.16). It would be interesting to investigate how fresh materials would perform in full gas conditions wherein the CO_2 present might function to keep the Au oxidized.

4.3 Effect of Other Pretreatments (O_2, He) on the Performance of 1% Au/La_2O_3 (AA,P)

The effect of pretreatment conditions has been reported in the literature for Au-based WGS and CO oxidation catalysts[1b, 2c, 13]. It is important not only to find the pretreatment that yields the most active catalyst, but also to attempt to understand the reason behind this improved activity. For this reason, O_2 and He pretreatments (both at 400 °C for 1 hour) were investigated in addition to the CO_2 treatment outlined previously. High temperature treatments in O_2 and He were chosen specifically because they can be used to investigate whether the activation by CO_2 noted above is due to a temperature effect alone, an oxidizing atmosphere effect alone, or – more likely – an effective combination of the two that is more in line with the recent findings of Gates, et al. wherein CO_2 can oxidize Au(0) on La_2O_3 at room temperature[3c]. Extending this work further, it could be possible that higher temperature treatments of Au on La_2O_3 are able to redisperse Au, in addition to oxidizing it.

During high temperature pretreatments the effluent from the reactor is monitored by mass spectrometry to help understand how the surface is changing when the Au/La_2O_3 is exposed to different atmospheres at high temperature. The pretreatments in O_2 (Figure 4.17), He (Figure 4.18) and CO_2 (Figure 4.19) show

the desorption of different species from the surface, which would indicate that different chemistries exist. During the O_2 pretreatment (Figure 4.17), the only species seen to desorb in detectable amounts is H_2O with a very broad peak; the desorption of neither CO_2 (indicating the desorption of loosely bound CO_2 at low temperatures or the decomposition of surface carbonaceous species at higher temperatures) nor H_2 is observed. The desorption of H_2O at elevated temperatures indicates that the underlying La_2O_3 structure is changing. As previously mentioned, the La_2O_3 material used in this study is amorphous and likely contains a very high amount of hydroxide (*i.e.* crystalline water) in the bulk, leading to a structure more appropriately called $LaO(OH)_x$. The results of Figure 4.17 suggests that by adding the Au, the decomposition of this hydroxide structure is promoted, leading to the reconstruction of the support to a lanthanum material with less H_2O in the lattice through a reaction of the type below.

$$LaO(OH)_x + O_2 \rightarrow La_2O_3 + H_2O$$

Even though the lanthanum support has been calcined to 650 °C before the addition of Au, the presence of Au may be enough to promote the further oxidation of the $LaO(OH)_x$ to La_2O_3, at least on the surface. XRD or XPS analysis is required to further validate this hypothesis. The catalyst is observed to be purple in color after a WGS-TPSR suggesting the presence of some reduced Au(0) species.

On the contrary, no H_2O is seen to desorb in either the He (Figure 4.18) or the CO_2 (Figure 4.19) pretreatments. Also, no CO_2 desorbs during the He pretreatment; as previously discussed, CO_2 is adsorbed during the CO_2

pretreatment. The lack of H_2O suggests that the underlying $LaO(OH)_x$ support was unaltered. It is possible that the CO_2 pretreatment forms surface hydroxycarbonates with the $LaO(OH)_x$ and this preserves the Au in place with enough –OH groups around it to remain active. In this manner, despite the net oxidizing environment during the CO_2 pretreatment, the $LaO(OH)_x$ support is not oxidized to La_2O_3 as in the O_2 pretreatment. The He heat treatment, then, does not change the underlying $LaO(OH)_x$ support because the temperature of 400 °C is low for the decomposition temperature of the hydroxide. The H_2 species in the He and CO_2 pretreatments, and not observed in the O_2 pretreatment, might be due to small amounts of H_2O lost from the $LaO(OH)_x$ during the heat treatments where the H_2O signal might be too high to see such a small change. Again, XRD and XPS analysis would shed light on this structural change in the support. After a WGS-TPSR, the catalyst is still dark grey if it was pretreated in either He or CO_2, suggesting that the Au is still highly dispersed and oxidized.

The similarity in pretreatment spectra translates to similarities in the performance of the 1% Au/La_2O_3 (AA,P) materials in WGS TPSR tests. The 1% Au/La_2O_3 (AA,P,O_2) shows very low activity (Figure 4.20), even slightly lower than the fresh 1% Au/La_2O_3 (AA,P) (Figure 4.6). Alternatively, the 1% Au/La_2O_3 (AA,P,He) shows high catalytic activity (Figure 4.21), identical to that of the 1% Au/La_2O_3 (AA,P,CO_2) (Figure 4.9). All materials, regardless of their catalytic performance, showed stability during 12 hour isothermal hold tests in product-free conditions (Figure 4.22). In a similar fashion that a CO_2 treatment was seen to “reactivate” a fresh 1% Au/La_2O_3 (AA,P) after several cycles of WGS TPSR

(Figure 4.16), a CO_2 treatment was seen to moderately improve a 1% Au/La_2O_3 (AA,P,O_2) material after it had undergone cycles of WGS TPSR (Figure 4.23). This effect is potentially due to the ability of CO_2 to oxidize Au as previously discussed above. In this example (Figure 4.23) it is possible that the CO_2 has oxidized or even redispersed the Au. Further study is necessary to better understand this finding.

To investigate whether the activation observed in He and CO_2 pretreatments was due to the oxidizing potential of the pretreatment gas (*i.e.* the oxygen partial pressure in the pretreatment), a series of pretreatments with varying O_2 fractions (0%, 1%, 10%, and 20%) were performed followed by WGS-TPSR (Figure 4.24). In all of these pretreatments H_2O was seen to desorb from the surface, further indicating the oxidation of the underlying $LaO(OH)_x$ under oxygen environments. For simplicity, only the CO_2 signal for the WGS reaction is shown in Figure 4.24, though the H_2 signals matched in a stoichiometric 1:1 fashion. From these data it is apparent, that the fresh (calcined in static air at 250 °C for 2 hours) and the material pretreated in 1% O_2 –He at 400 °C for 1 hour perform similarly in WGS-TPSR. Additionally, as observed with the 20% O_2 – He pretreatment, the material pretreated in 10% O_2 – He at 400 °C for 1 hour was slightly less active than the fresh material. It is apparent, then, that the effect CO_2 has during the pretreatment is more than to just serve as an oxidizer.

4.4 Characterization of 1% Au/La_2O_3 (AA,P) Materials Before and After High Temperature Pretreatments

4.4.1 *in situ* XAS Studies

In an effort to better understand the nature and origin of the enhanced catalytic performance of the 1% Au/La_2O_3 (AA,P,CO_2) and 1% Au/La_2O_3 (AA,P,He) and the suppressed activity of the 1% Au/La_2O_3 (AA,P,O_2) (which runs contrary to previous observations with gold supported on ceria[14]), *in situ* XANES studies were conducted (Figure 4.26). The XANES spectra were collected under WGS reaction conditions (5% CO – 3 % H_2O – He) as the temperature was ramped to 300 °C and held there isothermally for 1 hour. Figure 4.25a shows that the initial white line intensity of the fresh 1% Au/La_2O_3 (AA,P) is very high, but it rapidly decreases as the temperature is ramped with it eventually stabilizing during the isothermal hold (also shown in Figure 4.15). The loss in intensity indicates that the Au loses some of its ionic character during the WGS reaction; however, because the white line is still present, the Au was not completely reduced. Figures 4.25b and 4.25c shows the white lines of the 1% Au/La_2O_3 (AA,P, CO_2) and 1% Au/La_2O_3 (AA,P,He), respectively. Both materials start off with a reduced white line intensity equal to that of the fresh material after it had seen time on stream. Additionally, with both materials the white line intensity does not decrease, indicating that the residual cationic Au is highly stable in these materials. Most interestingly, the white line intensity of the 1% Au/La_2O_3 (AA,P,O_2) is very high, and remains relatively high throughout the reaction (Figure 4.25d). This result indicates that the Au in this material remains

highly oxidized, and is perhaps Au(III) instead of Au(I). Alternatively, the high white line intensity could be due to oxygen adsorbed onto the Au species, which makes the Au appear more oxidized. Similar results have previously been observed by Deng, et al.[14b]. In her work, Deng observed that the white line intensity of Au/CeO_2 catalysts decreased at elevated WGS reaction temperatures (as observed here), but that this loss in white line was seen to parallel a loss in catalytic performance[14a]. The lower activity of the 1% Au/La_2O_3 (AA,P,O_2) compared to the He and CO_2 pretreated materials in spite of the more oxidized Au in the former suggests that active sites have been lost. In point of fact, with the oxidation of the $LaO(OH)_x$ in the O_2 pretreatment as discussed above, it is likely that the strong interaction between the Au and support –OH groups has been lost. So, even though the Au is still highly oxidized, it is not interacting with the support and has therefore lost a majority of its activity for the WGS reaction.

In a similar study, Ioannis Valsamakis investigated Au supported on $La_2O_2SO_4$ prepared by an anion adsorption method[15]. This $La_2O_2SO_4$ material was fully crystalline, and as such a support restructuring (i.e. loss of H_2O) was not observed during various CO_2, He or O_2 high temperature treatments. Indeed, the treatment effects observed in the Au/La_2O_3 (AA,P) system were not observed in the $Au/La_2O_2SO_4$ (AA,P) system. In the latter, a high temperature CO_2 treatment did not have as pronounced a promotional effect observed in this thesis, likely due to the inability of $La_2O_2SO_4$ to form surface carbonates that might better stabilize the active Au species. Additionally, the He pretreatment over the $Au/La_2O_2SO_4$ (AA,P) leads to a more active catalyst, but without a change in the underlying

support. This may then, as Valsamakis states, be due to a temperature effect wherein the Au is able to better form the necessary Au-O-support species active in the WGS reaction during the high temperature treatment and not due to a restructuring or oxidation of the underlying support.

4.4.2 Reducibility Measured by CO-TPR

Work with Au supported on reducible metal oxides (e.g. FeOx, CeO_2) has shown that the reducibility of the surface oxygen plays a major role in its performance in the WGS reaction[14b]. This reducibility can be measured by temperature programmed reduction (TPR) studies with H_2 or CO as the reductant; in this work CO was used to examine the reducibility of Au/La_2O_3. During CO-TPR, a feed of CO diluted in He is passed over the sample while the temperature is ramped in a linear fashion; the effluent gas is monitored by online mass spectrometry. The production of CO_2 and H_2 in stoichiometric amounts can be used as an indication that the CO is reacting with the –OH groups in the material under the assumed reaction:

$$H_2O^* \rightarrow OH^* + H^*$$

$$CO + OH^* \rightarrow COOH^* \rightarrow CO_2 + H^*$$

$$H^* + H^* \rightarrow H_2$$

wherein OH*, COOH*, and H* are surface-adsorbed species. The OH* is derived from adsorbed H_2O that has been activated (either by temperature or by the catalytic surface) and caused to dissociate, liberating a OH* and a H*, as shown by the reaction scheme above.

In general, the CO-TPR studies performed here were conducted after the Au/La_2O_3 material had been pretreated (if indicated), undergone a WGS TPSR and isothermal hold at 400 °C, cooled the room temperature in He and then rehydrated with a flow of 3% H_2O – He at room temperature for 30 minutes. This rehydration is necessary because when materials are not rehydrated after the WGS reaction, they have been observed to show minimal reducibility by CO-TPR believed to be due to residual surface hydroxyl groups that were not consumed during WGS. By examining the reducibility of the material after reaction and after a rehydration, a better picture of the "working" catalyst is obtained; *i.e.* an estimation of the total number of –OH groups present in the catalyst under WGS condition (where H_2O is constantly present) is attained.

Lanthanum oxide is an irreducible metal oxide. When the surface $LaO(OH)_x$ (without added Au) is hydrated at room temperature before CO-TPR, the H_2 is seen to evolve in three overlapping peaks centered at approximately 325, 375, and 450 °C. The CO_2 is seen to evolve as one broad peak centered at 450 °C and then a much higher temperature peak >600 °C, that is likely due to the decomposition of hydroxycarbonates formed from atmospheric CO_2 (Figure 4.26). The first peak in the H_2 signal, which is not accompanied by CO_2 desorption, may be due to H_2O loss and oxidation of the $LaO(OH)_x$ to La_2O_3. The non-stoichiometric evolution of H_2 and CO_2 at ~400 °C is likely due to the ability of $LaO(OH)_x$ to adsorb CO_2, which delays its release to higher temperatures. tThese peaks are from activated surface oxygen and/or hydroxycarbonates.

The addition of Au to metal oxide supports has been previously shown to improve their surface reducibility[8, 14b, 16], and excess oxygen has been measured. It is believed that this shift to lower temperatures is due to the activation of –OH groups around the Au sites, which are more reducible and presumably involved in the WGS catalysis. The more dispersed the Au species, the more –OH groups that can be stabilized around each $[Au\text{-}O]_x$. The 1% Au/La_2O_3 (AA,P) before and after the different pretreatments was examined with CO-TPR to evaluate the amount of these reducible –OH on the surface after each treatment. This calculation could be used to further elucidate the mechanism behind the He and CO_2 induced activation. In this work, because the $LaO(OH)_x$ itself showed now significant low-temperature activated oxygen, the –OH titrated are likely those that interact most closely with the supported Au species.

The CO-TPR of the 1% Au/La_2O_3 (AA,P) materials after WGS reaction and a room temperature rehydration procedure are presented in Figure 4.27. For simplicity, only the H_2 signals of the CO-TPR results are presented. The downward shift and improved reducibility of the supports after the Au addition compared to the bare support is evident. The 1% Au/La_2O_3 (AA,P,CO_2) (Figure 4.27a) and the 1% Au/La_2O_3 (AA,P,He) (Figure 4.26b) show the highest degree of reducibility, and thus the highest surface –OH content (Table 4.3). These –OH contents are calculated by integrating the H_2 signal up to 375 °C so that the same window of –OH is calculated for each catalyst. Since some materials are reducible at lower temperatures, their calculated –OH content should reflect this. By normalizing in this fashion, rate data taken at 375 °C can be normalized by the

total number of –OH groups activated up to that temperature (as will be performed below). Even the 1% Au/La_2O_3 (AA,P,He) – the most reducible material – has approximately 7 -25 times fewer reducible –OH species than the Au/CeO_2 and Au/FeOx catalysts whose H_2 consumption in H_2-TPR mode correspond to approximately –OH contents of 900 μmol OH g^{-1} (0.5% Au/Ce(La)Ox[14b]), 1800 μmol OH g^{-1} (1.0% Au/CeO_2[16]), and 2500 μmol OH g^{-1} (0.7% Au/FeOx[16]).

The important aspect from the CO-TPR measurements made with the various Au/La_2O_3 (AA,P) samples is that the addition of Au improves their reducibility compared to the bare La_2O_3. Additionally, the most active samples (i.e. the He and CO_2 treated materials) are the most reducible. Finally, the reducibility of these materials is more than an order of magnitude lower than the highly active Au/CeO_2 and Au/FeOx catalysts. This significant difference can be used to explain why the Au/La_2O_3 perform poorly in TPSR mode (and in steady-state mode, as shown below) when compared to the more reducible Au/CeO_2 catalysts. In a similar vein, the $Au/La_2O_2SO_4$ material previously mentioned[15] had only 80 μmol OH g^{-1}, and showed significantly less activated oxygen than the Au/CeO_2 or Au/FeOx.

4.4.3 Apparent Activation Energy (E_{app}) and Steady-State Rate Measurement

The Au/La_2O_3 (AA,P) materials were tested in the full reformate gas (11% CO – 26% H_2O – 26% H_2 – 7% CO_2 – He) to follow how they perform under real gas conditions at steady-state. The apparent activation energy (E_{app}) of the WGS

reaction over the Au/La_2O_3 catalysts was estimated by measuring steady-state rate data at low conversions (<15%). In these experiments, the temperature was ramped to the high temperature (400 °C) and the rates were measured in cool down mode at 25 °C intervals so that any thermally induced deactivation would occur at the start of the kinetic measurements and then remain constant throughout the test (Figure 4.28). The E_{app} of the 1% Au/La_2O_3 (AA,P,He) catalyst was found to be 49 ± 1 kJ mol^{-1}, which is good agreement with the reported activation energy over other Au-based catalysts[16].

The steady-state rate of each catalyst measured at 375 °C is presented in Table 4.2. The mass rate of each material is 1 – 2 orders of magnitude lower than the mass rate reported for Au/CeO_2 materials, even though the Au/La_2O_3 materials were tested at 100 – 150 °C higher temperatures[16]. Similarly, the Au/La_2O_3 materials were from 2 – 10 times less active than the Au/FeOx materials[14b, 16]. Rates were also normalized by the specific surface area and the specific –OH content (calculated from CO-TPR) to validate whether this markedly lower activity could be attributed to a surface area or reducibility effect (Table 4.4).

The 1% Au/La_2O_3 (AA,P) catalysts are approximately an order of magnitude less active when comparing rates normalized by the specific surface area (Table 4.4). However, the rates are comparable when normalized by the –OH content. The same trend is observed with the 1% $Au/La_2O_2SO_4$ (AA,P,He) prepared by Valsamakis[15]. This suggests that the amount of –OH available on the catalyst surface plays an intrinsic role in the material's activity towards the

WGS reaction. The –OH contents of the Au/CeO_2 and Au/FeOx catalysts must be taken with the concession that the measurement contains both the –OH groups associated with the Au species (as reported for the Au/La_2O_3 materials in this work) and those –OH from the reducible support (which is not the case with Au/La_2O_3). As previously reported by Zhai, efforts to increase the –OH environment around the precious metal in WGS catalysts leads to a marked improvement in their activity[17]. In her case, Zhai increased the –OH content through alkali metal doping. Nanoscale ceria and FeOx have a significantly higher –OH content due to their nature and reducibility. $LaO(OH)_x$, on the other hand, is irreducible, and the –OH groups active at low temperatures in the Au/La_2O_3 system are likely to be those stabilized around the Au sites, in a similar fashion as was reported with the $Pt(OH)_x$ species on SiO_2[17].

4.5 Summary

Anion adsorption is an attractive means to preferentially adsorb the fully speciated $[Au(OH)_4]^-$ complex onto La_2O_3 at a pH where a strong electrostatic interaction exists between the Au precursor and the support surface. Such a preparation has been shown to achieve highly dispersed Au. Catalysts prepared in this manner show promising activity in the WGS reaction but can be made significantly more active through high temperature CO_2 or He treatments. These treatments were shown to decrease the oxidation state of the supported Au, while preserving some degree of ionic character, while stabilizing the Au-O-$La(OH)_x$ interaction. During this pretreatment, the underlying $LaO(OH)_x$ structure is preserved. However in O_2 pretreatments the support seems to be oxidized further

to La_2O_3 with the loss of much of its associated –OH groups, leading to a Au species that does not interact strongly with the support and a catalyst that is less active.

While 1% Au/La_2O_3 (AA,P) is significantly less active than Au/CeO_2 and Au/FeOx catalysts with similar gold loading when mass rates (i.e. mol CO_2 g_{cat}^{-1} s^{-1}) are compared, normalization by the active oxygen (i.e. surface –OH groups participating in the reaction) shows that all materials are comparably active. A parallel study with a Au/$La_2O_2SO_4$ material, which contained less active surface oxygen and did not undergo structural changes in the support with high temperature treatments, showed similar active oxygen-normalized rates. Such a trend suggests that it is not simply bare Au atoms that are the active sites for the WGS reaction. Instead, these results show that an ensemble of species on the surface, a Au-O-$La(OH)_x$, is likely the active site. A more crystalline La_2O_3 (instead of $LaO(OH)_x$) has shown inferior properties when gold was deposited on it by DP[16]. Whether or not the same will be true when the AA technique is used on crystalline La_2O_3 supports remains to be investigated.

4.6 References

[1] a. H.-S. Oh, J. H. Yang, C. K. Costello, Y. M. Wang, S. R. Bare, H. H. Kung, M. C. Kung, *Journal of Catalysis* **2002**, *210*, 375-386; b. *Catalysis by Gold, Vol. 6*, Imperial College Press, London, **2006**.

[2] a. D. Pierre, M.S. Thesis, Dept. of Chemical & Biological Engineering, Tufts University, **2007**; b. J. H. Yang, J. D. Henao, C. Costello, M. C. Kung, H. H. Kung, J. T. Miller, A. J. Kropf, J.-G. Kim, J. R. Regalbuto, M. T. Bore, H. N. Pham, A. K. Datye, J. D. Laeger, K. Khara, *Applied Catalysis A: General* **2005**, *291*, 73-84; c. *Catalyst Preparation*, CRC Press, Boca Raton, FL, **2007**; d. S. Ivanova, V. Pitchon, Y. Zimmermann, C. Petit, *Applied Catalysis A: General* **2006**, *298*, 57-64.

[3] a. J. C. Fierro-Gonzalez, V. A. Bhirud, B. C. Gates, *Chemical Communications* **2005**, 5275-5277; b. M. Mihaylov, E. Ivanova, Y. Hao, K. Hadjiivanov, B. C. Gates, H. Knözinger, *Chemical Communications* **2008**, *2*, 175-177; c. M. Mihaylov, E. Ivanova, Y. Hao, K. Hadjiivanov, H. Knözinger, B. C. Gates, *Journal of Physical Chemistry C* **2008**, *112*, 18973-18983.

[4] a. S. Ivanova, C. Petit, V. Pitchon, *Applied Catalysis A: General* **2004**, *267*, 191-201; b. S. Ivanova, V. Pitchon, C. Petit, *Journal of Molecular Catalysis A: Chemical* **2006**, *256*, 278-283; c. S. Ivanova, V. Pitchon, C. Petit, H. Herschbach, a. Dorsselaer, E. Leize, *Applied Catalysis A: General* **2006**, *298*, 203-210; d. A. Hugon, N. E. Kolli, C. Louis, *Journal of Catalysis* **2010**, *274*, 239-250.

[5] J. Peck, C. Tait, B. Swanson, G. Brown Jr, *Geochimica et Cosmochimica Acta* **1991**, *55*, 671-676.

[6] a. A. N. Pestryakov, N. Bogdanchikova, A. Simakov, I. Tuzovskaya, F. Jentoft, M. Farias, A. Diaz, *Surface Science* **2007**, *601*, 3792-3795; b. A. N. Pestryakov, V. V. Lunin, a. N. Kharlanov, N. E. Bogdanchikova, I. V. Tuzovskaya, *The European Physical Journal D - Atomic, Molecular and Optical Physics* **2003**, *24*, 307-309; c. J. Guzman, A. Corma, *Chemical Communications* **2005**, 743-745.

[7] J. P. Gaviría, L. G. Navarro, A. E. Bohé, *The Journal of Physical Chemistry A* **2012**, *116*, 2062-2070.

[8] Q. Fu, Ph.D. Thesis, Dept. of Chemical & Biological Engineeing, Tufts Univerisity, **2004**.

[9] J. A. Dean, *Lange's Handbook of Chemistry*, 15 ed., McGraw-Hill, Columbus, **1998**.

[10] F. Menegazzo, M. Manzoli, a. Chiorino, F. Boccuzzi, T. Tabakova, M. Signoretto, F. Pinna, N. Pernicone, *Journal of Catalysis* **2006**, *237*, 431-434.

[11] a. S. Bernal, J. Diaz, R. Garcia, J. M. Rodriguez-Izquierdo, *Journal of Materials Science* **1985**, *20*, 537-541; b. S. Bernal, F. J. Botana, R. García, J. M. Rodríguez-Izquierdo, *Reactivity of Solids* **1987**, *4*, 23-40.

[12] R. P. Turcotte, J. O. Sawyer, L. Eyring, *Inorganic Chemistry* **1969**, *8*, 238-246.

[13] a. Newsome, *Catalysis Reviews* **1980**, *21*, 275-318; b. C. Ratnasamy, J. P. Wagner, *Catalysis Reviews* **2009**, *51*, 325-440.

[14] a. W. Deng, A. I. Frenkel, R. Si, M. Flytzani-Stephanopoulos, *Journal of Physical Chemistry C* **2008**, *112*, 12834-12840; b. W. Deng, Ph.D. Thesis, Dept. of Chemical & Biological Engineering, Tufts University, **2008**.

[15] I. Valsamakis, Ph.D. Thesis, Dept. of Chemical & Bioloical Engineering, Tufts University, **2012**.

[16] Y. Zhai, Ph.D. Thesis, Dept. of Chemical & Biological Engineering, Tufts University, **2011**.

[17] Y. Zhai, D. Pierre, R. Si, W. Deng, P. Ferrin, A. U. Nilekar, G. Peng, J. a. Herron, D. C. Bell, H. Saltsburg, M. Mavrikakis, M. Flytzani-Stephanopoulos, *Science* **2010**, *329*, 1633-1636.

Table 4.1 Speciation of $[AuCl_4]^-$ Under Various Conditions[1b]

Table 4.1: Gold speciation in $HAuCl_4$ solutions at room temperature as a function of pH.

$HAuCl_4$ solution	pH or range of pH of predominance of the various Au^{III} speciation					Characterisation technique	References
	$[AuCl_4]^-$	$[Au(OH)Cl_3]^-$	$[Au(OH)_2Cl_2]^-$	$[Au(OH)_3Cl]^-$	$[Au(OH)_4]^-$		
10^{-2} M in NaCl (1M)[a]	pH 1.4–6.2	pH 6.2–8.1	pH 8.1–11	pH 11–12	pH 12?	Raman, UV-visible	18
10^{-1}–10^{-3} M[a]	pH 2	pH 7.5	pH 9.2			XANES, EXAFS	19
2×10^{-2} M[b]	pH 1–3.8	pH 3.8–5.2	pH 5.2–6.6	pH 8.2–11.2	pH 11.2–12	Raman	20
$1 - 2.5 \times 10^{-3}$ M	pH ≤ 4				pH 7	EXAFS	30

[a]pH range of predominance of the various Au^{III} speciation.
[b]Each pH range corresponds to a single species except at pH 6.6–8.2: mixture of $Au(OH)_2Cl_2^-$ and $Au(OH)_3Cl^-$.

This table is taken from Ref. [1b]. References listed in Table 4.1 are taken from Ref. [1b].

Table 4.2 Performance of 1%, 3% and 5% Au/La_2O_3 (AA,P)

Sample	Au Loading (at. %)	Light-Off Temperature (°C) (Cycle 1, Cycle 2, Cycle 3)	CO Conversion (%) at 400 °C
1% Au/La_2O_3 (AA,P)	1.0	175, 175, 175	70, 70, 70
1% Au/La_2O_3 (AA,L)	0.7	175, 175, 175	70, 70, 70
3% Au/La_2O_3 (AA,P)	2.9	125, 150, 150	100, 100, 100
3% Au/La_2O_3 (AA,L)	1.0	175, 175, 175	70, 70, 70
5% Au/La_2O_3 (AA,P)	4.8	75, 100, 100	100, 100, 100
5% Au/La_2O_3 (AA,L)	1.0	125, 125, 125	100, 100, 100

Table 4.3 Specific –OH Content (Below 375 °C) of

1% Au/La_2O_3 (AA,P) Materials

Sample	-OH Content (μmol g^{-1})
1% Au/La_2O_3 (AA,P,CO_2)	213
1% Au/La_2O_3 (AA,P,He)	360
1% Au/La_2O_3 (AA,P,O_2)	102
1% Au/La_2O_3 (AA,P)	152

Table 4.4 Steady-State Rates at 375 °C of 1% Au/La_2O_3 (AA,P) Materials

Sample	Rate per g_{cat} ($\mu mol\ CO_2\ g_{cat}^{-1}\ s^{-1}$)	Rate per m^2 ($\mu mol\ CO_2\ m^{-2}\ s^{-1}$)	Rate per mol OH ($\mu mol\ CO_2\ (mol\ OH)^{-1}\ s^{-1}$)
1% Au/La_2O_3 (AA,P,CO_2)	5.5	0.10	2.6×10^4
1% Au/La_2O_3 (AA,P,He)	3.1	0.056	8.6×10^3
1% Au/La_2O_3 (AA,P,O_2)	0.016	2.9×10^{-4}	160
1% Au/La_2O_3 (AA,P)	0.65	0.012	4.3×10^3
Ce(La)Ox[14b]	1.3	0.008	
0.5% Au/Ce(La)Ox*[14b]	145	0.9	3.6×10^5
0.7% Au/FeOx[14b]	30	0.8	1.2×10^4
1% Au/CeO_2*[16]	110	0.90	6.1×10^4
0.1% Au/Fe_2O_3[16]	16	0.4	6.4×10^3

*Extrapolated from lower temperature

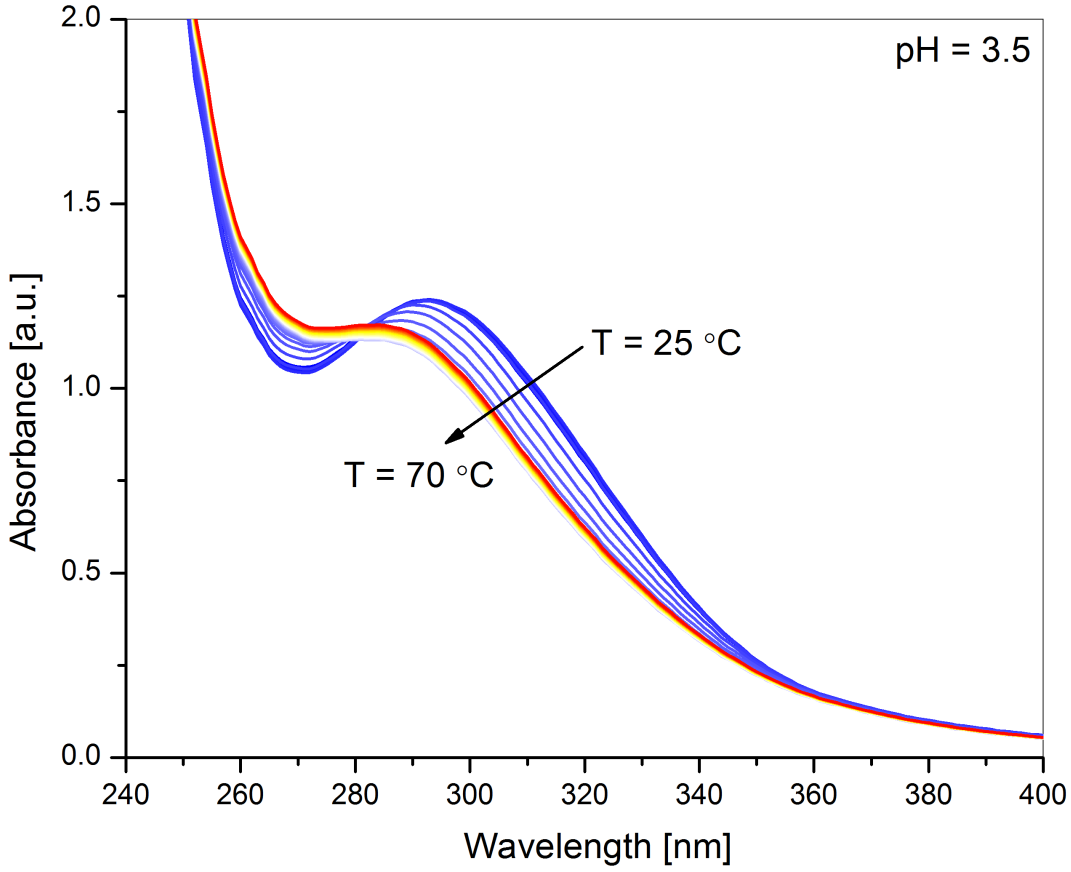

Figure 4.1 UV-Vis Absorption Spectra of Au Precursor Solution

(4×10^{-4} M) at pH = 3.5 with Increasing Temperature

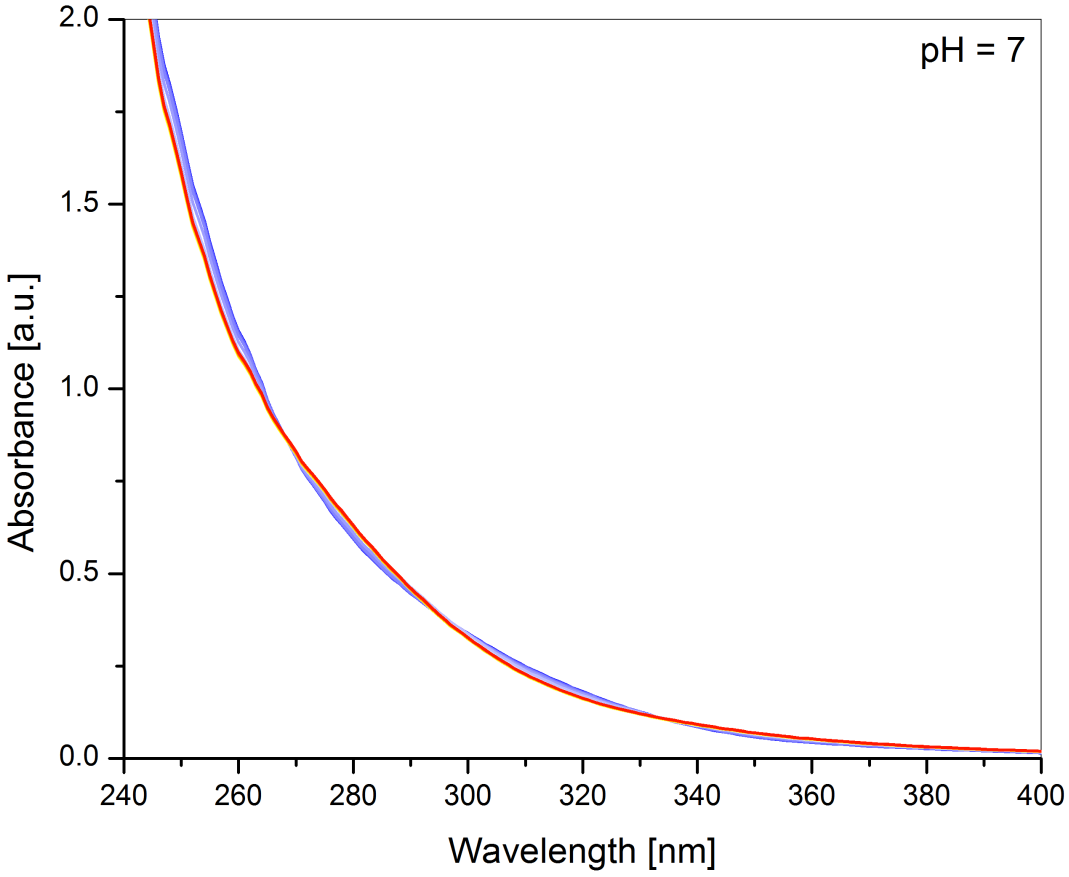

Figure 4.2 UV-Vis Absorption Spectrum of Au Precursor Solution

(4×10^{-4} M) at pH = 7 with Increasing Temperature

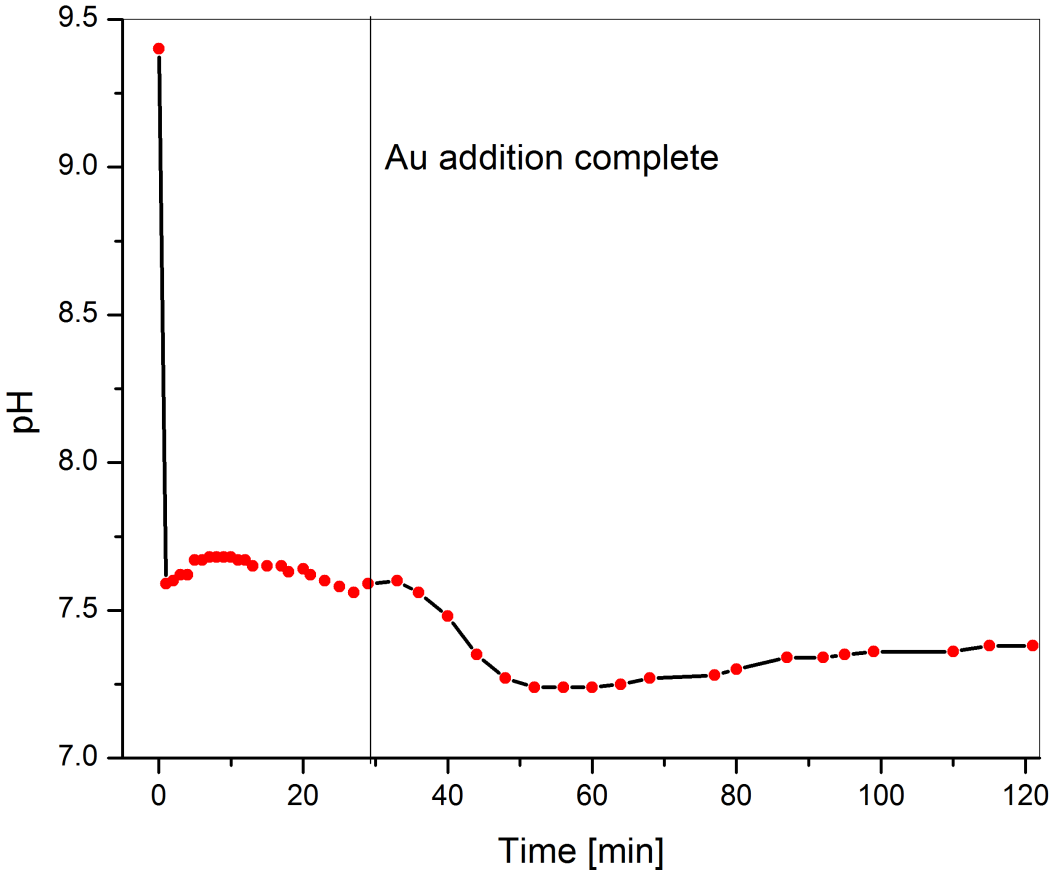

Figure 4.3 pH Profile during AA Preparation of 3% Au/La_2O_3 (AA,P)

Here the pH changes are slightly different than those reported above due to the higher design Au loading.

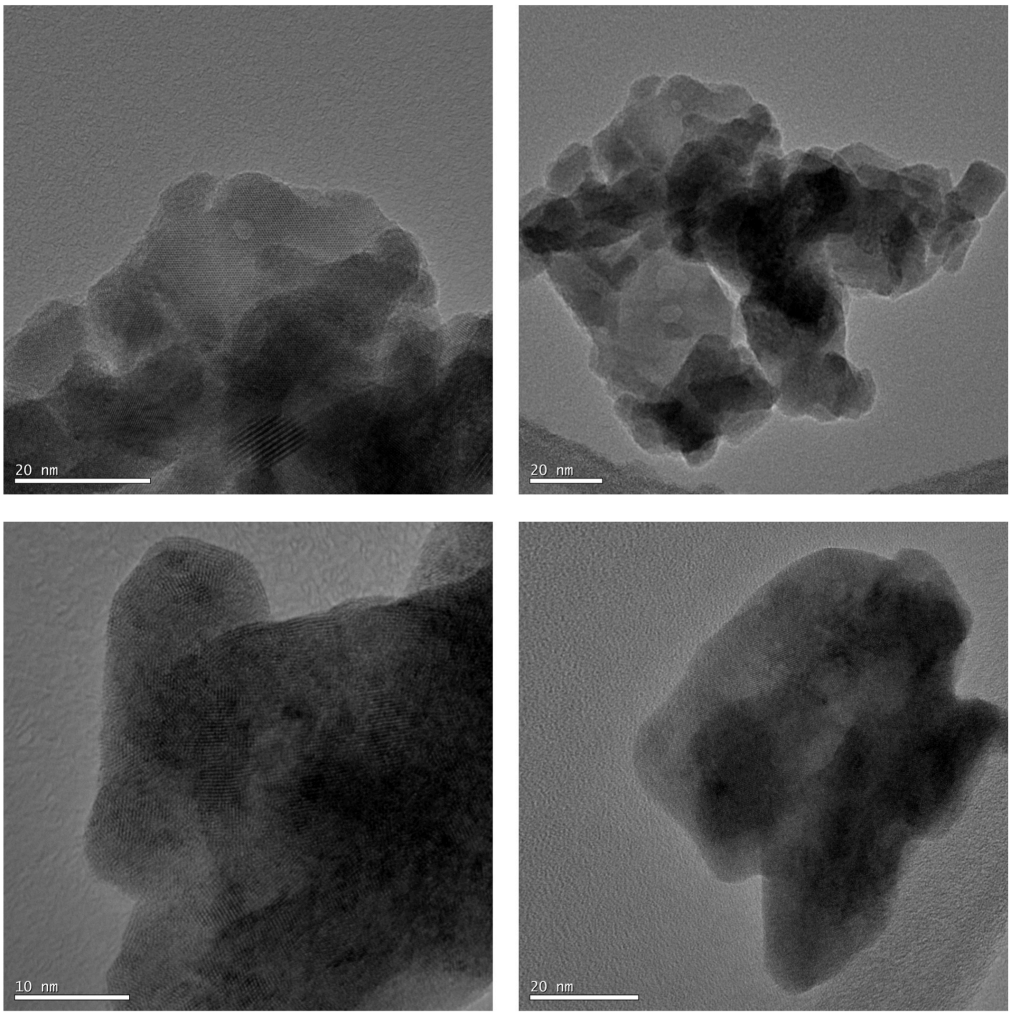

Figure 4.4 Transmission Electron Micrograph (TEM) Image of

1% Au/La_2O_3 (AA,P)

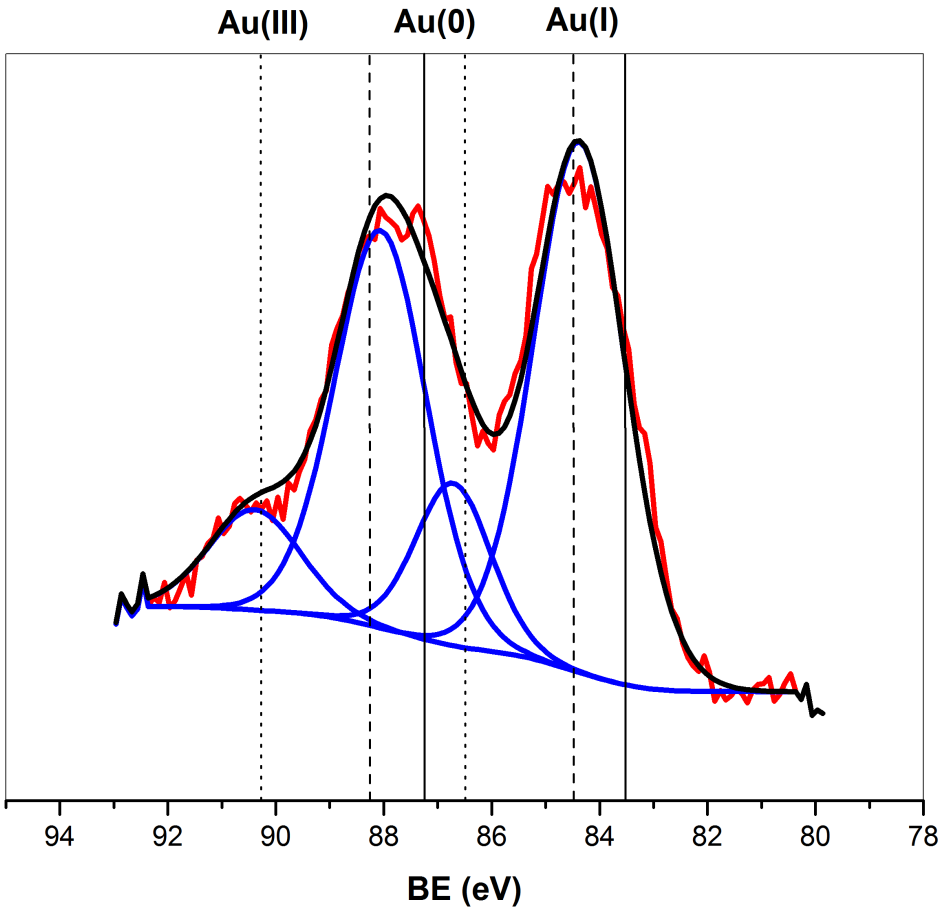

Figure 4.5 XPS of 1% Au/La_2O_3 (AA,P)

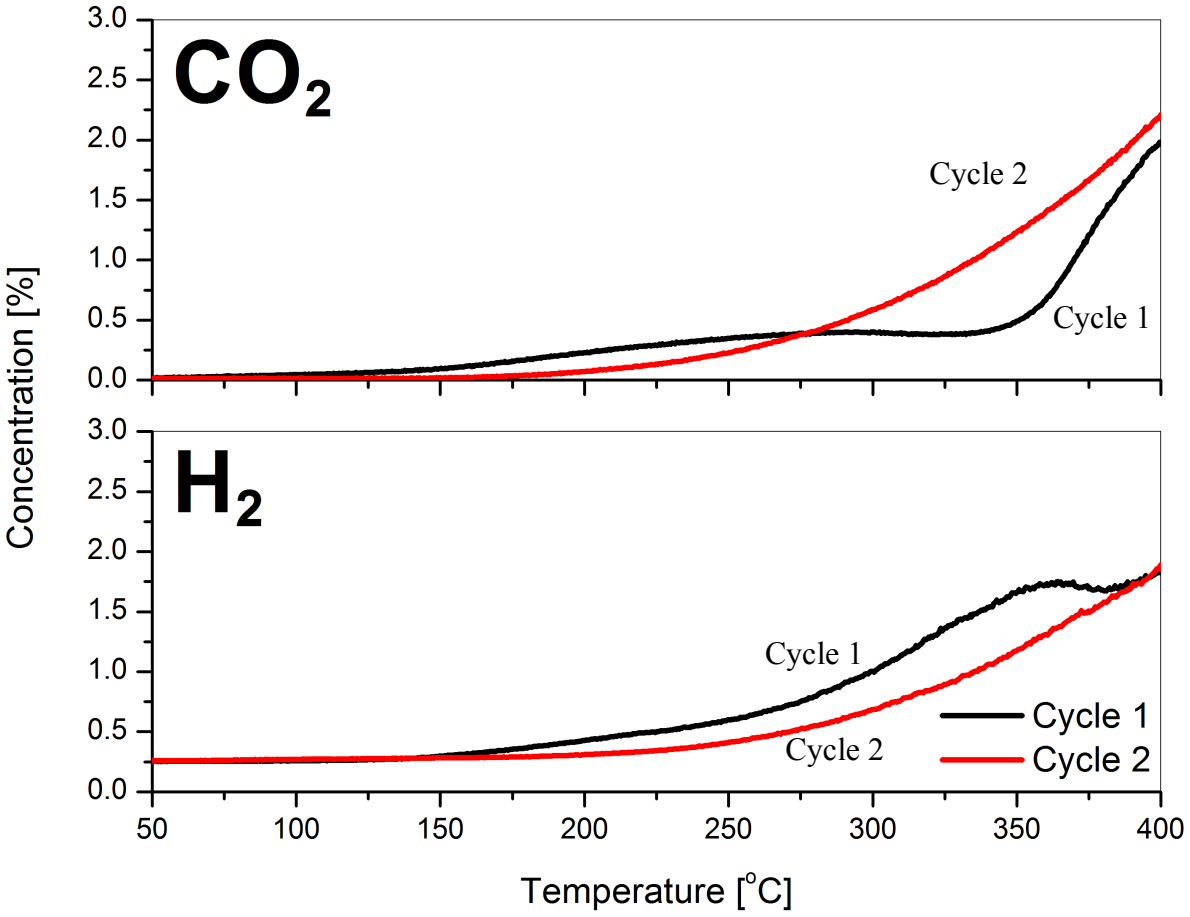

Figure 4.6 Cyclic WGS TPSR over 1% Au/La_2O_3 (AA,P)

30 mL min^{-1}, 10% CO – 3% H_2O – He, contact time 0.2 g s mL^{-1}

Sample cooled to room temperature in He between cycles

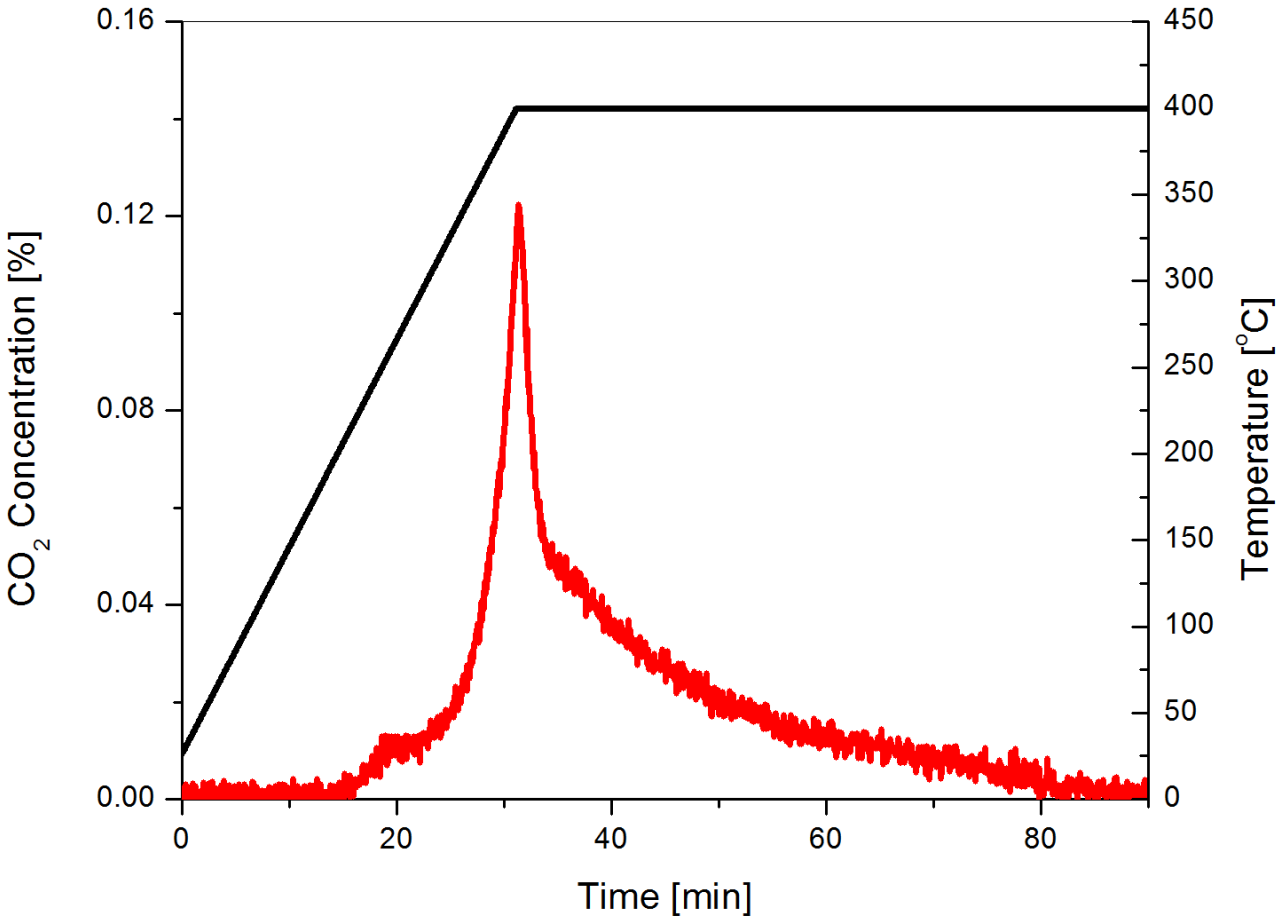

Figure 4.7 TPD of 1% Au/La_2O_3 (AA,P) after WGS TPSR

30 mL min^{-1}, He, contact time 0.2 g s mL^{-1}

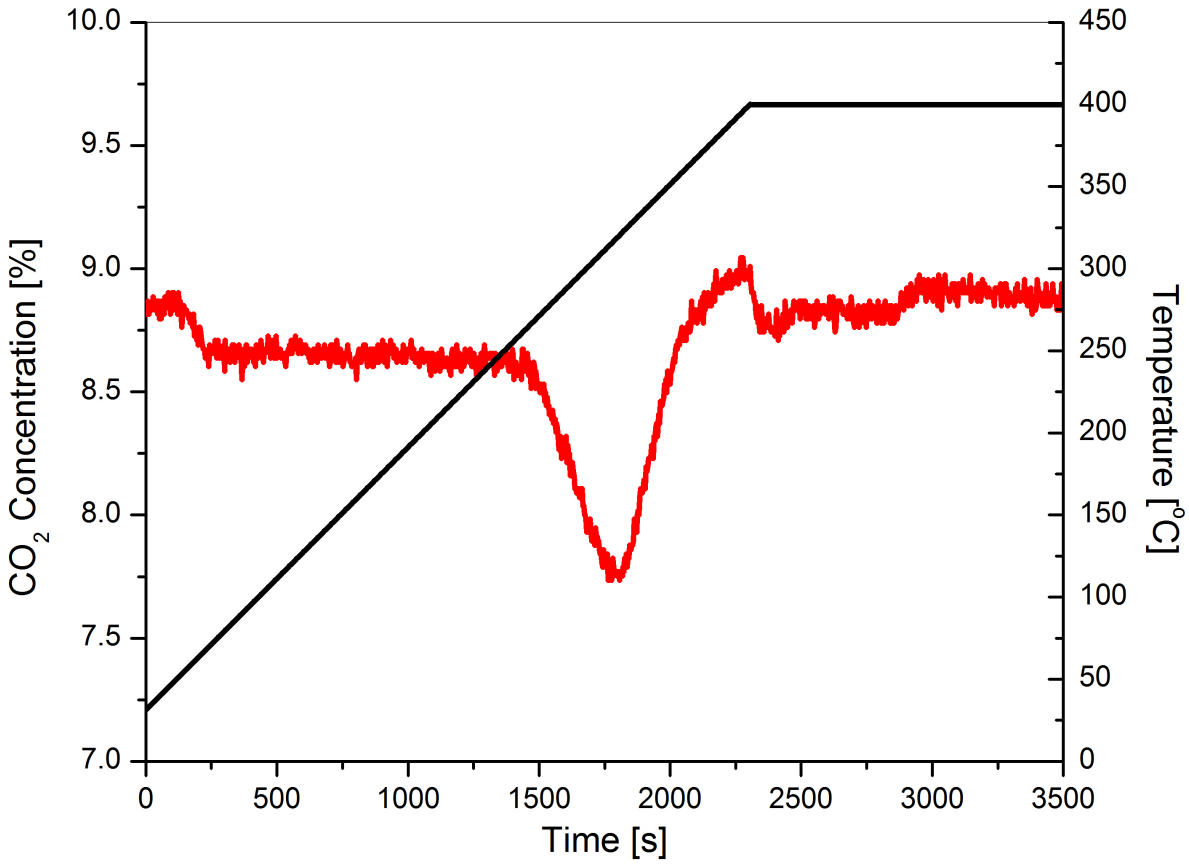

Figure 4.8a CO_2 Saturation of Bare La_2O_3

30 mL min^{-1}, 10% CO_2 – He, contact time 0.2 g s mL^{-1}

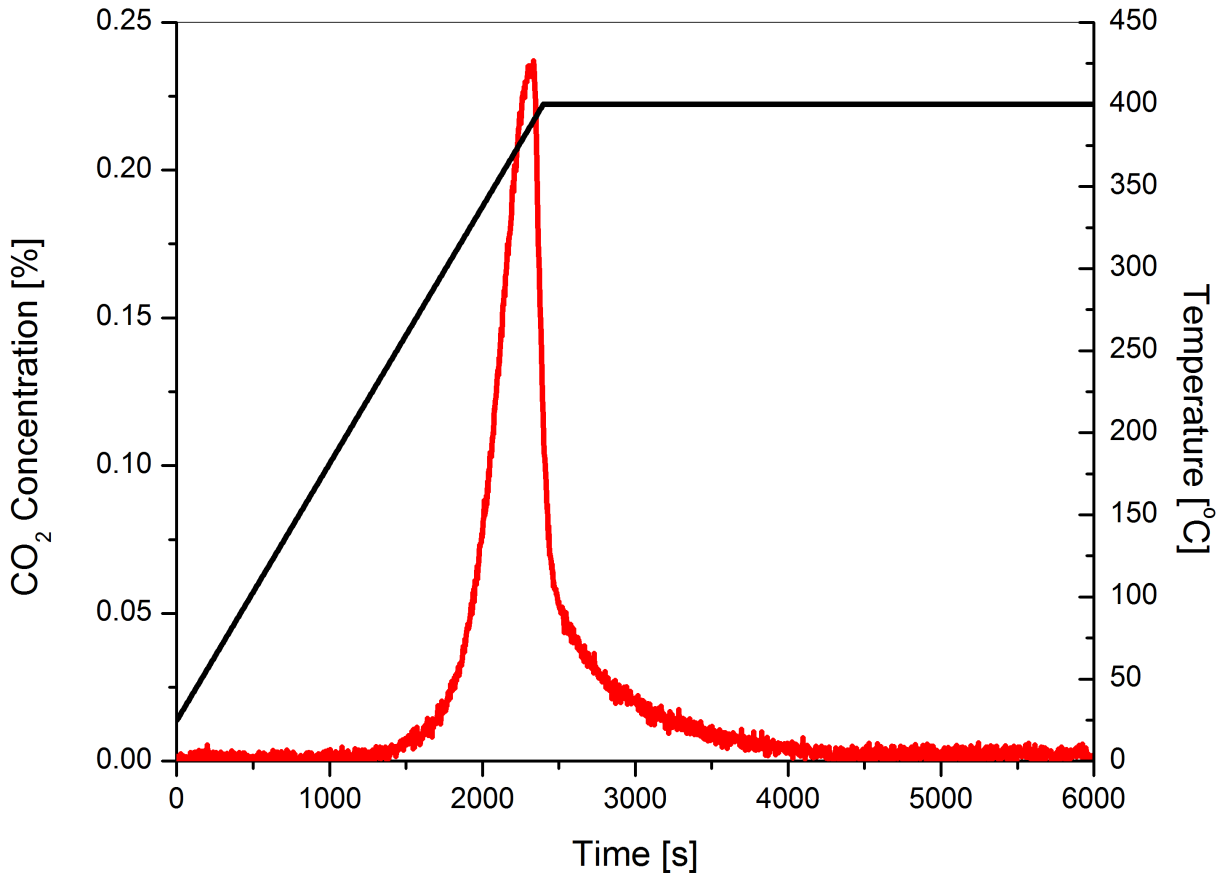

Figure 4.8b TPD of Bare La_2O_3 after CO_2 Saturation

30 mL min^{-1}, He, contact time 0.2 g s mL^{-1}

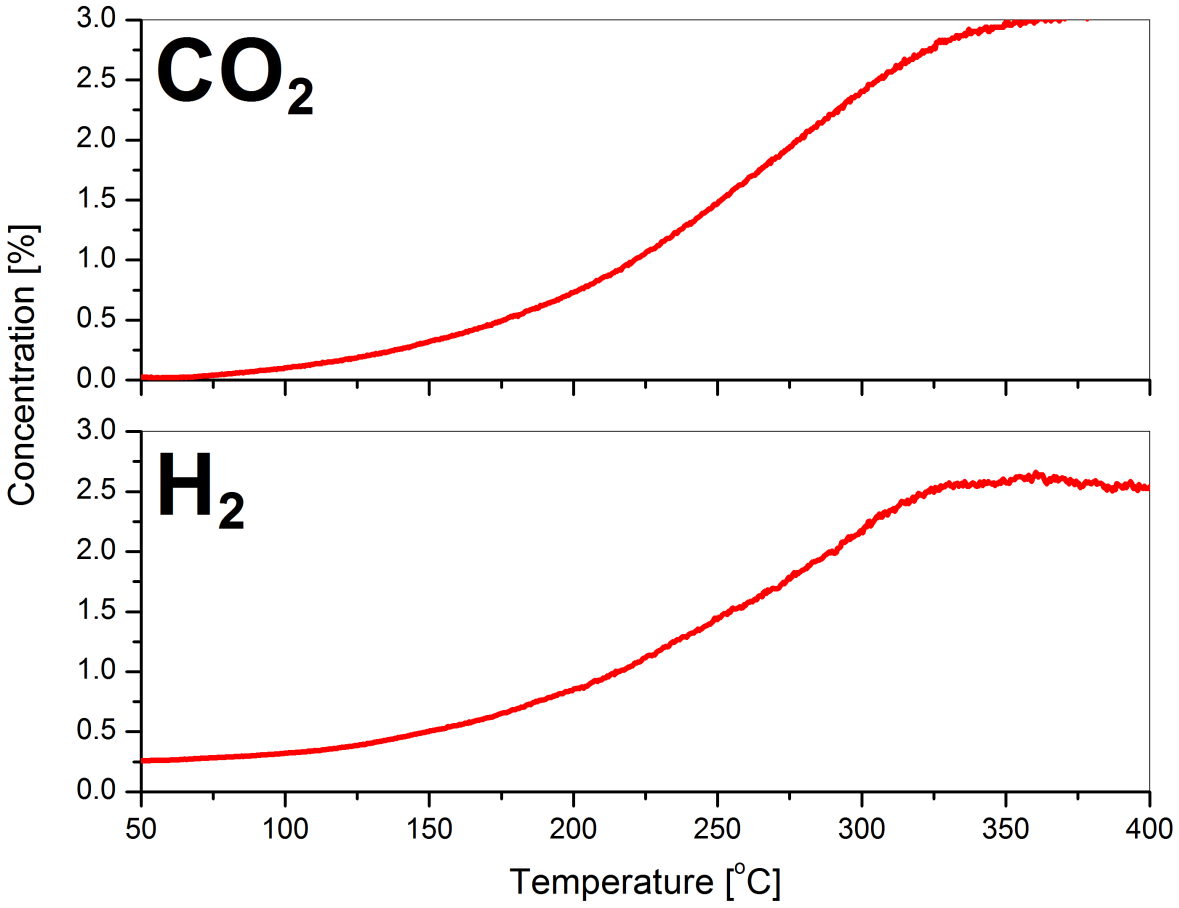

Figure 4.9 WGS TPSR of 1% Au/La_2O_3 (AA,P,CO_2)

Pretreatment: 30 mL min^{-1} (10% CO_2 – He), room temperature to 400 °C for 1 h

with a heating rate of 10 °C min^{-1}

Reaction conditions: 30 mL min^{-1}, 10% CO – 3% H_2O – He,

contact time 0.2 g s mL^{-1}

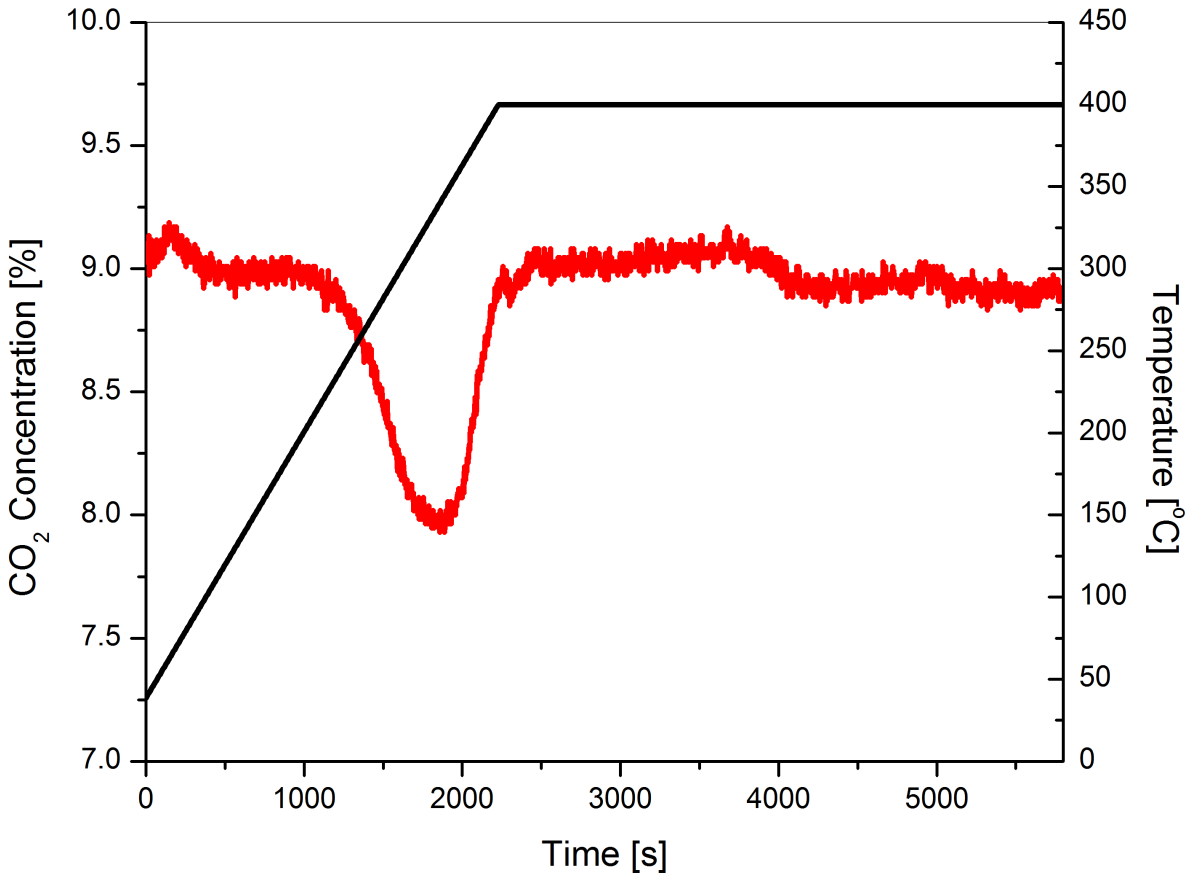

Figure 4.10 CO_2 Saturation of 1% Au/La_2O_3 (AA,P)

30 mL min^{-1}, 10% CO_2 – He, contact time 0.2 g s mL^{-1}

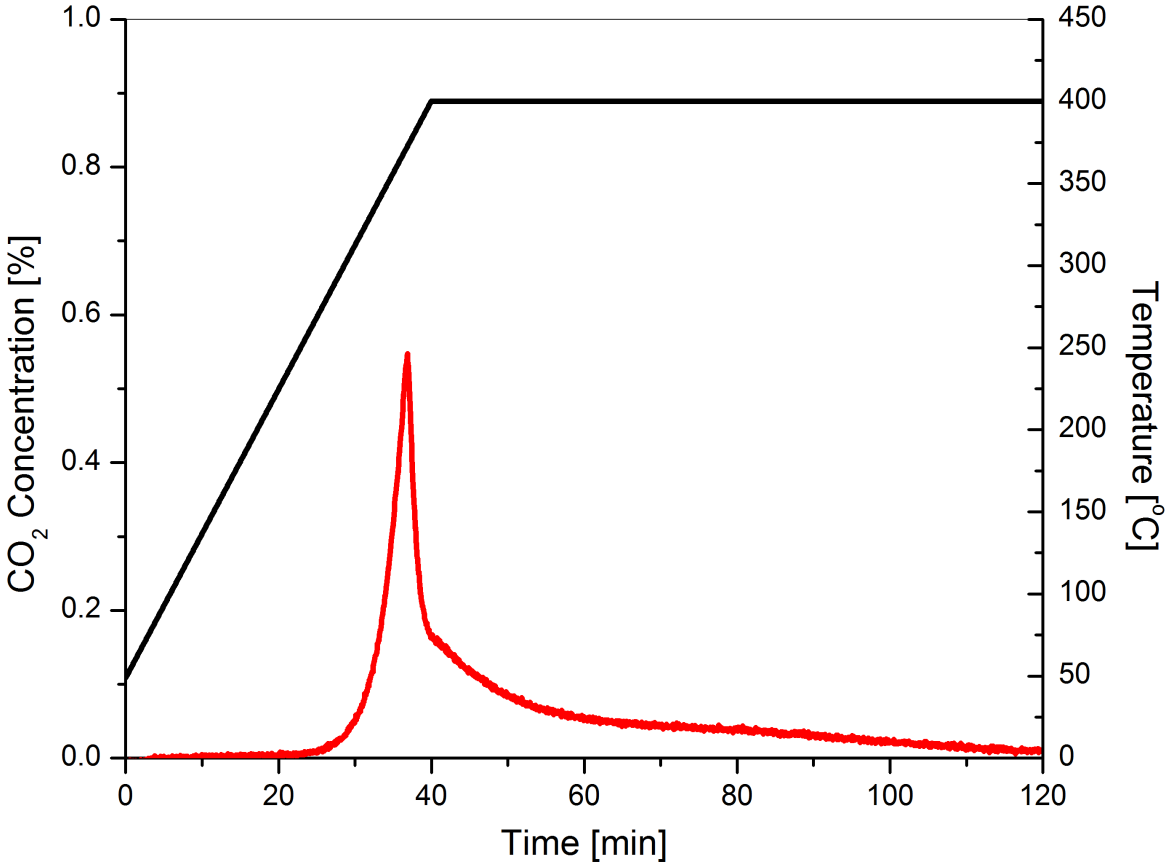

Figure 4.11 TPD of 1% Au/La_2O_3 (AA,P,CO_2) before WGS Reaction

30 mL min^{-1}, He, contact time 0.2 g s mL^{-1}

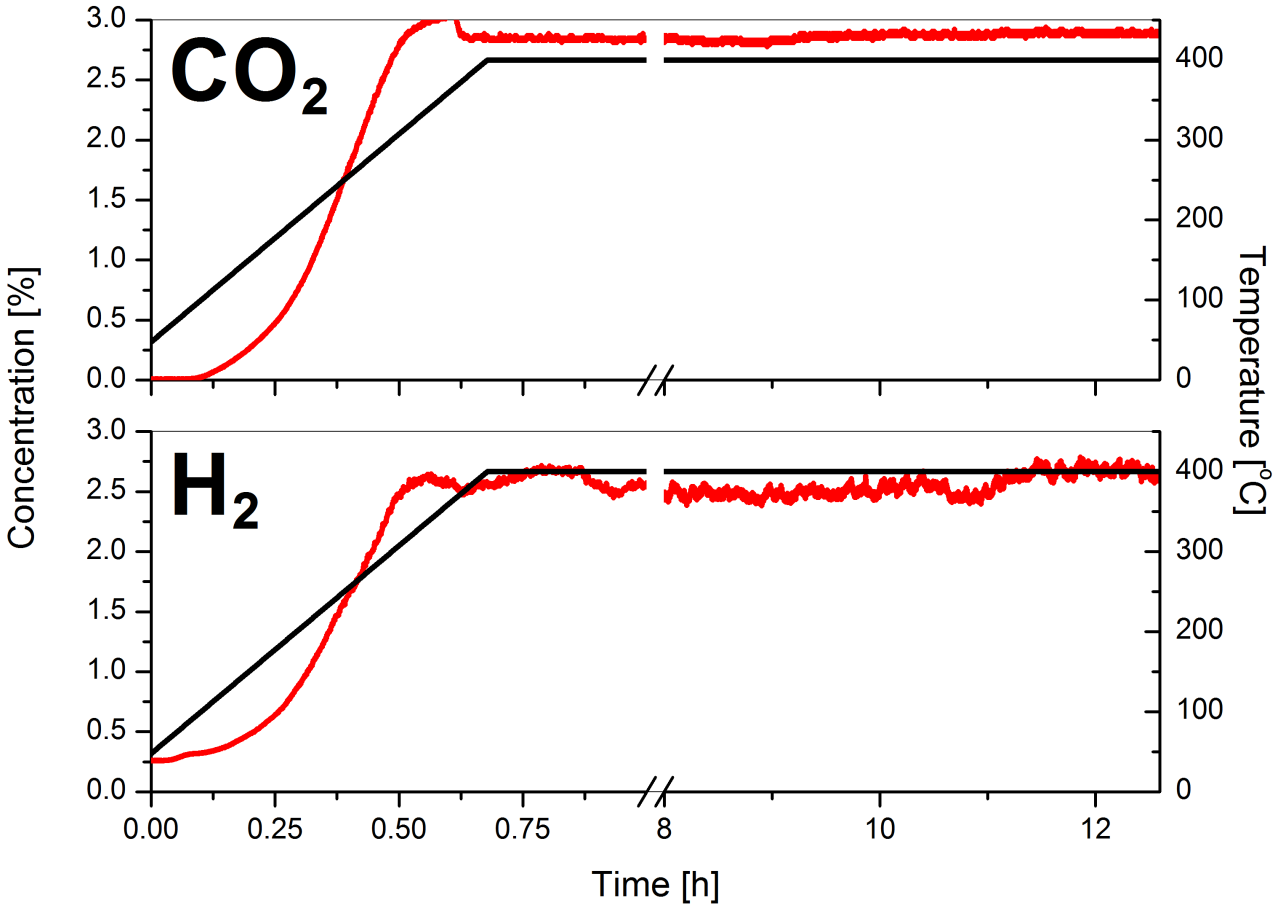

Figure 4.12 Isothermal WGS Test of 1% Au/La_2O_3 (AA,P,CO_2)

Pretreatment: 30 mL min^{-1} (10% CO_2 – He), room temperature to 400 °C for 1 h

with a heating rate of 10 °C min^{-1}

Reaction conditions: 30 mL min^{-1}, 10% CO – 3% H_2O – He,

contact time 0.2 g s mL^{-1}, isothermal for 12 h at 400 °C

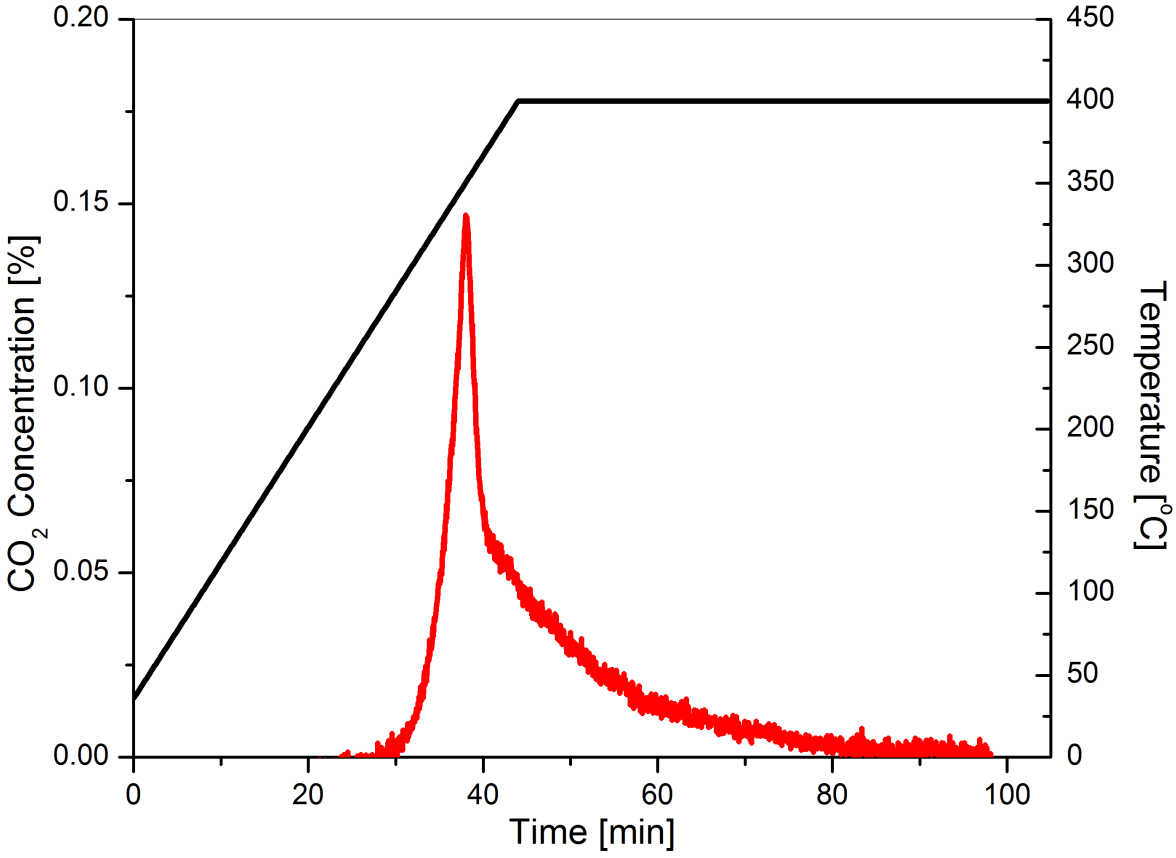

Figure 4.13 TPD of 1% Au/La_2O_3 (AA,P,CO2) after WGS Reaction

30 mL min^{-1}, He, contact time 0.2 g s mL^{-1}

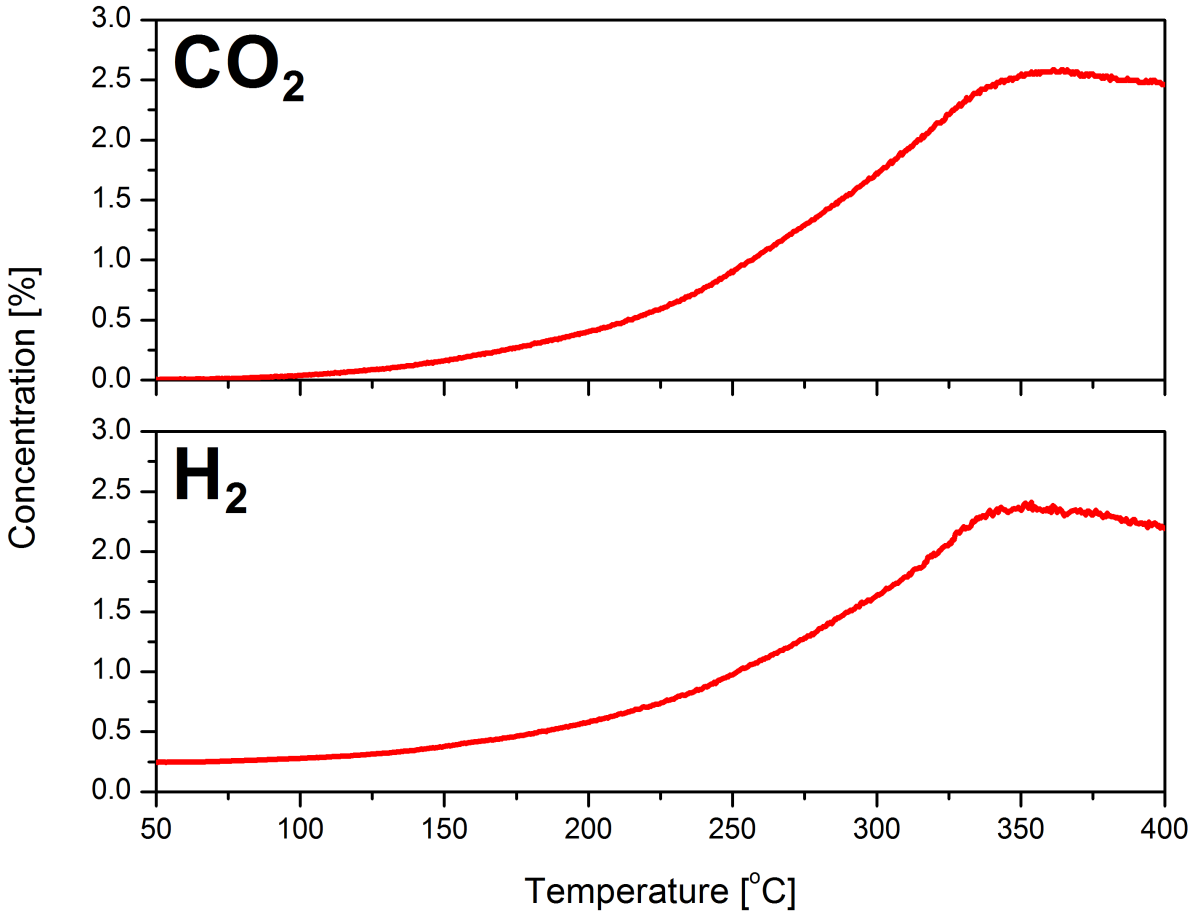

Figure 4.14 WGS TPSR of 1% Au/La_2O_3 (AA,P,CO_2) after TPD

30 mL min^{-1}, 10% CO – 3% H_2O – He, contact time 0.2 g s mL^{-1}

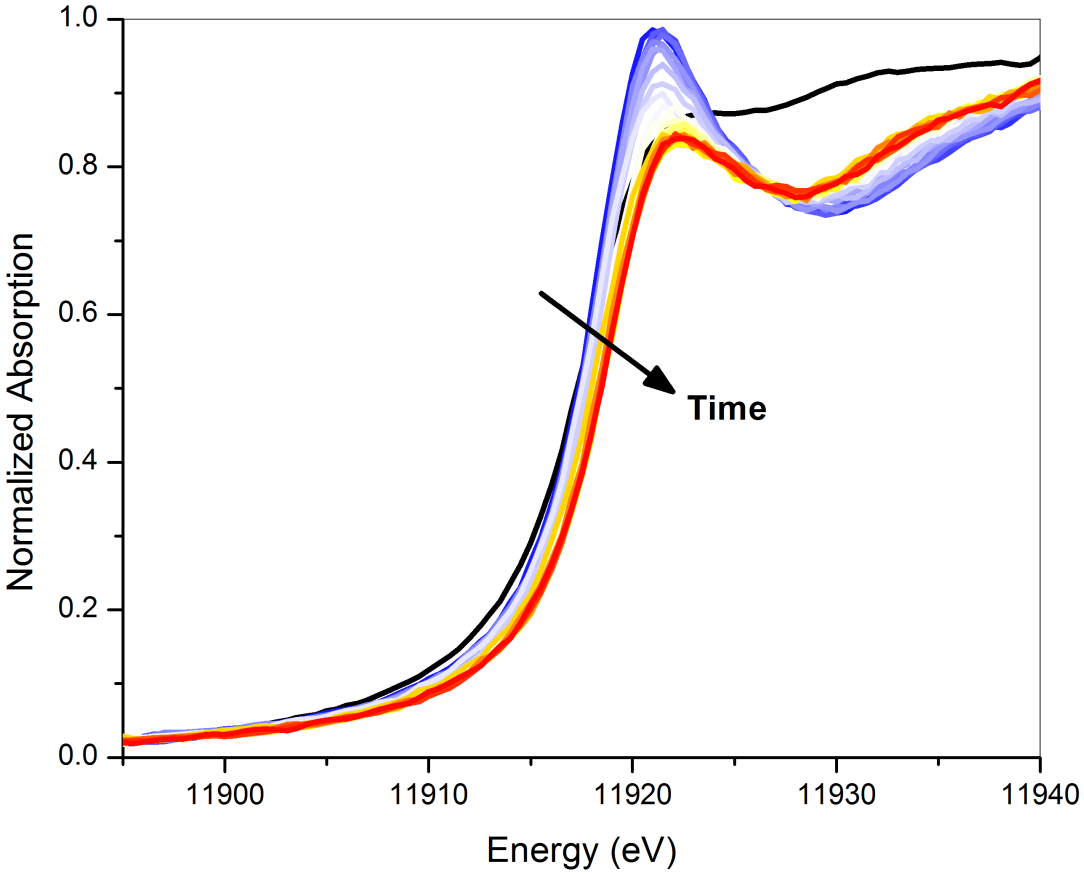

Figure 4.15 *in situ* XANES Spectra of 1% Au/La2O3 (AA,P) during WGS Reaction

Reaction conditions: 20 mL min^{-1},5% CO – 3% H_2O – He, contact time ~0.09 g s mL^{-1}, room temperature to 300 °C for 1 h with a heating rate of 5 °C min^{-1}

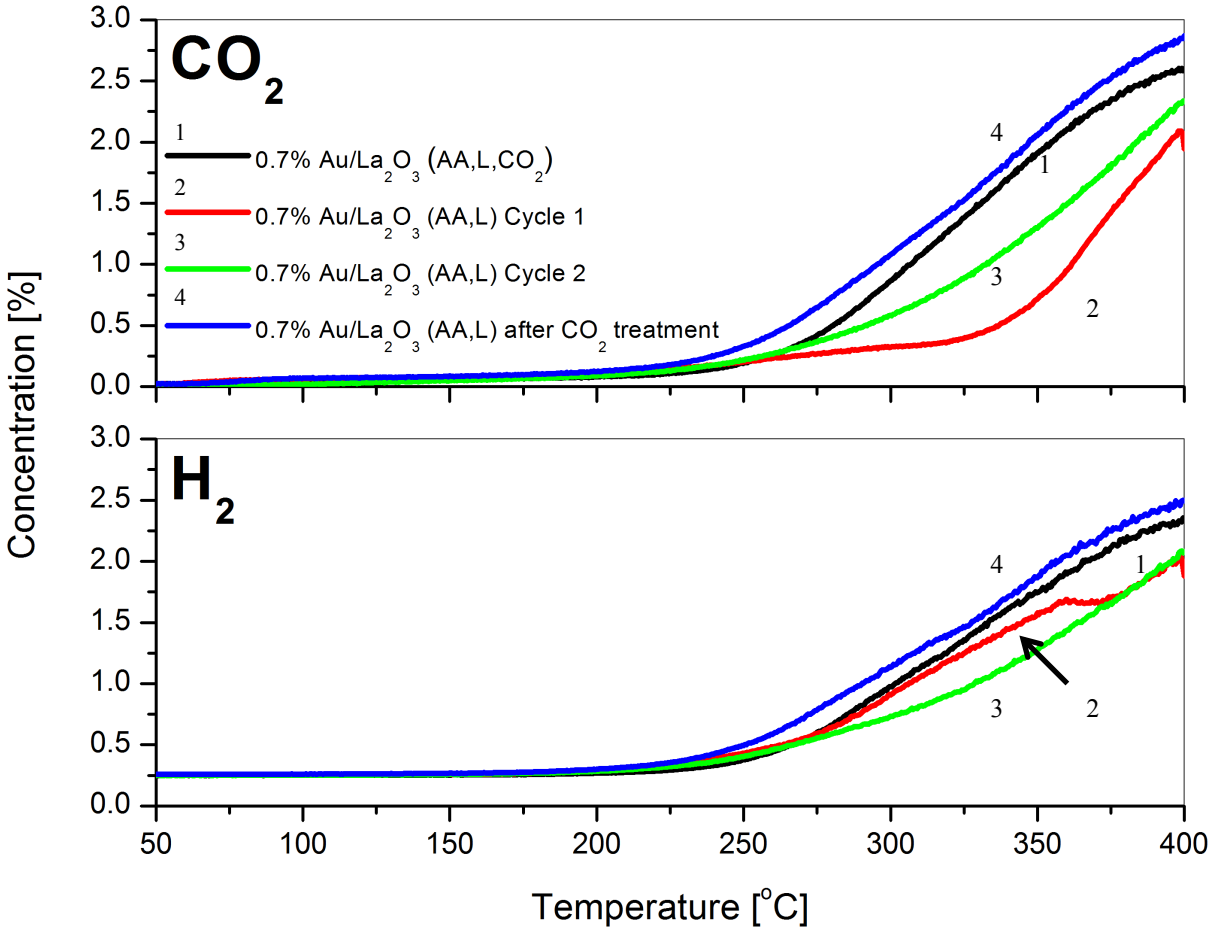

Figure 4.16 WGS Performance of 0.7% Au/La2O3 (AA,L) before and after *in situ* CO_2 Treatment

CO_2 treatment: 30 mL min^{-1} (10% CO_2 – He), room temperature to 400 °C for 1 h with a heating rate of 10 °C min^{-1}

Reaction conditions: 30 mL min^{-1}, 10% CO – 3% H_2O – He, contact time 0.2 g s mL^{-1}

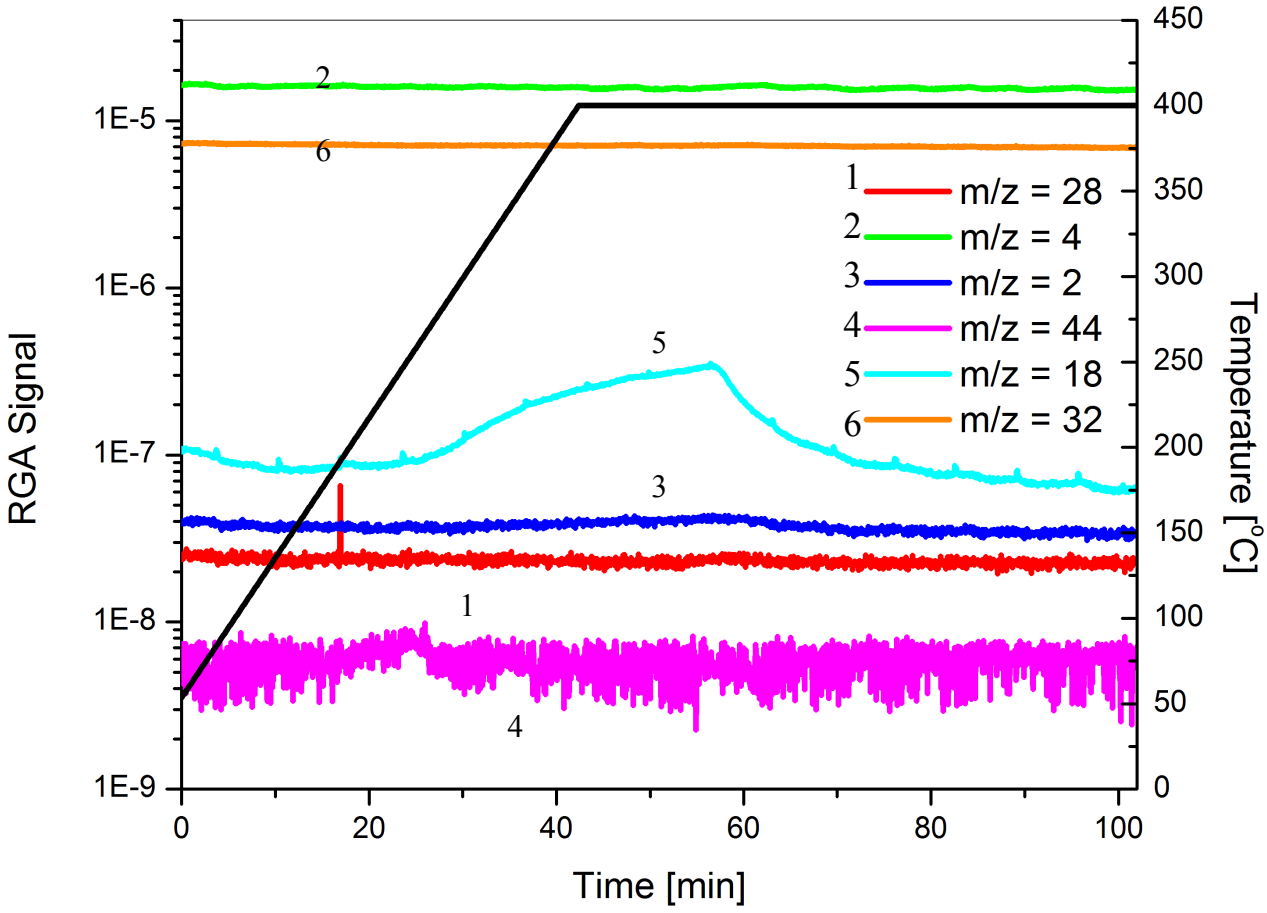

Figure 4.17 High Temperature O_2 Pretreatment of

1% Au/La_2O_3 (AA,P,O_2)

30 mL min^{-1} (20% O_2 – He), room temperature to 400 °C for 1 h with a heating

rate of 10 °C min^{-1}

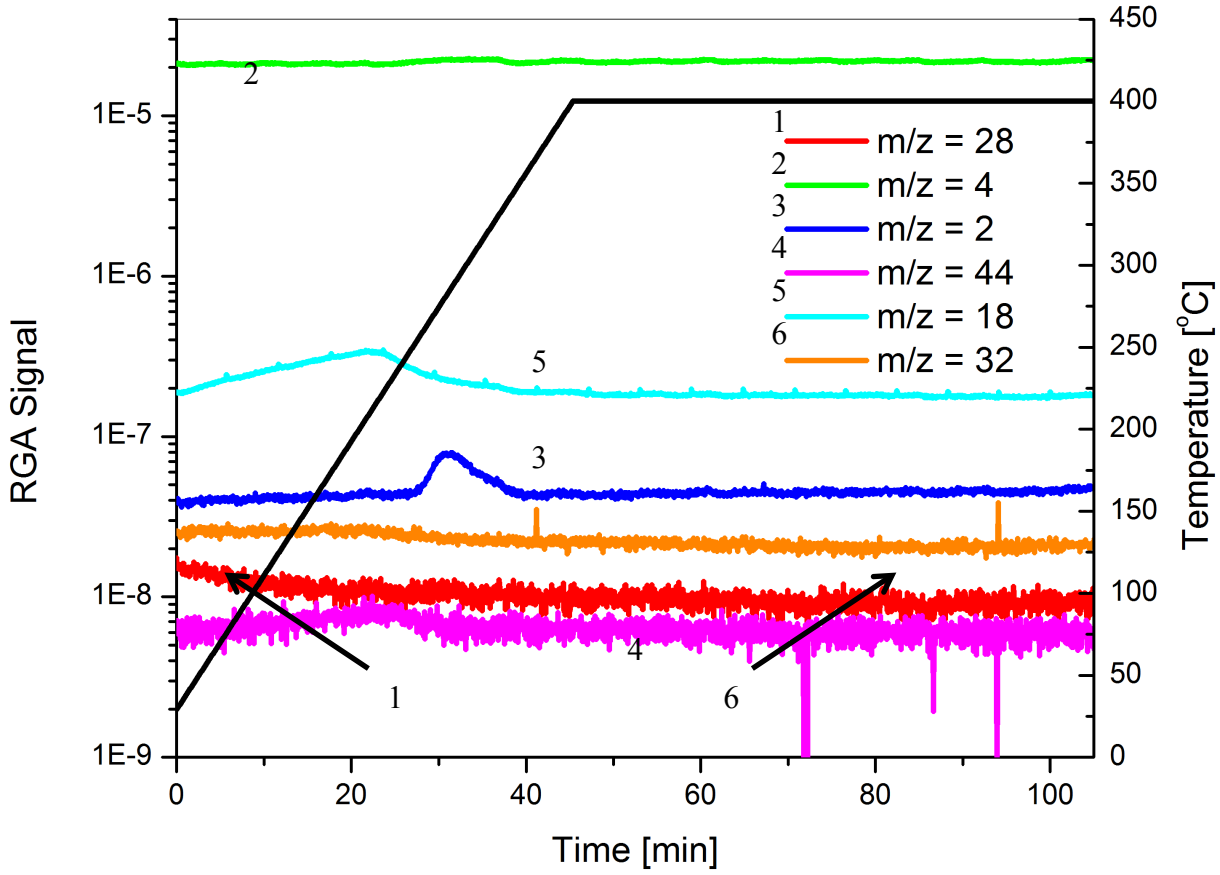

Figure 4.18 High Temperature He Pretreatment of

1% Au/La_2O_3 (AA,P,He)

30 mL min^{-1} (He), room temperature to 400 °C for 1 h with a heating rate of

10 °C min^{-1}

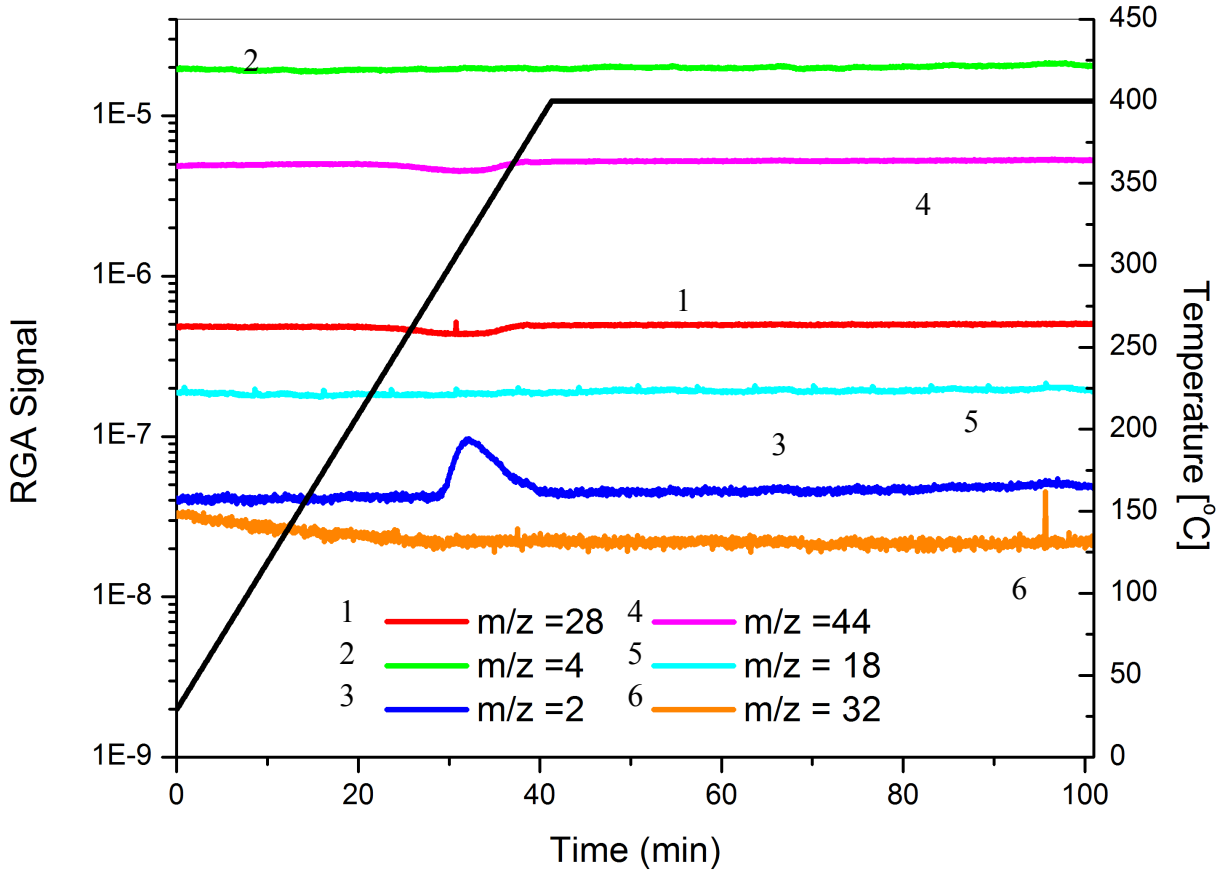

Figure 4.19 High Temperature CO_2 Pretreatment of

1% Au/La_2O_3 (AA,P,CO_2)

30 mL min^{-1} (10% CO_2 – He), room temperature to 400 °C for 1 h with a heating

rate of 10 °C min^{-1}

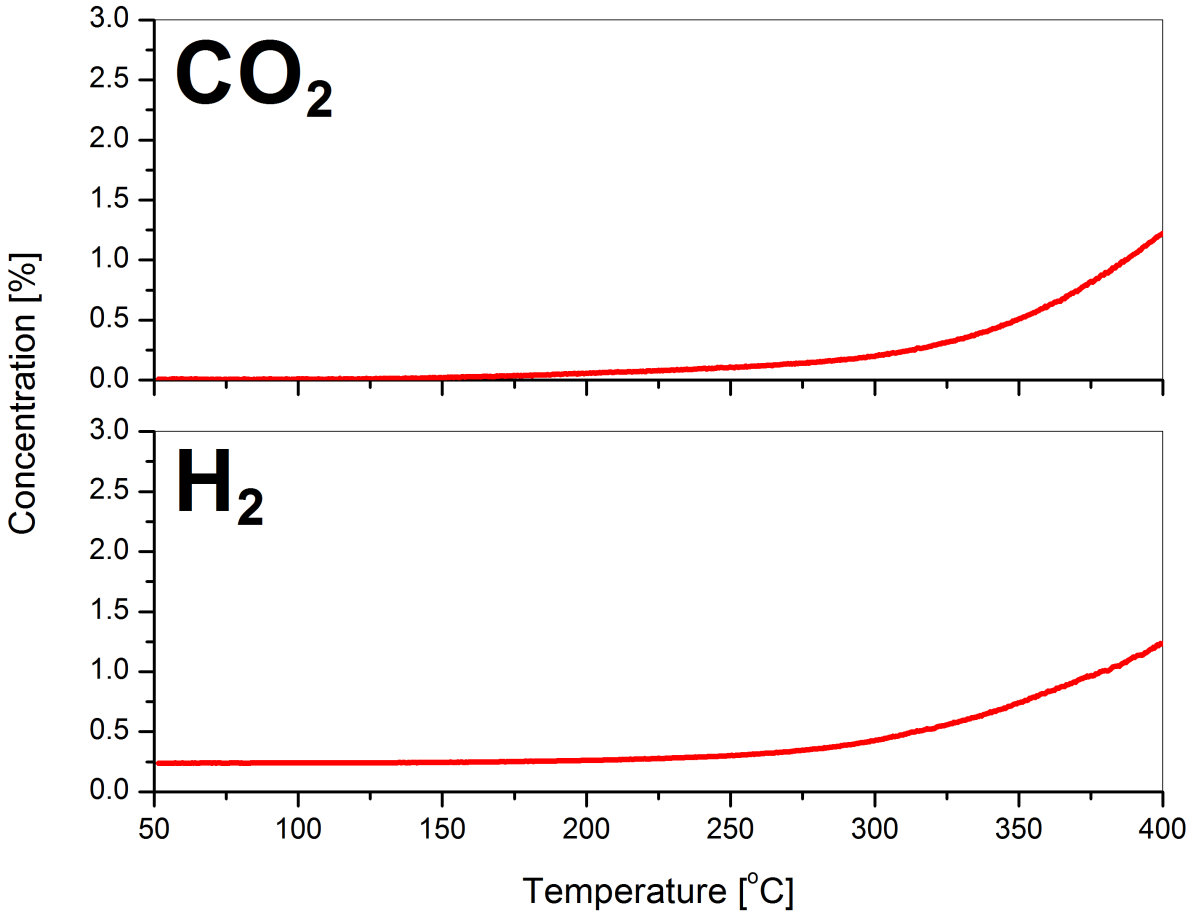

Figure. 4.20 WGS TPSR of 1% Au/La_2O_3 (AA,P,O_2)

Pretreatment: 30 mL min^{-1} (20% O_2 – He), room temperature to 400 °C for 1 h

with a heating rate of 10 °C min^{-1}

Reaction conditions: 30 mL min^{-1}, 10% CO – 3% H_2O – He,

contact time 0.2 g s mL^{-1}

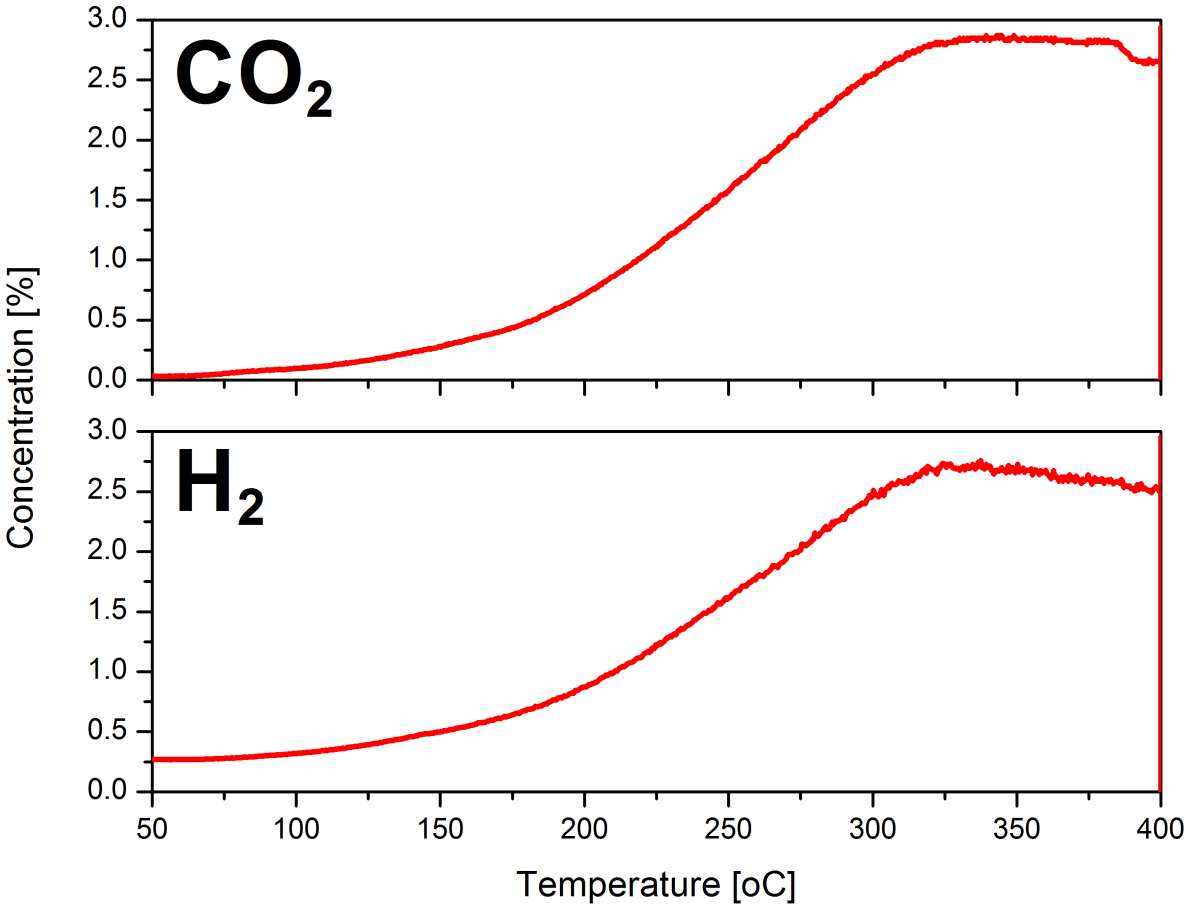

Figure 4.21 WGS TPSR of 1% Au/La_2O_3 (AA,P,He)

Pretreatment: 30 mL min^{-1} (He), room temperature to 400 °C for 1 h with a heating rate of 10 °C min^{-1}

Reaction conditions: 30 mL min^{-1}, 10% CO – 3% H_2O – He, contact time 0.2 g s mL^{-1}

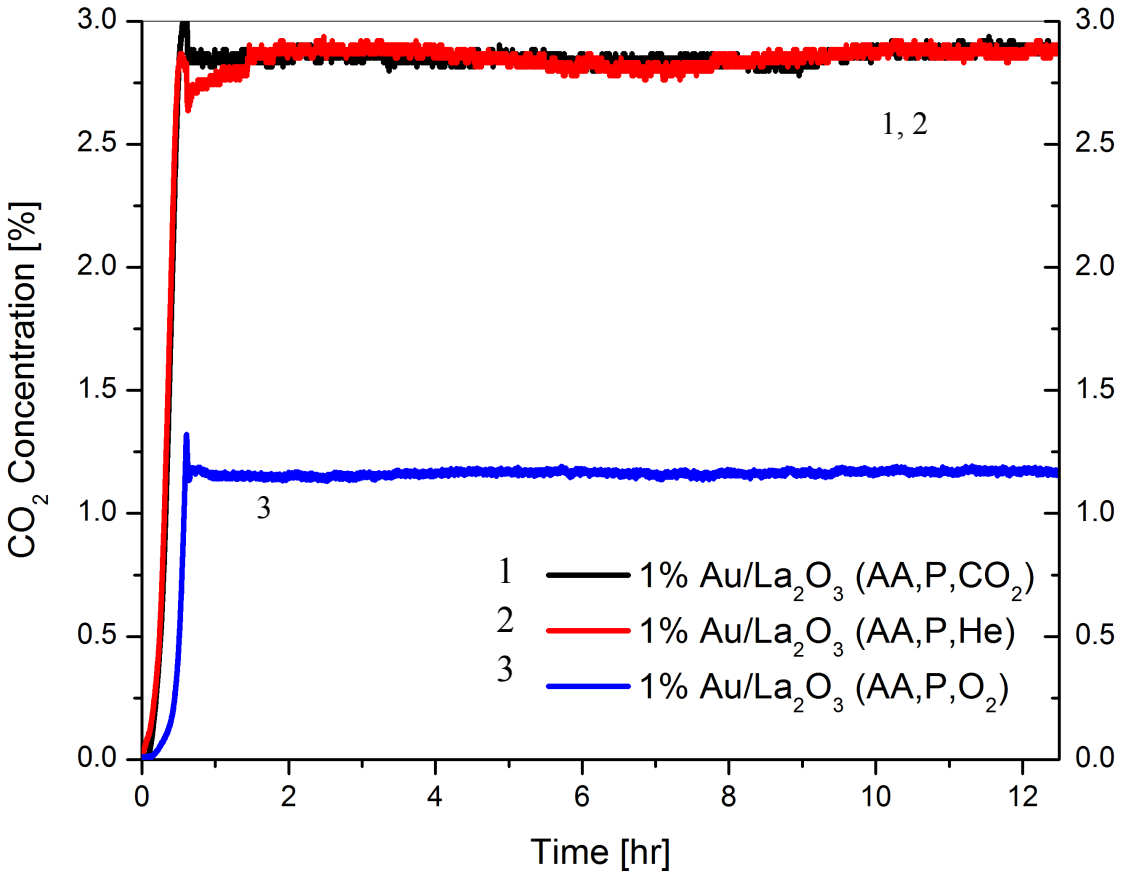

Figure 4.22 Isothermal WGS Stability of 1% Au/La_2O_3 (AA,P,CO_2), 1% Au/La_2O_3 (AA,P,He), and 1% Au/La_2O_3 (AA,P,O_2) (CO_2 signal shown)

Pretreatments: 30 mL min^{-1} (10% CO_2 – He, He, 20% O_2 - He), room temperature to 400 °C for 1 h with a heating rate of 10 °C min^{-1}

Reaction conditions: 30 mL min^{-1}, 10% CO – 3% H_2O – He, contact time 0.2 g mL s^{-1}, room temperature to 400 °C (10 °C min^{-1}) isothermal for 12 h

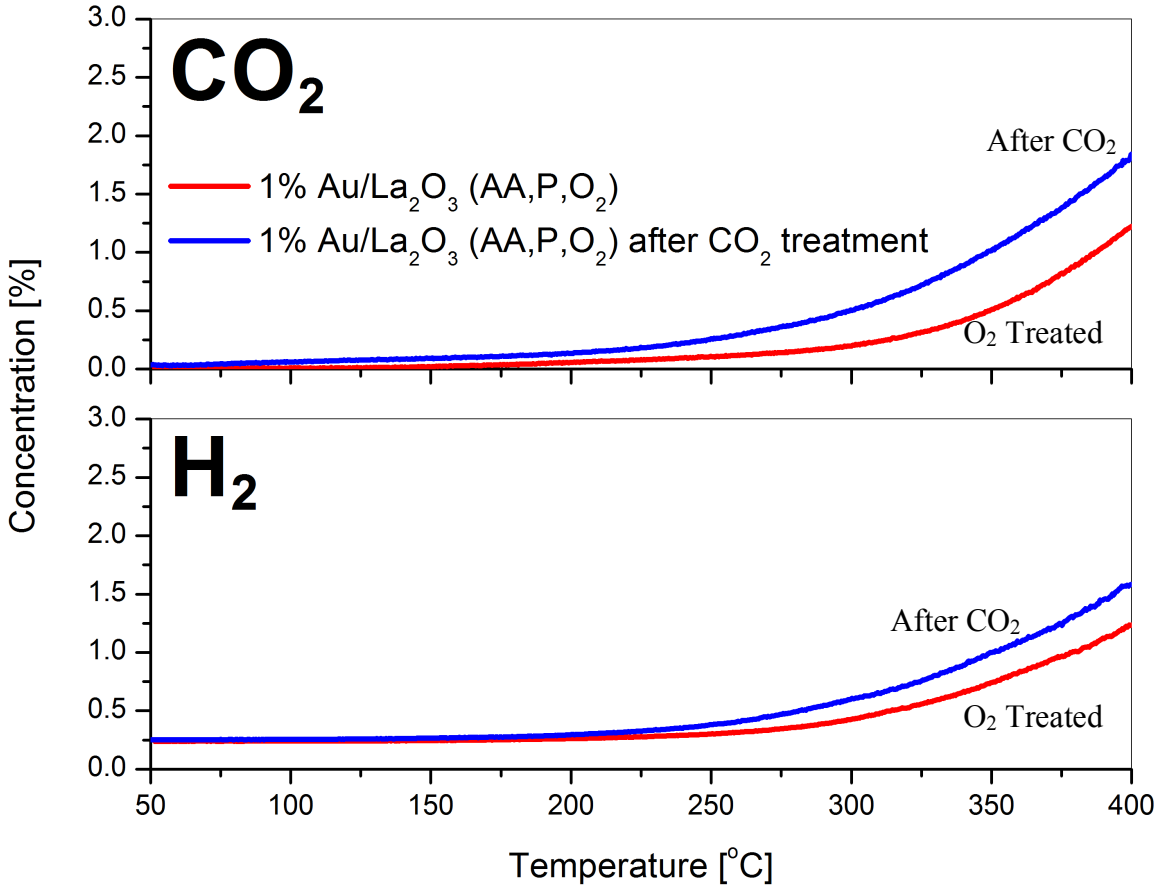

Figure 4.23 Comparison of WGS TPSR Performance of

1% Au/La_2O_3 (AA,P,O_2) before and after CO_2 Treatment

Pretreatment: 30 mL min^{-1} (20% O_2 – He), room temperature to 400 °C for 1 h

with a heating rate of 10 °C min^{-1}

in situ CO_2 treatment: 30 mL min^{-1} (10% CO_2 – He), room temperature to 400 °C

for 1 h with a temperature ramping rate of 10 °C min^{-1}

Reaction conditions: 30 mL min^{-1}, 10% CO – 3% H_2O – He,

contact time 0.2 g mL s^{-1}

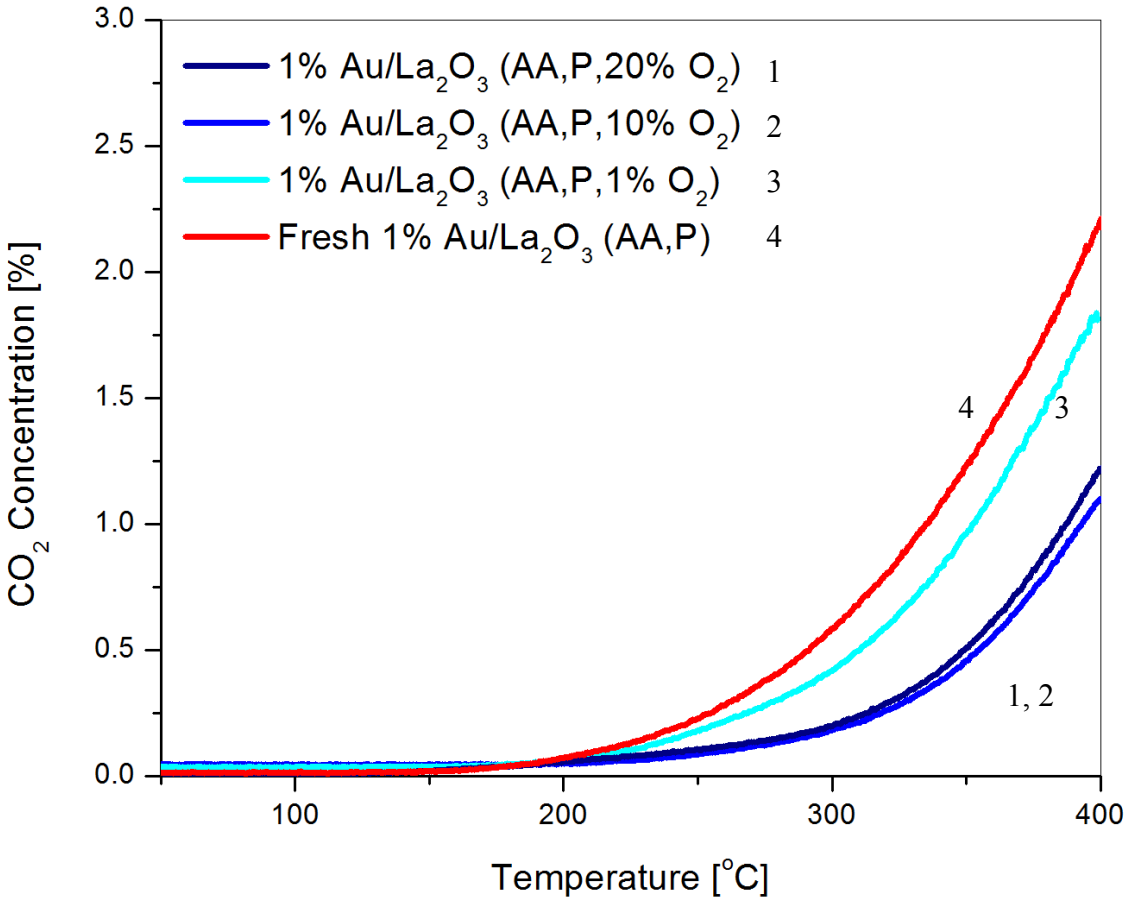

Figure 4.24 Effect of Oxygen Partial Pressure in Pretreatment Gas on WGS-TPSR Performance of 1% Au/La_2O_3 (AA,P)

Pretreatment: 30 mL min^{-1} (1%, 10%, 20% O_2 – He), room temperature to 400 °C for 1 h with a heating rate of 10 °C min^{-1}

Reaction conditions: 30 mL min^{-1}, 10% CO – 3% H_2O – He, contact time 0.2 g mL s^{-1}

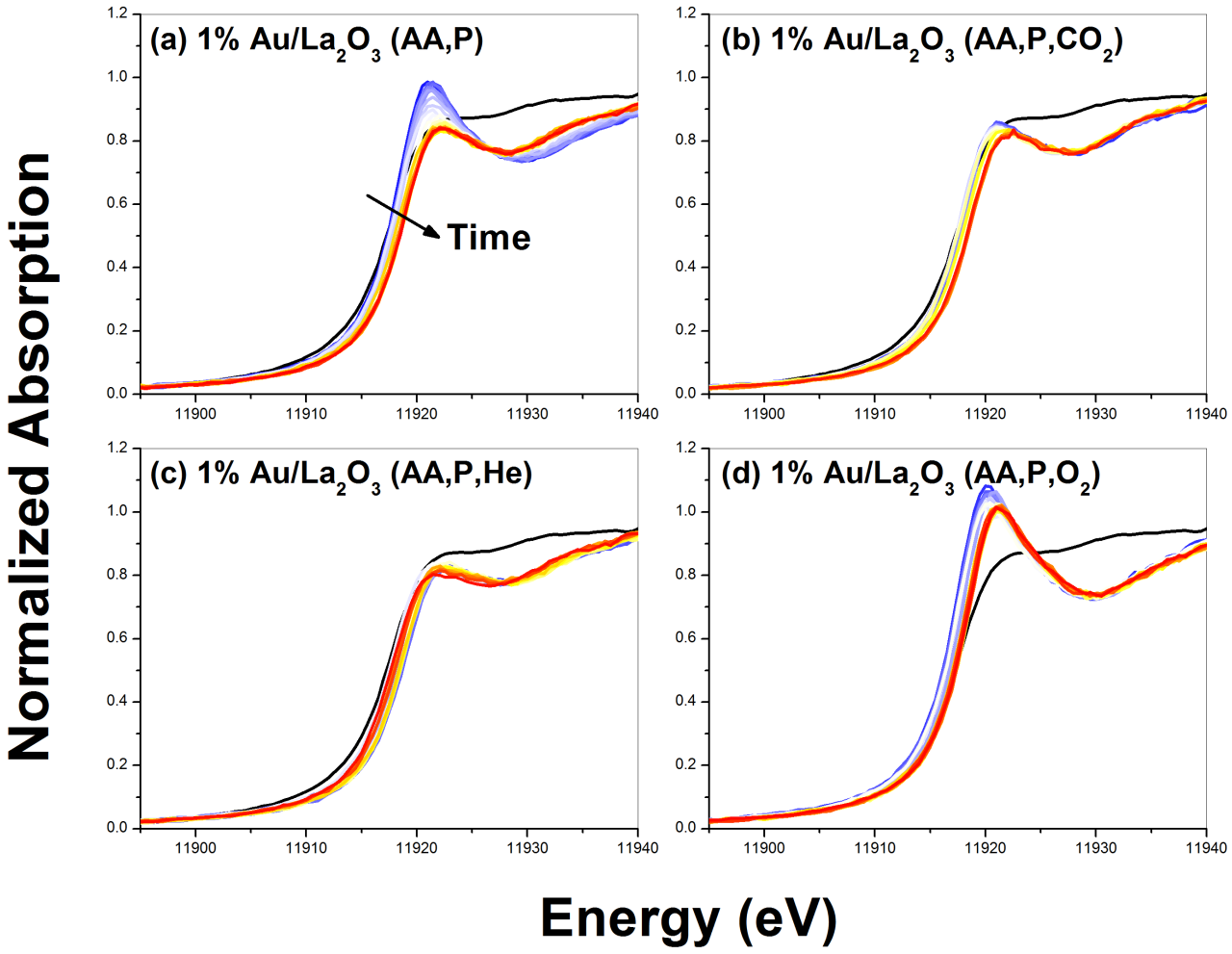

Figure 4.25 Summary of *in situ* XANES Spectra of 1% Au/La2O3 (AA,P)

Materials after Pretreatments

Reaction conditions: 20 mL min^{-1}, 5% CO – 3% H_2O – He, room temperature to

300 °C with an isothermal hold for 1 h, heating rate of 5 °C min^{-1}

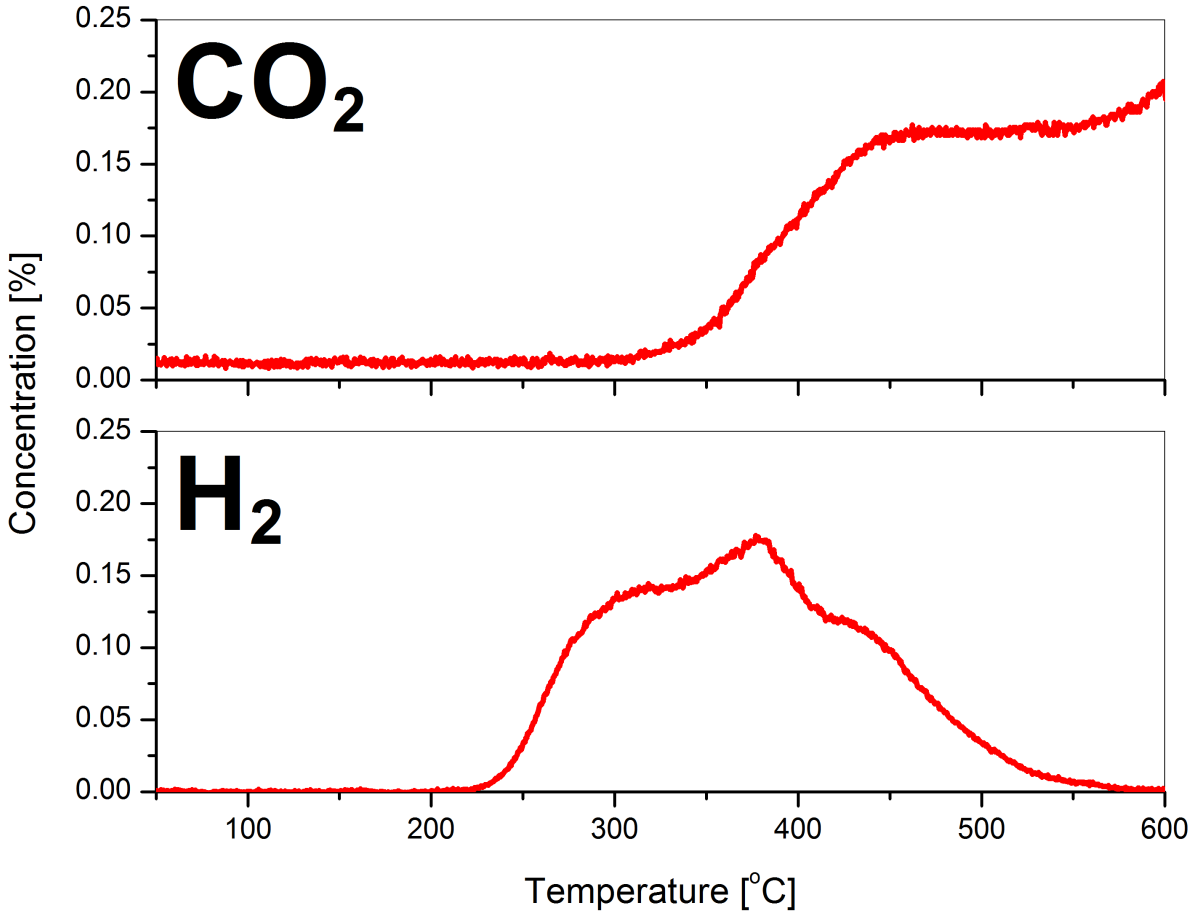

Figure 4.26 CO-TPR of Bare La_2O_3

30 mL min^{-1}, 10% CO – He, heating rate of 10 °C min^{-1}

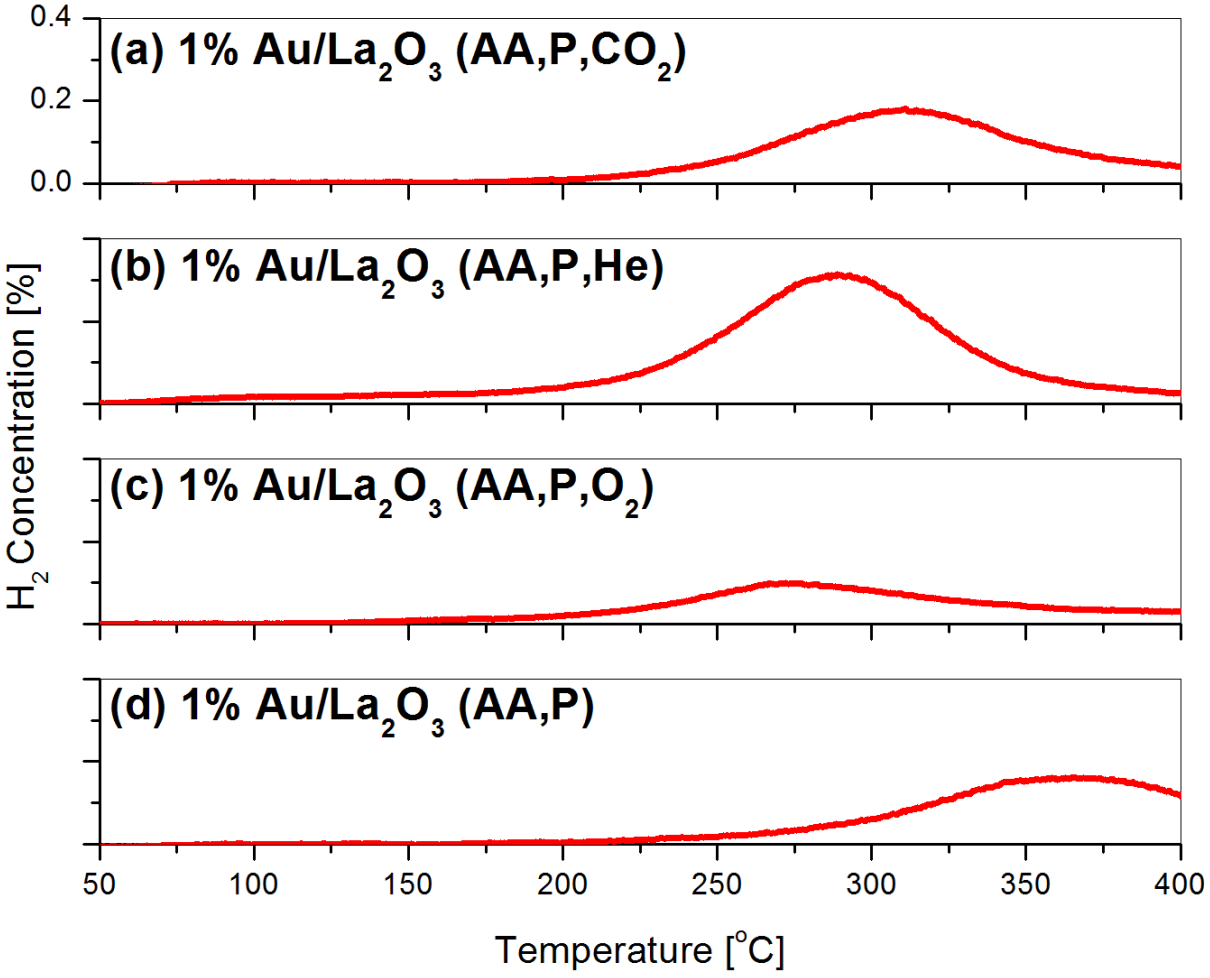

Figure 4.27 CO-TPR of 1% Au/La_2O_3 (AA,P) Materials

Pretreatments: 30 mL min^{-1} (10% CO_2 – He, He, 20% O_2 - He), room temperature to 400 °C for 1 h with a heating rate of 10 °C min^{-1}

CO-TPR: 30 mL min^{-1}, 10% CO – He, heating rate of 10 °C min^{-1}

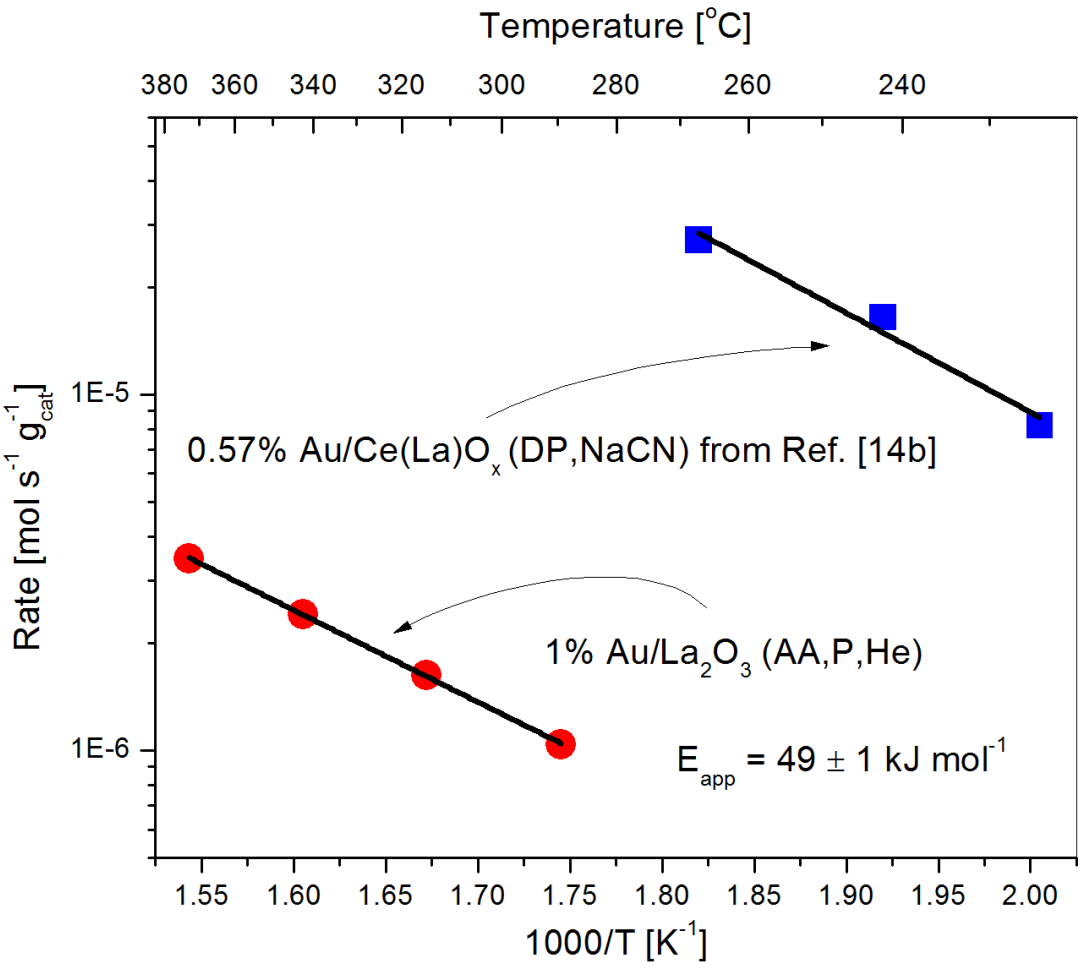

Figure 4.28 Apparent Activation Energy (E_{app}) of 1% Au/La_2O_3 (AA,P,He)

Gas composition: 11% CO – 26% H_2O – 26% H_2 – 7% CO_2 - He

Chapter 5. Summary and Recommendations

5.1 Summary

In this thesis, the preparation of lanthanum oxide-supported Au catalysts was investigated. These Au/La_2O_3 materials were shown to be active for the water-gas shift (WGS) reaction.

Several formulations of lanthanum-based Au catalysts were investigated. A colloidal deposition technique was used to prepare a control Au/La_2O_3 (C) system to show that simply having Au on the La_2O_3 surface did not yield an active WGS catalyst. Additionally, a co-precipitation (CP) method was also investigated to prepare a $Au/La(OH)_3$ (CP) that, through careful pretreatment, was reported to contain ionic gold clusters decorated with hydroxyl groups. However, this material was shown to be inactive in the low temperature window for which the $Au/La(OH)_3$ structure was stable. A traditional deposition-precipitation (DP) preparation was used to prepare Au/La_2O_3 (DP). These catalysts were moderately active for the WGS reaction but the Au was shown to interact weakly with the La_2O_3 surface as formed 1-2 nm particles and was removed with NaCN leaching.

Anion adsorption (AA) was investigated as a means to more effectively disperse Au on the La_2O_3 surface while simultaneously removing residual Cl from the precursor complex. In the literature this technique was shown to produce promising CO oxidation catalysts. During AA, the Au is speciated completely to $[Au(OH)_4]^-$ and then adsorbed onto the support surface. This adsorption is driven by an electrostatic attraction established between the positively charged support

surface and the negatively charged precursor. The Au/La_2O_3 (AA) materials were shown to contain highly dispersed Au that could not be removed by NaCN leaching, suggesting it was interacting strongly with the La_2O_3 surface.

When tested for the WGS reaction, the 1% Au/La_2O_3 (AA) showed moderate initial activity. The catalyst was also observed to adsorb CO_2 during the reaction. In an investigation of what role CO_2 adsorption might play, it was discovered that high temperature pretreatments in either CO_2 or He further activated 1% Au/La_2O_3 (AA) for the WGS reaction, lowering the light off temperature by over 100 °C. Further characterization of these materials by XAS showed that the Au was partially reduced after the high temperature treatments (compared to the fresh material). The support material used in this study is represented as La_2O_3 for consistency with the relevant literature, but in reality it would be better described as a $LaO(OH)_x$ species that is highly amorphous and contains OH and crystalline H_2O in its structure. The high temperature O_2 treatment was shown to further oxidize the $LaO(OH)_x$ to La_2O_3; during this oxidation the support surface lost much of its active oxygen and its ability to stabilize Au-O-$La(OH)_x$, which is the active site for the WGS reaction. The high temperature CO_2 treatment, on the other hand, was able to form surface hydroxycarbonates that are likely able to stabilize the active Au species during the WGS reaction, and prevent further oxidation of the support. Similarly, the support was not affected during the high temperature He treatment. In effect, the $LaO(OH)_x$ support is much better at stabilizing the necessary Au species (Au-O-

$La(OH)_x$) than the La_2O_3. While the starting Au/La_2O_3 (AA,P) is in fact the former lanthanum species, this $LaO(OH)_x$ can be altered.

Investigation of the reducibility of these materials with temperature programmed reduction (CO-TPR) studies proved that the most active materials contained the highest content of activated surface oxygen, in accordance with previous observations in our group. However, the 1% Au/La_2O_3 (AA) catalysts had significantly lower mass reaction rates than Au/CeO_2 and Au/FeOx samples with similar Au loading. Further normalization of the reaction rates by the material surface area did not bring the reaction rates into agreement. Normalization by the activated oxygen (as –OH, and calculated by TPR), though, showed that the amount of active oxygen is the determinant factor in the overall activity of a WGS catalyst whether it is composed of a reducible or irreducible metal oxide. These active oxygen groups are likely the species most closely interacting with the Au through a possible Au-O-$La(OH)_x$ species.

5.2 Recommendations for Future Study

5.2.1 Determining the Au-OH Species Present

A more mechanistic understanding of the surface chemistry taking place during WGS catalysis on Au/La_2O_3 is warranted and would further our knowledge of how Au, OH and the WGS reaction are linked. In particular, *in* and *ex situ* studies of the types of –OH and carbonate species present in this system would greatly clarify the effect different pretreatments have on the Au/La_2O_3. Infared (IR) or Ramen spectroscopy would help elucidate the type of –OH groups on the surface. Additionally, detailed XPS analysis of the support surface would

shed light on the type of O groups present. Finally, XRD analysis performed on the used materials would indicate whether any bulk changes have taken place in the support. These measurements would allow for a more quantitative explanation for the observations made here and perhaps help further bridge the gap between the role irreducible metal oxides play in the WGS reaction. It is important to better understand how the high temperature treatments have affected both the $LaO(OH)_x/La_2O_3$ and the Au. It would also be useful to study Au supported on more crystalline La_2O_3 (i.e. hydrolysis lanthana calcined at temperatures >800 °C) because this would provide a system in which the effect of the support change would be mitigated and even fewer activated oxygen species would be present. The $Au/La_2O_2SO_4$ provides a useful parallel to the work presented here, but our understanding is still incomplete.

The work performed with anion adsorption here was used to prepare an active WGS catalyst. However, the preparation conditions are those taken loosely from reports in the literature. A more detailed study of these preparations, along with an optimization study, might yield insight into a method to preparing an even more active material. An understanding of Au uptake on La_2O_3, the maximal achievable loading and how these parameters affect WGS activity would provide more guidance in preparing Au/La_2O_3. Additionally, this work has demonstrated the –OH groups play a significant role during the WGS catalysis, and whether or not the –OH content can be augmented with alkali doping remains to be seen.

This Au/La_2O_3 system provides a useful template on which the Au-OH interaction can be studied because, unlike in Au/FeOx and Au/CeO_2 systems

where the support contributes a significant fraction of –OH, the majority of TPR titratable oxygen groups in Au/La_2O_3 seem to be those bound on the Au surface complex.

A parametric study on the influence of CO and H_2O concentrations on the WGS performance of these materials is also warranted. During WGS-TPSR tests the materials were exposed to a net reducing atmosphere and a slightly reducing environment during the kinetics measurements. However, how these materials performing in a fuel lean mixture should also be investigated.

5.2.2 Potential Au/La_2O_3 Catalyzed Reactions

Lanthanum oxide-supported Au catalysts have been investigated for several reactions in the literature. However, these materials are generally prepared by methods investigated here that were shown to produce less than ideal catalysts. Anion adsorption could potentially be used to overcome the limitations of techniques like DP to produce even more active catalysts. In particular, CO oxidation and oxidative dehydrogentation (ODH) of butane have been catalyzed by Au/La_2O_3 in the literature with promising results. What effect using more highly dispersed Au prepared by AA might have remains to be seen. Additionally, the methanol reactions (steam reforming, decomposition) have been shown to be catalyzed by Au supported on basic metal oxides. The use of Au/La_2O_3 in the study of these reactions may further elucidate the role oxidized Au species and basic sites play.